Applications of Mass Spectrometry in the Analysis of Food Composition and Contaminants

Lead Guest Editor: Yan Zhang
Guest Editors: Hui-Min David Wang, Wei Chen, and Xiaozhi Tang

Applications of Mass Spectrometry in the Analysis of Food Composition and Contaminants

Applications of Mass Spectrometry in the Analysis of Food Composition and Contaminants

Lead Guest Editor: Yan Zhang
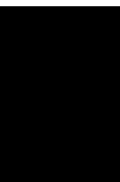Guest Editors: Hui-Min David Wang, Wei Chen, and Xiaozhi Tang

María B. Pérez-Gago (iD), Spain
Anand Babu Perumal (iD), China
Gianfranco Picone (iD), Italy
Witoon Prinyawiwatkul, USA
Eduardo Puértolas (iD), Spain
Sneh Punia, USA
Sara Ragucci (iD), Italy
Miguel Rebollo-Hernanz (iD), Spain
Patricia Reboredo-Rodríguez (iD), Spain
Jordi Rovira (iD), Spain
Swarup Roy, India
Narashans Alok Sagar (iD), India
Rameswar Sah, India
El Hassan Sakar (iD), Morocco
Faouzi Sakouhi, Tunisia
Tanmay Sarkar (iD), India
Cristina Anamaria Semeniuc, Romania
Hiba Shaghaleh (iD), China
Akram Sharifi, Iran
Khetan Shevkani, India
Antonio J. Signes-Pastor (iD), USA
Amarat (Amy) Simonne (iD), USA
Anurag Singh, India
Ranjna Sirohi, Republic of Korea
Slim Smaoui (iD), Tunisia
Mattia Spano, Italy
Barbara Speranza (iD), Italy
Milan Stankovic (iD), Serbia
Maria Concetta Strano (iD), Italy
Antoni Szumny (iD), Poland
Beenu Tanwar, India
Hongxun Tao (iD), China
Ayon Tarafdar, India
Ahmed A. Tayel (iD), Egypt
Meriam Tir, Tunisia
Fernanda Vanin (iD), Brazil
Ajar Nath Yadav, India
Sultan Zahiruddin (iD), USA
Dimitrios I. Zeugolis (iD), Ireland
Chu Zhang (iD), China
Teresa Zotta (iD), Italy

Contents

Rapid Identification of Chemical Constituents in *Hericium erinaceus* Based on LC-MS/MS Metabolomics

Fei Yang ⓘD, Honglin Wang ⓘD, Guoquan Feng ⓘD, Sulan Zhang ⓘD, Jinmei Wang ⓘD, and Lili Cui ⓘD

WILEY | Hindawi

Corrigendum

Corrigendum to "The Bridge between Screening and Assessment: Establishment and Application of Online Screening Platform for Food Risk Substances"

Kang Hu, Shaoming Jin, Hong Ding, and Jin Cao

National Institutes for Food and Drug Control, Beijing 100050, China

Correspondence should be addressed to Hong Ding; dinghong@nifdc.org.cn and Jin Cao; caojin@nifdc.org.cn

In the article titled "The Bridge between Screening and Assessment: Establishment and Application of Online Screening Platform for Food Risk Substances" [1], the Authors' Contributions statement was omitted. The Authors' Contributions statement is given below.

Authors' Contributions

Ding Hong, Cao Jin, Hu Kang, and Jin Shaoming jointly studied and formulated research ideas, technical solutions, and verification implementation. Kang Hu and Shaoming Jin contributed equally. Shaoming Jin was responsible for the collection, provision, and verification of experimental data. Kang Hu generated the Online Screening Platform and realized the function of computer software. Hong Ding was responsible for the overall work of the subject research. Jin Cao was responsible for the technical audit related to the laboratory. Kang Hu and Shaoming Jin wrote and prepared the original draft. Hong Ding and Jin Cao completed the review of the paper for publication.

References

[1] K. Hu, S. Jin, H. Ding, and J. Cao, "The Bridge between Screening and Assessment: Establishment and Application of Online screening Platform for Food Risk Substances," *Journal of Food Quality*, vol. 2021, Article ID 2275471, 9 pages, 2021.

Research Article

Accurate Determination, Matrix Effect Estimation, and Uncertainty Evaluation of Three Sulfonamides in Milk by Isotope Dilution Liquid Chromatography-Tandem Mass Spectrometry

Chaonan Han [1,2] **Xiuqin Li**,[1] **Hui Jiao**,[1] **Yan Gao**,[1] **and Qinghe Zhang**[1]

[1]*Division of Chemical Metrology and Analytical Science, National Institute of Metrology, Beijing 100029, China*
[2]*Heilongjiang Green Food Science Research Institute, Harbin 150000, China*

Correspondence should be addressed to Yan Gao; gaoyan@nim.ac.cn and Qinghe Zhang; zhangqh@nim.ac.cn

Liquid chromatography-tandem mass spectrometry (LC-MS/MS) is the most commonly used method for sulfonamide determination. Its accuracy, however, can be affected by many factors. In this study, sulfadiazine (SDZ), sulfadimidine (SMZ), and sulfadimethoxine (SDM) in milk were selected to investigate an accurate determination method and the potential influencing factors in the use of ultrahigh-performance liquid chromatography-tandem mass spectrometry (UHPLC-MS/MS). Milk samples were extracted by 25 mL perchloric acid solution (pH = 2) and cleaned up using HLB solid-phase extraction (SPE) cartridges. Four kinds of filters, including PTFE, GHP, nylon, and glass fiber, were compared, and PTFE was selected since it had the best recoveries of target sulfonamides (SAs). Three quantitative methods, including external standard (ES), matrix matching (MM), and isotope dilution mass spectrometry (IDMS), were compared, among which IDMS exhibited the best accuracy. The matrix effect under different mobile phase compositions and of different sample matrices were evaluated and discussed. Ion suppression effects were observed during the determination of all SAs, which got stronger with the increase of the methanol composition percent in the mobile phase. After correction by IDMS, the matrix effect could be neglected. Matrix spiked recoveries at three spiked levels (1 μg/kg, 10 μg/kg, and 20 μg/kg) ranged from 96.8% to 103.8% by IDMS. The expanded relative uncertainties were in the range of 2.02% to 5.75%. The method exhibited wide application range, high accuracy, good stability, and high sensitivity.

1. Introduction

Sulfonamides (SAs) are a kind of generic, highly effective, low-toxicity, and low-cost antibacterial agents [1]. The use of SAs as antibacterial synergist can expand the scope and enhance the activity of antibacterial. Therefore, SAs are widely used in milk production for the prevention and treatment of bacterial diseases. However, due to the potential toxicity, excessive intake of SAs may lead to human diseases, such as urinary system damage, digestive disorders, vomiting diarrhea, hemolytic anemia, drug-resistant strains, human immunity reduction, and tumor tendency [2, 3].

Therefore, many countries and regions have issued regulations on maximum residue limits (MRL) for SAs in food and feed. It is stipulated in the International Codex Alimentarius Commission (CAC) that the total amount of SAs in food and feed shall not exceed 100 μg/kg [4]. The United Nations Food and Agriculture Organization (FAO) stipulates a residue limit for SAs in animal food at 100 ng/mL [5]. According to the European Union (EU) regulation, single SAs concentration in milk and meat should not exceed 25 μg/kg, and the total amount should not exceed 100 μg/kg [6]; China's Ministry of Agriculture and Rural Affairs stipulates that the total concentration of SAs in milk should be lower than 100 ng/mL, and the MRL of sulfamethazine is 25 μg/L [7].

At present, the detection methods of SAs residues mainly include microbial detection [8], fluorescence spectrophotometry [9], immunoassay [10], and high-performance liquid chromatography coupled mass spectrometry (HPLC-MS). However, the sensitivity and selectivity were limited.

Liquid chromatography coupled to tandem mass spectrometry (LC-MS/MS) [11, 12] is a highly sensitive, specific, and reliable tool for contaminants detection in food and has become the most universal approach for multianalyte analysis. It is applied in an expanding field of food analysis, particularly in multiresidue detection [13, 14]. However, the complex food matrix (such as carbohydrates, proteins, or fats) can induce ion suppression or enhancement of the target analytes, which may hamper the accuracy of mass spectrometric quantification [15–18]. Matrix effect (ME) cannot be neglected in LC-MS/MS analysis, which makes the extraction and clean-up processes challenging [19–22]. Strategies have been developed to minimize or eliminate the MEs, such as improving chromatographic selectivity to avoid coelution, mobile phase modifiers, dilution, and efficient clean-up [23–25]. Although these approaches were claimed to be effective for chosen mode analytes, there are inherent drawbacks for further extension [26, 27]. With identical chemical and chromatographic properties compared with the target compound, isotope labeled internal standards can compensate for matrix effects. Therefore, the isotope dilution mass spectrometry (IDMS) method exhibits high accuracy and repeatability for the quantitative analysis of organic compounds in complex matrices, which could overcome the difficulty in the correction of recovery and the influence of inject volume, mobile phase, and instrument fluctuation during the sample detection [28–34].

The accuracy and reliability of the method are crucial in veterinary drugs analysis. In this study, three kinds of SAs with different polarities, SDZ (pKow = 0.34), SMZ (pKow = −0.76), and SDM (pKow = −1.17) (pKow obtained from KowWin software), were selected. The experimental conditions were optimized and discussed thoroughly. The extraction and clean-up methods were optimized. Four kinds of filters were compared. Three quantitative methods, external standard (ES), matrix matching (MM), and isotope dilution mass spectrometry (IDMS), were compared. Matrix effects were evaluated, and the potential influencing factors were discussed. Moreover, the uncertainty of the method was estimated. The developed method was validated for accuracy and precision through the matrix spiked experiment, intra-/interday variation, limits of detection (LOD), limits of quantification (LOQ), linearity, and uncertainties.

2. Materials and Methods

2.1. Materials and Reagents.
The certified reference materials (CRMs) of sulfadiazine (SDZ; GBW (E) 081146), sulfadimidine (SMZ; GBW (E) 081145), and sulfadimethoxine (SDM; GBW (E) 061416) were obtained from the National Institute of Metrology, China (Beijing, China). The isotope standards ($^{13}C_6$-sulfadiazine, $^{13}C_6$-sulfadimidine, and $^{13}C_6$-sulfadimethoxine) were purchased from TRC (Toronto, Canada). Formic acid, methanol, and water (HPLC-MS grade) were purchased from Thermo Fisher Scientific (Waltham, MA, USA). Perchloric acid (analytical grade) was purchased from XiYa chemical reagents company (Shanxi, China). Oasis® HLB SPE cartridges (6 cc, 150 mg) were purchased from Waters (Milford, MA, USA).

Stock solutions were made for individual sulfonamides at the concentration of 1000 μg/kg in methanol and stored away from light at 4°C. For linearity studies, the samples were freshly prepared using appropriate dilution of the stock solution with initial LC mobile phase (methanol-water; 15 : 85; v : v, containing 0.2% formic acid). Standard solutions of three sulfonamides mixture were prepared in the range of 0.1 to 50 μg/kg with isotopic internal standards at 10 μg/kg. Spiked milk samples were prepared at three concentrations of 1, 10, and 20 μg/kg, respectively. All standard solutions were stored in amber glass bottles at 4°C.

2.2. Milk Samples.
Skim and whole-fat milk samples of Yili (China), Arla (Germany), and LVLINB (Austria) were purchased from supermarket. The nutrient contents of milk are shown in Table S1.

2.3. Sample Preparation.
A previously homogenized milk sample (1.00 g) was weighed into a 50 mL centrifuge tube. 10 ng internal standard (100 ng/g working solutions) was added. Then, 25 mL perchloric acid solution (pH = 2) was added to each tube, and the mixture of each tube was vortex-mixed for 1 min and then extracted by ultrasonic for 10 min.

HLB solid-phase extraction cartridge (6 cc, 150 mg) was preconditioned with 5 mL methanol and 5 mL perchloric acid solution (pH = 2) sequentially at a flow rate of 1 mL/min. The extraction solution was gradually loaded to the HLB cartridge. Then, the centrifuge tube was washed with 5 mL perchloric acid solution and the wash solution was also loaded to the cartridge. The cartridge was washed with 5 mL water and then dried under vacuum for 1 min, and the SAs were eluted with 3 mL methanol at a flow rate of 1 mL/min. The elution liquid was evaporated under a gentle nitrogen stream at 40°C until the remaining amount was around 200 μL. The residual liquid was reconstituted with 1 mL methanol-water (15 : 85; v : v, containing 0.2% formic acid), vortex-mixed for 1 min, and filtered through a 0.22 μm PTFE filter into a glass LC vial for LC-MS/MS analysis.

2.4. UHPLC-MS/MS Conditions.
UHPLC-/MS/MS system, which consisted of a LC30AD liquid chromatography (Shimadzu Corp., Japan) and QTRAP 5500 mass spectrometry (SCIEX Corp., CA, America), was used for SAs analysis. The separation of SAs was achieved on an Acquity UPLC CSH™ C18 column (100 × 3.0 mm, 1.7 μm particle size; Waters, USA). A gradient LC elution method was employed by 0.2% formic acid aqueous solution as mobile phase A and acetonitrile (containing 0.2% formic acid) as mobile phase B. The gradient elution was carried out as follows: 15% B maintained for 3 min; increased to 35% B linearly in 2 min and then increased to 100% B in 4 min and maintained for 1 min; changed to 15% B and maintained for 2 min. The injection volume was 5 μL. The flow rate was set at 0.25 mL/min, and the column temperature was set at 38°C.

The QTRAP 5500 mass spectrometer equipped with an electrospray ionization (ESI) source was performed in positive ionization multiple-reaction monitoring (MRM)

mode. The ion source temperature (TEM) was set at 600°C, and ion spray voltage (IS) was set at 5.5 kV. Ion source gas 1 (GS1) and ion source gas 2 (GS2) were used as the drying and nebulizer gases at a back pressure of 60 psi and 65 psi, respectively. Curtain gas (CUR) was 25 psi. N_2 was used for all the gases. Parameters such as declustering potential (DP) and collision energy (CE) for the analyte are shown in Table S2.

2.5. Matrix Effect Estimation.
The ME factors were investigated by comparing the signal intensity and spiked quality of matrix-matched standard solution with that of the standard solution at the same concentrations. If the peak areas and mass obtained in neat solution standards were set as A and m and the corresponding peak areas for standards spiked after extraction into milk extracts as A' and m', the ME factors can be calculated as follows [35]:

$$ME = \frac{A'/m'}{A/m}. \tag{1}$$

ME factor <1 indicated ion suppression effect and ME factor >1 indicated ion enhancement effect.

2.6. Validation of the Method.
The LOD and LOQ were defined as $3 \times$ signal-to-noise ratio (S/N) and $10 \times$ S/N, respectively. To determine the linearity of the method, standard solutions of three sulfonamides mixture were prepared at the concentration of 0.1, 0.5, 1, 10, 20, and 50 μg/kg with isotopic internal standards at the concentration of 10 μg/kg.

To evaluate the recovery and precision, blank milk samples were spiked with three sulfonamides mixture standard solution at three concentrations of 1, 10, and 20 μg/kg, respectively. The precision was evaluated as intraday and interday by measuring the corresponding relative standard deviations (RSDs) at two spiked concentrations (1 μg/kg and 20 μg/kg) on six sequential runs by analyzing six replicates. Intraday precision (the so-called repeatability) was measured on a single day, whereas interday precision was evaluated on six consequent days.

3. Results and Discussion

3.1. Optimization of UHPLC-MS/MS Conditions.
Acquity UPLC CSH™ C18 column (100×3.0 mm, 1.7 μm) and XTerra MS C18 (100×2.1 mm, 3.5 μm) column were compared under the same experimental condition. The results showed that all compounds can be separated on both columns, and the target compounds had shorter retention time on XTerra MS C18 column. All the compounds had higher signal-to-noise ratio values in the Acquity UPLC C18 CSH™ column. Finally, the Acquity UPLC CSH™ C18 column was selected for the experiment.

Methanol and acetonitrile with different concentrations of formic acid (0.1% and 0.2%) were compared, respectively. For methanol and acetonitrile with the same formic acid concentration (0.1% formic acid), the responses of SDZ and SDM were about 20% and 5% higher by using methanol, while the responses of SMZ were similar. The response of

SMZ was about 20% higher on using methanol with 0.2% formic acid than that on using methanol with 0.1% formic acid. Methanol containing 0.2% formic acid was selected for the following experiments, as this condition provided the highest response. The chromatography of 3 SAs is illustrated in Figure S1.

The optimization of parameters can directly affect the sensitivity and accuracy of mass spectrometry. To obtain maximum sensitivity for the identification and detection of the three sulfonamides, compound-dependent parameters such as cone voltage and collision energy were optimized by direct infusion of different standard solutions at 100 μg/kg and at a flow rate of 7 μL/min using the built-in syringe pump directly connected to the interface. Precursor ions and product ions were determined, and the transition with the best sensitivity was selected for quantification, whereas an additional transition was acquired for confirmation (Table S2).

3.2. Optimization of Pretreatment Method.
Based on the national standard method (GB/T 22966-2008), the pretreatment method was improved and optimized. During the experiment, it was found that the filter membrane had a certain effect on the recovery rates of the analytes, so the selection of filter membrane was mainly optimized. This has rarely been discussed in previous studies.

Four kinds of filter membranes, including PTFE (0.45 μm, 25 mm), GHP (0.2 μm, 13 mm), nylon (0.2 μm, 15 mm), and glass fiber (1.0 μm, 15 mm) filters, were chosen to study the adsorption behavior by comparing the absolute recoveries of standard solution. The recovery is shown in Figure 1.

The adsorption of target compounds through PTFE filter was very low, and the recoveries ranged from 98.4% to 100.5%. It was obviously observed that the recovery of SMZ was only 65.7% after filtering through GHP filter; the recoveries of SDZ and SDM were 94.9% and 97.2%, respectively. Nylon filter had apparent adsorption for three SAs, with the recoveries ranging from 72.1% to 89.6%, and glass fiber filter recoveries were between 98.0% and 99.2%. Therefore, the PTFE filter was selected in this study because it has the lowest adsorption for the target compounds.

3.3. Comparison of Quantitation Methods.
The choice of quantitation method had a significant impact on the accuracy of the results. For the three compounds, the quantitation methods were compared using the skimmed milk of Yili under gradient elution conditions as shown in Figure 2. The recoveries by external standard method ranged from 17.8% to 61.2%, which were the lowest of all modes, and the difference between target compounds was large. The external standard method was greatly affected by the matrix, having a serious effect on the accuracy and reliability of the results. Blank sample matrix was applied to compensate for matrix effect by using a matrix matching method. Although the recoveries of matrix matching method ranged from 80.9% to 95.2%, which were better than those of external standard method, the recovery of individual target compound was still unsatisfactory. Besides, the ME factors of different milk
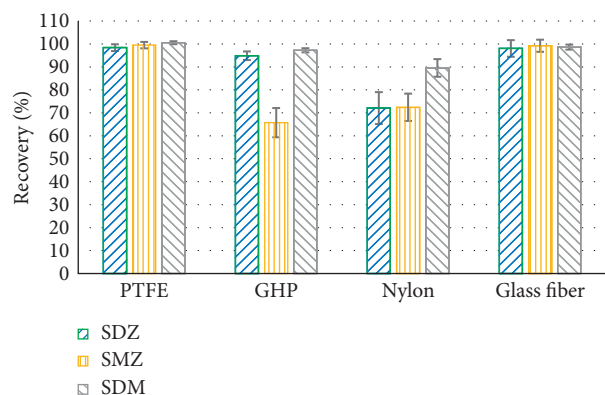
Figure 1: Absolute recoveries of filter after filtration of standard solution ($n = 3$).

Figure 2: The recoveries of compounds in different quantitative modes with gradient elution.

samples might be different, and it was very time-consuming and difficult to obtain the same blank matrix samples. The recoveries of IDMS method ranged from 99.7% to 100.7%. Due to similar physical and chemical properties between the isotope labeled internal standard and the target compound, their behaviors in the process of pretreatment and instrumental analysis were basically consistent, which greatly reduces the interference of the matrix effect. Moreover, the quantitative analysis by IDMS method had the lowest deviation and the best stability among the three methods.

Recoveries of IDMS method were the best under the two isocratic conditions and the gradient elution condition (as shown in Figure S2). Besides, the results of IDMS were similar under the three elution conditions while the recoveries varied by MM and ES, especially ES. The results indicated that IDMS method had a higher accuracy and better stability than MM and ES, leading to an extensive range of application. It was one of the most commonly used methods to detect trace components in complex matrix.

The quantitation methods for six different milk samples of skim and whole-fat milk purchased from local market were also compared. The recoveries of six matrix samples were analyzed by ES, MM, and IDMS, respectively. The results are shown in Table S3. External standard and matrix matching method were used to calculate the recovery, which was very unstable and can be greatly affected by the matrix. The recovery rates of IDMS method ranged from 96.6% to 102.2%, which can effectively reduce the matrix effect, exhibiting a high stability and wide applicability. The results indicated that the IDMS method can provide a stable and reliable method for the detection and analysis of SAs in milk.

3.4. Estimation of Matrix Effects.

Although some interfering components can be eliminated during the extraction, clean-up, and chromatographic separation process, analytical errors and inaccurate results still existed due to the interfering substances in complex matrix. The consequences of matrix effect were the over- or underestimation of the actual concentration of analytes present in samples, affecting both trueness and precision of the analytical method. The methods used to evaluate the matrix effects in LC-MS/MS analysis included postcolumn
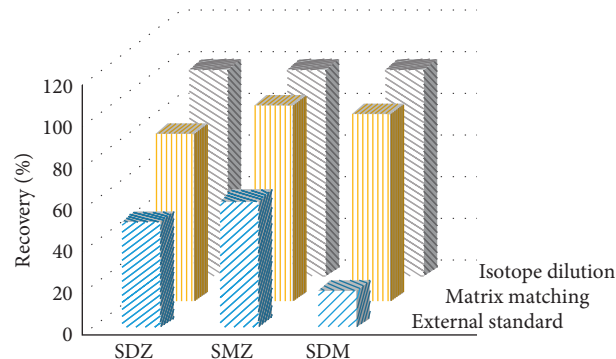
injection and postextraction addition [16–18, 36]. The method of postextraction addition can quantify the matrix effect, and it was widely used in the verification procedure.

First, the matrix effects of analytes in different milk matrix samples were compared (Table 1). The results showed that all compounds showed ion suppression effect in different milk samples. The ME factors for SDZ, SMZ, and SDM were in the following ranges: from 0.63 to 0.87; from 0.64 to 0.73; and from 0.18 to 0.30, respectively. There was a little difference in the matrix effect of different brands of skim-fat milk or whole-fat milk. However, the ME factors of skim-fat milk samples were lower than those of whole-fat milk, which indicated that the ion suppression effects of skim-fat milk were greater. The reason was unclear, and it may be related to the composition content in milk samples.

The ME factors (Yili skim-fat milk) of the target analytes at four liquid chromatography elution conditions were calculated, respectively. As shown in Figure 3, the ME factors of three compounds were lower than 1 under different phase compositions, which indicated ion suppression effect of target compounds in all mobile phase conditions. The ion suppression effects of SDZ and SMZ were lower under gradient condition than isocratic, and the ME factors in isocratic condition of 50% methanol were minimum. With the increase of the methanol composition percent in the mobile phase, the inhibitory effect got stronger, inferring that coeluting components in the matrix (interferents) under high methanol composition may get better atomization effect and higher ionization efficiency. The enhancement of the competitive ion lead to stronger ion suppression effect on the target compounds. Moreover, there may be more coeluting matrix with higher methanol composition.

After the correction by isotope labeled internal standards, the MEs for SDZ, SMZ and SDM were in the following ranges: from 0.937 to 1.001; from 0.973 to 0.999; from 1.006 to 1.021, respectively, indicating that IDMS could compensate for matrix effect to a large content.

3.5. Uncertainty Evaluation.

The uncertainty of the ID-UHPLC-MS/MS analysis was evaluated by the combination of individual uncertainty including purity of SAs CRMs

TABLE 1: The matrix effect factors of the target analytes in six milk samples ($n = 3$).

	Yili		Arla		LVLINB	
	Skim	Whole	Skim	Whole	Skim	Whole
SDZ	0.63	0.81	0.86	0.87	0.83	0.87
SMZ	0.64	0.73	0.67	0.66	0.68	0.70
SDM	0.20	0.24	0.18	0.25	0.18	0.30
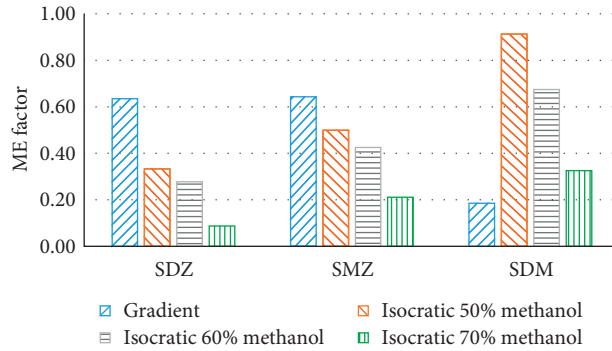
FIGURE 3: The matrix effect factors of the target analytes with four kinds of mobile phase elution conditions ($n = 3$).

($u_{\mathrm{rel,p}}$), balance weighing ($u_{\mathrm{rel,w}}$; including weighing of standards and standard solutions, isotope labeled standards and standard solutions, and milk samples), and the method precision ($u_{\mathrm{rel,rep}}$; $s/\sqrt{n}$).

The uncertainty from balance weighing referred to weights of CRMs of pure SAs and isotope labeled SAs, solvents, standard solutions, milk samples, and isotope labeled SAs solutions. The uncertainty of balance was evaluated as rectangular distribution. The standard uncertainty of balance weighting (u_{b}) is the combination of repeatability and weighting tolerance. The sample weighing is obtained by two times weighing operation, and each weight is an independent observation.

When a different candidate is weighed for the analysis (w_i), the relative uncertainty is determined by formula (2). The uncertainty from balance weighing $u_{\mathrm{rel,w}}$ is calculated by combining all uncertainties from weighing using formula (3):

$$u_{\mathrm{rel,i}} = \frac{u_{\mathrm{b}}}{w_i}, \tag{2}$$

$$u_{\mathrm{rel,i}} = \sqrt{\sum u_{\mathrm{rel,i}}^2}. \tag{3}$$

The uncertainty of method precision was in the range of 0.25%–2.46%. The combined relative standard uncertainty (u) was calculated by formula (4). The expanded relative uncertainties (U) with a coverage factor of 2 ($k = 2$) was calculated by formula (5):

$$u = \sqrt{u_{\mathrm{rel,p}}^2 + u_{\mathrm{rel,w}}^2 + u_{\mathrm{rel,rep}}^2}, \tag{4}$$

$$U = 2 \times u. \tag{5}$$

The individual uncertainty, relative uncertainties, and expanded relative uncertainties of three spiked levels are listed in Table 2. The relative uncertainties of three SAs were

TABLE 2: Estimated individual uncertainty, relative uncertainty (u), and expanded relative uncertainty (U, $k = 2$) of three spiked levels (%).

Spiked levels	Uncertainty	SDZ	SMZ	SDM
1 μg/kg ($n = 6$)	$u_{\mathrm{rel,p}}$	2.01	1.00	1.01
	$u_{\mathrm{rel,w}}$	1.80	1.80	1.80
	$u_{\mathrm{rel,rep}}$	0.99	0.28	1.00
	u	2.87	2.08	2.30
	U	5.75	4.16	4.59
10 μg/kg ($n = 6$)	$u_{\mathrm{rel,p}}$	2.01	1.00	1.01
	$u_{\mathrm{rel,w}}$	0.18	0.18	0.18
	$u_{\mathrm{rel,rep}}$	0.58	0.26	0.17
	u	2.10	1.05	1.04
	U	4.20	2.10	2.08
20 μg/kg ($n = 6$)	$u_{\mathrm{rel,p}}$	2.01	1.00	1.01
	$u_{\mathrm{rel,w}}$	0.09	0.09	0.09
	$u_{\mathrm{rel,rep}}$	0.42	0.10	0.38
	u	2.06	1.01	1.08
	U	4.11	2.02	2.16

in the range of 1.01% to 2.87%; the expanded relative uncertainties were in the range of 2.02% to 5.75%.

3.6. Method Validation.
Table S4 summarizes the calibration equations, linearity, correlation coefficient, LOD, and LOQ with the developed UHPLC-MS/MS method. All studied SAs presented good linearity in a wide range of concentrations from 0.1 μg/kg to 50 μg/kg. Correlation coefficients (R^2) were higher than 0.999, suggesting a good linearity of the method. LOD and LOQ were estimated as $3 \times S/N$ and $10 \times S/N$, respectively. LOD ranged from 0.018 μg/kg to 0.075 μg/kg, while LOQ ranged from 0.029 μg/kg to 0.166 μg/kg. The low LOQ obtained by this method allowed the quantification at concentrations lower than the MRL stipulated in current legislation. Recovery was evaluated at three spiked levels (1 μg/kg, 10 μg/kg, and 20 μg/kg), as shown in Table 3. Six replicates of

TABLE 3: Recoveries of SDZ, SMZ, and SDM in the different spiked levels and the method precisions at two different concentrations combined with LC-MS/MS method of the three sulfonamides from milk samples ($n = 6$).

Compounds	Recovery (%)			Intraday precision RSD (%)		Interday precision RSD (%)	
	1 μg/kg	10 μg/kg	20 μg/kg	1 μg/kg	20 μg/kg	1 μg/kg	20 μg/kg
SDZ	99.2	100.6	96.8	2.43	1.03	0.45	1.02
SMZ	98.2	101.2	100.6	0.69	0.25	0.90	0.87
SDM	100.7	100.9	103.8	2.69	0.74	1.40	1.18

spiked samples at the three concentration levels were prepared. For all compounds, satisfactory recoveries (96.8%–103.8%) were achieved. Intraday and interday precisions were evaluated at 1 μg/kg and 10 μg/kg spiked levels. For all analytes, the repeatability RSDs for intraday precision were within the range of 0.25–2.69% and those of interday precision were less than 1.40%, indicating that the method was accurate and precise. The sensitivity and precision of the three SAs in this method were better than the Ministry of Agriculture Announcement No.781-12-2006 standard [37].

4. Conclusions

An ID-UHPLC-MS/MS method has been developed and validated for the accurate determination of sulfonamides in milk. After solid-phase extraction and filtration, the sample was analyzed by UHPLC-MS/MS system. The matrix effects were evaluated and discussed. The results showed that there were obvious differences in matrix effect with different mobile phases and different milk matrices. IDMS was used for the quantitation since it could effectively reduce the influence of matrix and other factors. The optimized method was fully validated through estimation of recovery, linearity, LOD/LOQ, and intra-/interday reproducibility, exhibiting good sensitivity, accuracy, and precision. The uncertainty estimation indicated that the developed method has proper metrological quality as reference method in not only daily SAs determination but also value assignment of related CRMs.

Data Availability

Data are available in the supplementary information file.

Conflicts of Interest

The authors declare that there are no conflicts of interest regarding the publication of this study.

Acknowledgments

Supplementary Materials

Table S1: nutrients in milk (per 100 mL). Table S2: the optimal parameters of multiple-reaction monitoring of SAs. Table S3: recoveries of different quantitative modes including external standard, matrix matching, and isotope dilution in six milk samples ($n = 3$). Table S4: linearity, LOD, and LOQ of the method. Figure S1: chromatography of three SAs. Figure S2: recoveries of different quantitative analysis modes of three target compounds in different elution conditions. (*Supplementary Materials*)

References

[1] Q. Shen, R. Jin, J. Xue, Y. Lu, and Z. Dai, "Analysis of trace levels of sulfonamides in fish tissue using micro-scale pipette tip-matrix solid-phase dispersion and fast liquid chromatography tandem mass spectrometry," *Food Chemistry*, vol. 194, pp. 508–515, 2016.

[2] L. Wang, B. Yang, X. Zhang, and H. Zheng, "Novel two-dimensional liquid chromatography-tandem mass spectrometry for the analysis of twenty antibiotics residues in dairy products," *Food Analytical Methods*, vol. 10, no. 6, pp. 2001–2010, 2017.

[3] F. L. D. Pontes, J. C. Gasparetto, T. M. G. de Francisco et al., "Development and validation of a multiclass method for the analysis of veterinary drug residues in eggs using liquid chromatography-tandem mass spectrometry," *Food Analytical Methods*, vol. 10, no. 4, pp. 1063–1077, 2017.

[4] Codex Alimentarius Commission, Maximum Residue Limits for Veterinary Drugs in Foods, Updated as at the 35th Session of the Codex Alimentarius Commission, CAC/MRL, 2012, http://www.fao.org/fao-who-codexalimentarius.

[5] L. Jank, M. T. Martins, J. B. Arsand et al., "Liquid chromatography-tandem mass spectrometry multiclass method for 46 antibiotics residues in milk and meat: development and validation," *Food Analytical Methods*, vol. 10, no. 7, pp. 2152–2164, 2017.

[6] Commission Regulation (EU) No. 37/2010 of 22 December 2009, On Pharmacologically Active Substances and Their Classification Regarding Maximum Residue Limits in Foodstuffs of Animal Origin, http://citeseerx.ist.psu.edu/showciting?cid=18868500.

[7] Ministry of Agriculture and Rural Affairs of the People's Republic of China, GB 31650-2019, The Maximum Veterinary Drug Residues in Veterinary Drug Residues.

[8] H.-H. Chung, J.-B. Lee, Y.-H. Chung, and K.-G. Lee, "Analysis of sulfonamide and quinolone antibiotic residues in Korean milk using microbial assays and high performance liquid chromatography," *Food Chemistry*, vol. 113, no. 1, pp. 297–301, 2009.

[9] R. Dez, L. Sarabia, and M. C. Ortiz, "Rapid determination of sulfonamides in milk samples using fluorescence spectroscopy and class modeling with n-way partial least squares," *Analytica Chimica Acta*, vol. 585, pp. 350–360, 2007.

[10] D. V. Yaroshenko and L. A. Kartsova, "Matrix effect and methods for its elimination in bioanalytical methods using

chromatography-mass spectrometry," *Journal of Analytical Chemistry*, vol. 69, no. 4, pp. 311–317, 2014.

[11] C. L. Chitescu, A. I. Nicolau, A. Csuma, and C. Moisoiu, "Simultaneous analysis of four sulfonamides in chicken muscle tissue by HPLC," *Food Additives & Contaminants: Part A*, vol. 28, no. 8, pp. 1013–1020, 2011.

[12] J. Ma, S. Fan, L. Sun, L. He, Y. Zhang, and Q. Li, "Rapid analysis of fifteen sulfonamide residues in pork and fish samples by automated on-line solid phase extraction coupled to liquid chromatography-tandem mass spectrometry," *Food Science and Human Wellness*, vol. 9, no. 4, pp. 363–369, 2020.

[13] C. Nebot, P. Regal, J. M. Miranda, C. Fente, and A. Cepeda, "Rapid method for quantification of nine sulfonamides in bovine milk using HPLC/MS/MS and without using SPE," *Food Chemistry*, vol. 141, no. 3, pp. 2294–2299, 2013.

[14] J. Kang, S.-J. Park, H.-C. Park et al., "Multiresidue screening of veterinary drugs in meat, milk, egg, and fish using liquid chromatography coupled with ion trap time-of-flight mass spectrometry," *Applied Biochemistry and Biotechnology*, vol. 182, no. 2, pp. 635–652, 2017.

[15] P. Kaczyński, "Clean-up and matrix effect in LC-MS/MS analysis of food of plant origin for high polar herbicides," *Food Chemistry*, vol. 230, pp. 524–531, 2017.

[16] Y. Wang, S. Li, F. Zhang et al., "Study of matrix effects for liquid chromatography-electrospray ionization tandem mass spectrometric analysis of 4 aminoglycosides residues in milk," *Journal of Chromatography A*, vol. 1437, pp. 8–14, 2016.

[17] X. Q. Li, Z. Yang, Q. H. Zhang, and H. M. Li, "Evaluation of matrix effect in isotope dilution mass spectrometry based on quantitative analysis of chloramphenicol residues in milk powder," *Analytica Chimica Acta*, vol. 807, pp. 75–83, 2014.

[18] H. Li, J. Wu, C. Chen, W. Xin, and W. Zhang, "Simultaneous determination of 74 pesticide residues in Panax notoginseng by QuEChERS coupled with gas chromatography tandem mass spectrometry," *Food Science and Human Wellness*, vol. 10, no. 2, pp. 241–250, 2021.

[19] P. Svoboda, H. Vlčková, and L. Nováková, "Development and validation of UHPLC-MS/MS method for determination of eight naturally occurring catechin derivatives in various tea samples and the role of matrix effects," *Journal of Pharmaceutical and Biomedical Analysis*, vol. 114, pp. 62–70, 2015.

[20] M. Yadav, V. Trivedi, V. Upadhyay et al., "Comparison of extraction procedures for assessment of matrix effect for selective and reliable determination of atazanavir in human plasma by LC-ESI-MS/MS," *Journal of Chromatography B*, vol. 885-886, pp. 138–149, 2012.

[21] P. Svoboda, D. Sander, K. Plachká, and L. Nováková, "Development of matrix effect-free MISPE-UHPLC-MS/MS method for determination of lovastatin in Pu-erh tea, oyster mushroom, and red yeast rice," *Journal of Pharmaceutical and Biomedical Analysis*, vol. 140, pp. 367–376, 2017.

[22] P. Yang, J. S. Chang, J. W. Wong et al., "Effect of sample dilution on matrix effects in pesticide analysis of several matrices by liquid chromatography-high-resolution mass spectrometry," *Journal of Agricultural and Food Chemistry*, vol. 63, pp. 5169–5177, 2015.

[23] W. X. Zhu, J. Z. Yang, W. Wei, Y.-f. Liu, and S.-s. Zhang, "Simultaneous determination of 13 aminoglycoside residues in foods of animal origin by liquid chromatography-electrospray ionization tandem mass spectrometry with two consecutive solid-phase extraction steps," *Journal of Chromatography A*, vol. 1207, pp. 29–37, 2008.

[24] R. Pascoe, J. P. Foley, and A. I. Gusev, "Reduction in matrix-related signal suppression effects in electrospray ionization mass spectrometry using on-line two-dimensional liquid chromatography," *Analytical Chemistry*, vol. 73, no. 24, pp. 6014–6023, 2001.

[25] C. Ferrer, A. Lozano, A. Agüera, A. J. Girón, and A. R. Fernández-Alba, "Overcoming matrix effects using the dilution approach in multiresidue methods for fruits and vegetables," *Journal of Chromatography A*, vol. 1218, no. 42, pp. 7634–7639, 2011.

[26] W. Guo, G. Li, Y. Yang, C. Yang, L. Si, and J. Huang, "LC-MS/MS analysis of pramipexole in mouse plasma and tissues: elimination of lipid matrix effects using weak cation exchange mode based solid-phase extraction," *Journal of Chromatography B*, vol. 988, pp. 157–165, 2015.

[27] O. González, M. Van Vliet, C. W. N. Damen, F. M. van der Kloet, R. J. Vreeken, and T. Hankemeier, "Matrix effect compensation in small-molecule profiling for an LC-TOF platform using multicomponent postcolumn infusion," *Analytical Chemistry*, vol. 87, no. 12, pp. 5921–5929, 2015.

[28] E. Pagliano, Z. Mester, and J. Meija, "Calibration graphs in isotope dilution mass spectrometry," *Analytica Chimica Acta*, vol. 896, pp. 63–67, 2015.

[29] K. Habler, M. Gotthardt, J. Schüler, and M. Rychlik, "Multi-mycotoxin stable isotope dilution LC-MS/MS method for Fusarium toxins in beer," *Food Chemistry*, vol. 218, pp. 447–454, 2017.

[30] L. Qin, Y.-Y. Zhang, X.-B. Xu et al., "Isotope dilution HPLC-MS/MS for simultaneous quantification of acrylamide and 5-hydroxymethylfurfural (HMF) in thermally processed seafood," *Food Chemistry*, vol. 232, pp. 633–638, 2017.

[31] L. Wang, R. B. Cardenas, and C. Watson, "An isotope dilution ultra high performance liquid chromatography-tandem mass spectrometry method for the simultaneous determination of sugars and humectants in tobacco products," *Journal of Chromatography A*, vol. 1514, pp. 95–102, 2017.

[32] S. Yong, H. Liu, L. Wong et al., "Liquid chromatography-isotope dilution tandem mass spectrometry method for the measurement of urea in human serum and assignment of reference values to external quality assessment samples," *International Journal of Mass Spectrometry*, vol. 414, pp. 87–93, 2017.

[33] T.-T. Feng, J.-H. Wu, X. Liang, M. Du, L. Qin, and X.-B. Xu, "Isotope dilution determination for the trace level of 4(5)-methylimidazole in beverages using dispersive liquid-liquid microextraction coupled with ESI-HPLC-MS/MS," *Food Chemistry*, vol. 245, pp. 687–691, 2018.

[34] Y.-R. Lin, M.-F. Huang, Y.-Y. Wu et al., "Reductive amination derivatization for the quantification of garlic components by isotope dilution analysis," *Food Chemistry*, vol. 230, pp. 1–5, 2017.

[35] J. F. Bienvenu, G. Provencher, P. Bélanger et al., "Standardized procedure for the simultaneous determination of the matrix effect, recovery, process efficiency, and internal standard association," *Analytical Chemistry*, vol. 89, pp. 7560–7568, 2017.

[36] A. Ćirić, H. Prosen, M. Jelikić-Stankov, and P. Đurđević, "Evaluation of matrix effect in determination of some bioflavonoids in al food samples by LC-MS/MS method," *Talanta*, vol. 99, pp. 780–790, 2012.

[37] Ministry of Agriculture and Rural Affairs of the People's Republic of China, Ministry of Agriculture Announcement No.781-12-2006 Standard.

WILEY | Hindawi

Research Article

The Bridge between Screening and Assessment: Establishment and Application of Online Screening Platform for Food Risk Substances

Kang Hu ⬤, Shaoming Jin ⬤, Hong Ding ⬤, and Jin Cao ⬤

National Institutes for Food and Drug Control, Beijing 100050, China

Correspondence should be addressed to Hong Ding; dinghong@nifdc.org.cn and Jin Cao; caojin@nifdc.org.cn

Academic Editor: Wei Chen

In order to improve the risk identification ability of the technical support system of food safety supervision, an online screening platform for food risk substances (hereafter referred to as "platform") was established. The platform aims at the qualitative analysis of unknown compounds and consists of three parts: a standard spectrum library, screening model, and online comparison module. The standard library contains the standard spectra of 527 food risk substances by high-performance liquid chromatography/high-resolution mass spectrometry. The screening comparison algorithm, the core of the screening model, is obtained through the improvement of the existing spectral library search algorithm. The inspector uploads the original spectrum file through the online comparison module; the online comparison module calls the corresponding script to convert the original spectrum file into a standard spectrum file and then uses the screening and comparison algorithm to achieve online real-time comparison. The comparison results are used to determine whether the sample to be tested contains the food risk substances contained in the standard library, so as to realize the preliminary screening of potential food risk substances. The platform supports the spectrogram data format of mainstream instrument manufacturers. The standard spectrogram database can be coconstructed and shared by cooperative laboratories to effectively enrich the types of food risk substances. Through laboratory comparison, data calibration, and model optimization, the screening accuracy of the platform can reach more than 97%. The platform adopts the Internet online screening method, which greatly facilitates the risk investigation and control of national food safety inspection and testing institutions. At the same time, the construction of the screening platform for food risk substances based on high-performance liquid chromatography/high-resolution mass spectrometry, the Internet, big data, and other technologies will provide a new technical means for food safety risk management and control. Hence, it can build a bridge between the screening of risk substances and illegally added substances, as well as risk assessment, risk management, and control.

1. Introduction

With the development of the market economy and the improvement of the country's overall strength, China, the largest food producer and consumer since 2010 has a gradually increasing food quality. But because of the large amount of food consumption and the long food industrial chain, China has witnessed numerous food safety incidents, which have aroused widespread concern in society. The Chinese government has increased the monitoring of food risks through a series of policies and measures and has established a food safety risk management and control mechanism based on source control, process control, and end-product monitoring. In the mechanism, a sampling inspection and risk-screening system have been established at the technical level. This greatly improves the ability of food safety management and control and significantly improves food safety issues [1].

As the basic and supporting technology of food testing, instrumental analysis technology has developed rapidly in recent years. Liquid chromatography (LC) and gas chromatography (GC) have excellent performance in the separation of compounds. In view of the high selectivity and high sensitivity of mass spectrometry (MS) in the qualitative and

quantitative analysis of trace substances, many countries rely on GC–MS and LC–MS [2–4] and other analytical techniques in the detection and screening of food risk substances. LC–MS technology has a wide range of analysis, and it can detect almost all compounds, thus solving the problem that GC cannot analyze thermally unstable compounds. It has a strong ability to separate substances, even if the analyzed mixture is not completely separated. It can also perform qualitative and quantitative analysis through characteristic ion mass chromatograms to obtain the structural information and molecular weight of each component. The detection sensitivity is high, and sample detection at the microgram level is possible. The analysis time is short, and the detection time of a single sample is generally less than 15 minutes, which can significantly shorten the analysis time [5–9]. When using the LC–MS technology to detect and screen food risk substances, in addition to relevant equipment for detection, it also needs to rely on professional screening software that includes compound standard MS databases of compounds and comparison algorithms [10–12]. At present, most of the inspectors in various countries are limited to professional screening software provided by various instrument and equipment manufacturers when carrying out the screening and comparison of food risk substances. The standard MS database contained in this screening software is not only expensive but also unable to cover all of them. Screening procedures for risk substances are cumbersome, and there are various problems such as the high cost of manpower and material resources [13, 14]. In the context of the wide variety of substances at risk for food safety and the lack of professional network sharing databases, the establishment of a universal cross-instrument brand high-performance liquid chromatography/high-resolution mass spectrometry sharing screening software used for quickly screening for risk substances in food has become a major subject of research by food safety regulatory technical support institutions [15–17].

In view of the technical bottlenecks encountered by food inspection agencies in the screening of food risk substances, the relevant team of the National Institutes for Food and Drug Control conducted extensive investigation and research and used integrated technologies such as high-performance liquid chromatography/high-resolution mass spectrometry, the Internet, and big data [18, 19]. It finally established a food risk substance screening platform for food inspectors across the country, which has been officially launched. The platform refers to the European Union's analytical method guidelines [20], which aim to qualitatively analyze unknown compounds in mass spectrometry files from different instrument manufacturers. When carrying out the screening of food risk substances, the inspectors preprocess the relevant food samples according to the screening preprocessing technical standards researched and formulated by the National Institutes for Food and Drug Control. High-performance liquid chromatography/high-resolution mass spectrometry is then used to perform the detection. After testing, the generated data files are uploaded to the online comparison module of the screening platform through the Internet. The online comparison module calls the screening model for real-time analysis and comparison and then sends back the screening results to the inspectors. The inspectors refer to the screening results and combine other information to make comprehensive judgments to complete the preliminary screening of risky substances.

The platform can automatically identify the original mass spectrometry files of instruments from various brand manufacturers and perform a unified data format conversion; hence, there is no restriction on the brand and version of the instrument. The standard library of the platform can be jointly built and shared by cooperating laboratories, which can effectively enrich the types of food risk substances in the database and has good scalability. The screening model of the platform is based on the SS combination algorithm, and the algorithm has been optimized and improved through a large number of screening comparison experiments, which effectively guarantee the accuracy and scientific nature of the screening results given by the platform. The platform adopts the Internet online screening method, which is more efficient than the traditional risk-screening work mode and can greatly facilitate the risk investigation and control work of food safety inspection agencies.

2. Materials and Methods

The platform consists of three parts: a standard spectrum library, screening model, and online result comparison module. The standard spectrum library serves as the underlying basic database for risk screening. The screening model is used for screening and comparing the risk substances. The online result comparison module allows users to upload spectrometry files and obtain screening results in real time. Java language is used in the page development of the platform, and the mainstream technologies such as SpringBoot (https://spring.io/projects/spring-boot) and jQuery (https://jquery.com/) are applied. The underlying model is developed through Python, mainly using third-party libraries such as pymzML and Pandas [21].

2.1. Standard Spectrum Library. The platform builds a standard spectrum library based on high-resolution MS data for 527 banned and restricted compounds found in food matrixes [22, 23]. At present, the spectrum library mainly integrates the standard spectral data of Agilent brand instruments, which mainly covers the mass-to-charge ratio of the parent ion and the mass-to-charge ratio of the first 15 second-order fragment ions, as well as the corresponding relative peak intensity, retention time, and some basic information of the compounds. The content of the high-resolution spectrum library with methomyl used as an example is shown in Table 1.

2.2. Screening Model. The screening model is the core of the whole platform, and the screening comparison algorithm is the core of the screening model, which is obtained by improving the existing spectral library search algorithm, specifically, SS combination algorithm. The SS combination algorithm, proposed by Stein and Scott, includes the cosine

TABLE 1: Content of a high-resolution spectrum library (example).

Name of compound in Chinese	Mieduowei	Retention time (° min)	4.52
Name of compound in English	Methomyl	Mass-to-charge ratio of parent ion	163.05357
Chemical formula	$C_5H_{10}N_2O_2S$	Adduct type	$[M + H]+$
Mass	162.04635	Collisional energy(°V)	40
CAS no.	16752-77-5	Polarity	Positive
Mass-to-charge ratio 1 of fragment ions	72.99807	Relative peak intensity 1	100
Mass-to-charge ratio 2 of fragment ions	46.99500	Relative peak intensity 2	49.03175
Mass-to-charge ratio 3 of fragment ions	58.02874	Relative peak intensity 3	47.68800
Mass-to-charge ratio 4 of fragment ions	44.97935	Relative peak intensity 4	35.73670
Mass-to-charge ratio 5 of fragment ions	71.99025	Relative peak intensity 5	33.51392
Mass-to-charge ratio 6 of fragment ions	42.03383	Relative peak intensity 6	24.29776
Mass-to-charge ratio 7 of fragment ions	56.04948	Relative peak intensity 7	16.21830
Mass-to-charge ratio 8 of fragment ions	88.02155	Relative peak intensity 8	6.12826
Mass-to-charge ratio 9 of fragment ions	31.01784	Relative peak intensity 9	3.93581
Mass-to-charge ratio 10 of fragment ions	61.01065	Relative peak intensity 10	3.00822
Mass-to-charge ratio 11 of fragment ions	58.99500	Relative peak intensity 11	2.85382
Mass-to-charge ratio 12 of fragment ions	45.98717	Relative peak intensity 12	2.27873
Mass-to-charge ratio 13 of fragment ions	73.07603	Relative peak intensity 13	1.48801
Mass-to-charge ratio 14 of fragment ions	49.01065	Relative peak intensity 14	1.24759
Mass-to-charge ratio 15 of fragment ions	65.00556	Relative peak intensity 15	1.11706

similarity algorithm [24] (also called the weighted dot-product algorithm), represented here as SC (Uw, Vw), and the peak ratio algorithm, represented here as SD (Uw, Vw) [25, 26]. The calculation formula of the cosine similarity algorithm is expressed as follows:

$$S_C U^\omega, V^\omega = \frac{U^\omega \cdot V^\omega}{\|U^\omega\| \cdot \|V^\omega\|}, \tag{1}$$

where V represents the compound in the library, U represents the unknown compound, ω is the mass-to-charge ratio and peak intensity information, and U and V are the matrix form of ω. ω is obtained by multiplying the mass-to-charge ratio and relative peak intensity of the compound by taking the exponent of a weighting factor. The calculation formula of ω is expressed as follows:

$$\omega_q^n = (\alpha^n)^x (\beta^n)^y, \quad n = 1, 2, \ldots, q, \tag{2}$$

where $x = 1.3$ and $y = 0.53$ are weighting factors. α and β refer to the mass-to-charge ratio and relative peak intensity, respectively. The calculation formula of the peak ratio algorithm is expressed as follows:

$$S_D (U^\omega, V^\omega) = \frac{\sum_i^{N_{Q\cap R}} ((u_i/u_{i-1})(v_{i-1}/v_i))^n}{N_{Q\cap R}}, \tag{3}$$

where u_i and v_i are nonzero peaks with the same mass-to-charge ratio. When the peak value of the former is smaller than the latter, $n = 1$; otherwise, $n = -1$. Finally, the SC and SD are, respectively, multiplied by the corresponding weights and then combined to calculate the final similarity. The calculation formula is as follows:

$$S_{SS}(U^\omega, V^\omega) = \frac{N_R S_C(U^\omega, V^\omega) + N_{Q\cap R} S_D(U^\omega, V^\omega)}{N_R + N_{Q\cap R}}. \tag{4}$$

Compared with the SS combination algorithm proposed by Stein and Scott, the improved combination algorithm has a larger difference in the strength of the same mass-to-charge ratio of the different spectra when the similarity of the mass spectra is low. In this case, the peak ratio calculation is preferred. When the degree of similarity is high, the number of the same mass-to-charge ratio increases, and the gap between the corresponding intensities of the same mass-to-charge ratio decreases. In this case, the cosine similarity calculation is preferred to further improve the similarity between the mass spectra. The premise of similarity calculation is to determine whether the parent ion is the same as the parent ion of the compounds in the standard spectral library. If the error of the parent ion is within 2 mDa, then it is considered the same. It is necessary to further compare the fragment ions and calculate the similarity and then combine with the relative retention time difference to select the best matching result with higher similarity and lower relative retention time difference. If considered as different, the mass spectrum is ruled out directly and no subsequent calculation would be performed.

2.3. Online Result Comparison Module. The online result comparison module is developed and constructed using web technology. The front end uses the components including jQuery, Echarts, ayUI, and JSmol, and the back end uses frameworks [27, 28] including SpringBoot, SpringMVC, SpringSecurity, and Mybatis (http://blog.mybatis.org/). The module includes the pages such as file uploading (shown in Figure 1), a summary of screening results (Figures 2 and 3), a detailed comparison of screening results (shown in Figures 4–6), and a basic information display of compounds (Figure 7). Its main function is to upload the mass spectrometry file to be screened, call the background screening model for comparison, and return the screening comparison results through the web page in real time. After the inspectors upload the file, the platform will call the data standardization software to convert the uploaded MS file

Library name: Pesticide and Veterinary Drug Residue Database
Tips:
(1). In order to make the matching results more scientific and have a higher accuracy rate, you can perform experiments under the same conditions according to the experimental conditions of the data acquisition in the library, and then upload the acquired data for analysis.
(2). If the experimental conditions of the data you upload are inconsistent with the given, it will have a certain impact on the accuracy of the results.

Figure 1: File upload page. The file upload page contains the library name and tips.

unknown compound	Precursor Ion	Retention Time (min) of the unknown	name of matched compound	CAS NO.
unknown:1	331.226230	7.737	17α-Hydroxyprogesterone	68-96-2
unknown:2	427.149780	3.381	4-Epianhydrotetracycline hydrochloride	4465-65-0
unknown:2	427.149780	3.381	Anhydrotetracycline hydrochloride	13803-65-1
unknown:3	521.230000	10.152	Alclometasone dipropionate	66734-13-2
unknown:3	521.230000	10.152	Beclomethasone dipropionate	5534-09-8
unknown:4	311.200240	8.243	Altrenogest	850-52-2

Figure 2: Screening results summary page (part 1). The page contains part of the information of the compound matched by the unknown object according to the algorithm.

score	Retention Time (min) of the matched	Retention Time difference	remark
0.78921	7.65	0.087	None
0.99977	3.27	0.111	None
0.91830	3.91	0.529	None
0.99191	10.11	0.042	None
0.54687	11.22	1.068	None
0.96668	8.13	0.113	None

Figure 3: Screening results summary page (part 2).

into a standard format file in mzML format. The data standardization software ProteoWizard [29] supports data standardization for mass spectrometry files generated by mainstream mass spectrometer manufacturers [14]. Thus, the construction and application of the platform are not limited by specific brand instruments. After the spectrometry file conversion is completed, the system calls Python's pymzML library to parse the mzML format file and reads the information of the parent ions and their corresponding fragment ions, such as peak intensity, retention time, and high-resolution accurate mass-to-charge ratio. It then calls the screening model to compare the unknown spectrum with the standard spectrum library. It should be noted that when preparing the data, the inspectors should preprocess the sample according to the specific standard procedures and confirm that the high-resolution LC/MS instrument used has been calibrated with good performance. They should also follow the recommended instrument method to collect data.

The online result comparison module realizes the interaction between the user and the server through the file stream and the data stream. The user uploads the test files through the file stream. Since most of the test files uploaded are large, the platform adopts Conris Ultra-High-Speed
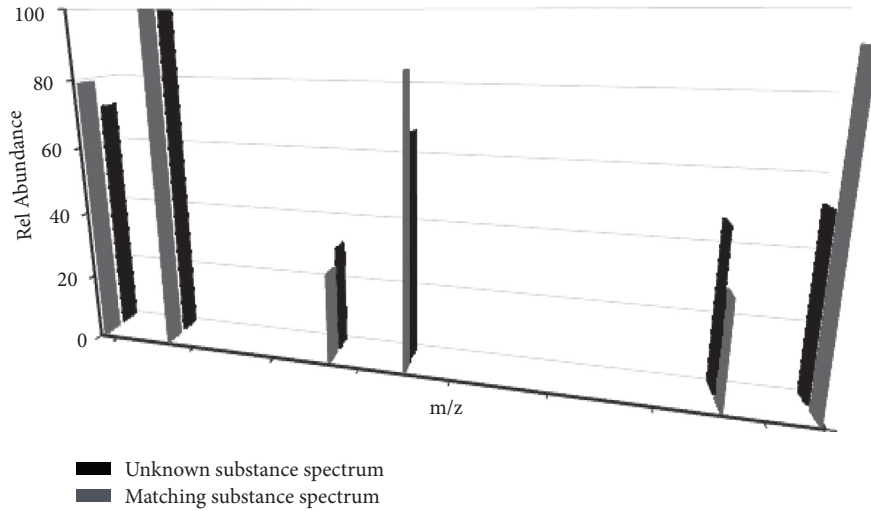
FIGURE 4: Detailed comparison page of screening results (3D histogram). In the 3D histogram, the *x*-axis represents m/z, the *y*-axis represents the matched substance and the unknown substance, and the *z*-axis represents the relative peak intensity.
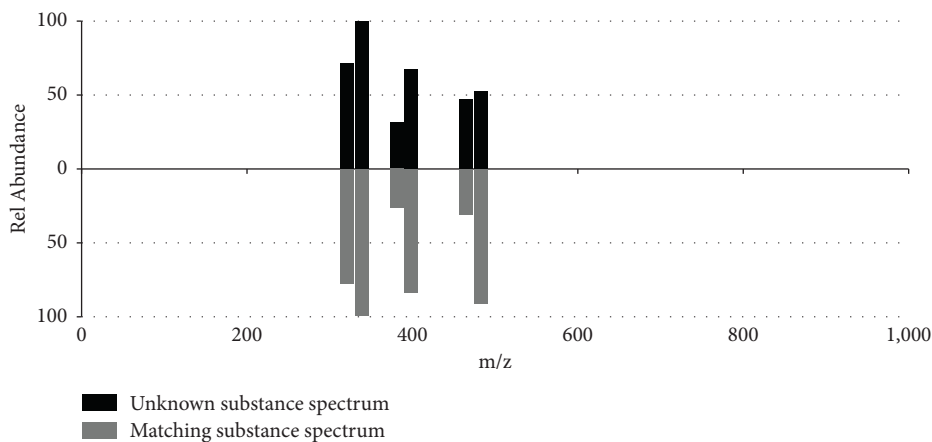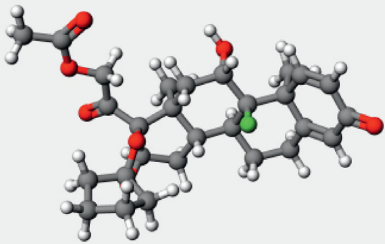
FIGURE 5: Detailed comparison page of the screening results (2D bar chart). In the 2D bar graph, the abscissa, ordinate, and upper half and lower halves of the graph, respectively, represent the m/z ratio, relative peak intensity, unknown substances, and matched substances.

Transfer Protocol [30] instead of the traditional FTP transfer protocol in order to improve the upload speed and greatly improves the speed of file upload. After a series of operations such as file conversion, data analysis, result sorting, and result display, the screening platform renders the screening results via various graphics in the form of data flow on the basic information display page for users to read. On the basis of the screening results, the user can determine whether the test files contain risk substances and accordingly make the preliminary determination whether the tested food is qualified.
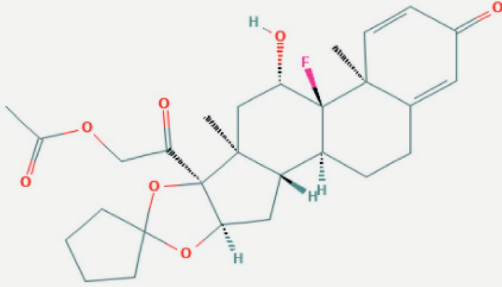
Each piece of information displayed on the screening results summary page includes the precursor ion, molecular formula, CAS number, and retention time of the unknown compound and the matched compound in the standard library. In the screening results, there may be a situation in which an unknown compound matches multiple compounds in the standard library. The inspector can

preliminarily judge the most likely compound based on the matching score and the retention time difference between the unknown and the matched compounds. The detailed comparison page of the screening results displays the 2D bar chart of comparison and 3D bar chart of comparison of the unknown and the matched compounds. The inspector can visually observe the similarities and differences between the two. Through viewing diagrams of 2D and 3D molecular geometry and basic compound information (including the relevant physical and chemical properties of the matched compound and various information such as inspection standards and methods) of the matched compound, the inspector can have an intuitive and detailed understanding of the matched compound. According to the information displayed on the platform, the inspector can preliminarily judge whether the tested sample contains risky substances, which can guide subsequent experiments to obtain scientific judgment results more quickly.

Retention Time (min) of the unknown	name of matched compound	score	Retention time(min) of the matched	Retention Time difference	remark
10.079	Amcinonide	0.98491	10.04	-0.039	

Figure 6: Detailed comparison page of screening results (molecular structure diagram). (a) 3D conformer. (b) 2D structure.

Basic Information   Testing standard   Domestic standards   Overseas standards   Spectrogram   Comparison of national limits

Ansinaide

Chinese common name	Ansinaide
English common name	Amcinonide
CAS code	51022-69-6
English chemical name	(11β, 16α)-21-(Acetyloxy)-16,17-[cyclopentylidenebis(oxy)]-9-fluoro-11-hydroxypregna-1,4-diene-3,20-dione
Chinese chemical name	Data collection
Molecular formula	C28H35FO7
Molecular weight	502.5744
Character description	White to light yellow powder
LD50/LC50	Data collection
toxicity	Skin corrosion/irritation category 2; serious eye damage/eye irritation category 2; specific target organ toxicity single exposure category 3; reproductive toxicity category 2
category	Hormones (glucocorticoids)

Figure 7: Compound basic information display page.

3. Results and Discussion

3.1. Model Validation. The platform uses a series of comparison methods to evaluate the screening model and then optimizes and adjusts the model based on the evaluation results. The comparison method screens the test files to be screened via the platform and the professional screening software of the corresponding manufacturer, compares the screening results, and then calculates the accuracy of the screening model. The calculation formula is as follows:

TABLE 2: High-resolution screening results.

Test file no.	Number of compounds correctly screened by Agilent professional screening software	Number of compounds screened before platform adjustment	Number of items correctly screened after platform adjustment	Accuracy of final screening results (%)
1	16	13	14	
2	36	32	34	
3	40	38	38	
4	50	47	48	97.29
5	62	62	62	
6	64	63	63	
7	65	65	65	
8	73	70	71	

$$\text{accuracy of screening model} = \frac{\text{number of compounds screened} \in \text{the platform}}{\text{number of compounds screened} \in \text{professional}}. \tag{5}$$
$$\text{screening software of manufacturer}$$

After the first model was constructed, eight test files with high resolution were uploaded to the platform for comparison. The screening results revealed the following: first, there were false-negative results in the screening results, namely, the compounds contained in the test files were not included in the screening results and, second, the isomers were not completely distinguished.

3.2. Model Optimization. To solve these problems, the research team optimized the model according to three technical directions: first, the number of selected spectra was reduced. Because each test file contained thousands of spectra, the more the spectra were selected initially, the more the screening results were obtained later, and the more difficult it was to select the best-matched results. The efficiency of the screening model would be greatly reduced if all the spectra were analyzed. Therefore, measures were taken to reduce the number of spectra corresponding to each parent ion selected from the test files for optimization. Specifically, the total energy of the spectra was sorted, and the spectrum with higher energy was selected for analysis. Before the model optimization, 30 spectra at most could be selected for one parent ion, but now 20 spectra at most are selected for one parent ion. Second, we took into consideration the similarity and retention time difference (the difference between the retention time of the mass spectrum and that of the compared compound in the standard spectrum library) to optimize the model to avoid the deviation of a single factor. Third, we increased the matching number of secondary fragment ions. According to the EU analytical method guidelines, if two compounds have the same precursor ion and have at least one same secondary fragment ion, then it can be determined that the two compounds are most likely to be the same compound. However, the limited number of the same fragment ions can affect the accuracy of model screening, and some isomers can produce the same fragment ions [31, 32]. The isomers can be distinguished effectively by taking the method that at least two secondary

fragment ions are the same under the premise of the same parent ion.

3.3. Model Revalidation. After the team optimized the model, they verified the screening model again. They uploaded the previous eight high-resolution test files for screening comparison. Screening results show that the proportion of compounds successfully identified by the model increased to 97.29%. The comparison of the two screening results is shown in Table 2.

4. Conclusion

The platform established in this paper has become stabilized after several times of model optimizing and testing. Currently, the first phase of the platform construction has been basically completed, and the platform has entered into small-scale trials. The present trials show that, by using this database, more than 300 banned and restricted compounds have been discovered in the actual food samples of daily monitoring and inspection. The platform has shown higher screening and identification for unknown compounds. It will continue to increase the standard spectrum library data of compounds; further expand the scope of screening; and continue to promote coconstruction, sharing, and verification through cooperative laboratories.

The construction of a food risk substance screening platform based on high-performance liquid chromatography/high-resolution mass spectrometry, the Internet, big data, and other technologies provides a new technical means for food safety risk management and control. It also builds a bridge between screening and risk assessment of risk substances and illegally added substances. It facilitates the full-chain online risk screening of food production and circulation, and it provides solid technical support for the intelligent supervision and inspection of food safety. It is reasonable to expect that this technology platform has a wider application prospect.

It is a new exploration to combine computer technology and spectrogram technology to create an online spectrogram real-time screening and comparison platform that is not subject to the limit of the instrument brand. It can be carried out not only in the food industry but also in various industries such as cosmetics, chemical industry, and environment industry to establish online spectrogram screening and comparison systems for all related industries to serve the industry risk management and control.

Data Availability

The data used to support the findings of this study are available from the corresponding author upon request.

Conflicts of Interest

The authors declare that there are no conflicts of interest regarding the publication of this paper.

Acknowledgments

References

[1] W. Xudong, *Take the Road of Food Safety Management with Chinese Characteristics*, China Food and Drug Website, Beijing, China, 2020.

[2] T. Wanli, Y. Shoufu, and D. Ming, "Determination of 11 pesticide residues in meat and meat products by solid phase extraction-gas chromatography tandem mass spectrometry," *Journal of Food Safety and Quality Testing*, vol. 11, no. 24, pp. 9124–9129, 2020.

[3] J. Yang, X. Wu, L. Hou, X. Zhang, L. Zhong, and L. Canxin, "Determination of 9 cholesterol oxides in food by gas chromatography-mass spectrometry," *Food Industry*, vol. 41, no. 12, pp. 301–304, 2020.

[4] A. Desmarchelier, T. Bessaire, M.-C. Savoy et al., "Screening of 154 veterinary Drug residues in foods of animal origin using LC-MS/MS: first action 2020.04," *Journal of AOAC International*, vol. 104, no. 3, pp. 650–681, 2021.

[5] R. Helmus, T. L. Ter Laak, A. P. van Wezel, P. de Voogt, and E. L. Schymanski, "patRoon: open source software platform for environmental mass spectrometry based non-target screening," *Journal of Cheminformatics*, vol. 13, no. 1, p. 10, 2021.

[6] J. Wei, R. Zhang, L. Shi, C. Dai, X. Xu, and X. Chu, "Research progress of analytical methods for screening exogenous risk substances in milk and dairy products based on two-dimensional chromatography and its combination technology," *Food Industry Science and Technology*, vol. 39, no. 23, pp. 339–345, 2018.

[7] J. Liigand, W. Tingting, J. Kellogg, J. Smedsgaard, and N. Cech, "Quantification for non-targeted LC/MS screening without standard substances," *Scientific Reports*, vol. 51, no. 6, pp. 2–4, 2020.

[8] J. Ma, S. Fan, L. Sun, L. He, Y. Zhang, and Q. Li, "Rapid analysis of fifteen sulfonamide residues in pork and fish samples by automated on-line solid phase extraction coupled to liquid chromatography-tandem mass spectrometry," *Food Science and Human Wellness*, vol. 9, no. 4, pp. 363–369, 2020.

[9] V. Parthasarathy and T. V. A. Kumar, "Screening of potential GCMS derived antimigraine compound from the leaves of Abrus precatorius Linn to target "calcitonin gene related peptide" receptor using in silico analysis," *Food Science and Human Wellness*, vol. 8, no. 1, pp. 34–39, 2019.

[10] H. R. Zhou, "Analysis on the problems and effective solutions of food sampling inspection at the grassroots level in China," *Food Industry*, vol. 2, p. 97, 2021.

[11] X. Wang, T. Shu, and Z. Ma, "Discussion on risk identification and prevention and control measures of food safety sampling inspection," *China Inspection and Test*, vol. 27, no. 6, pp. 56-57+66, 2019.

[12] L. S. Kato and C. A. Conte-Junior, "Safety of plastic food packaging: the challenges about non-intentionally added substances (NIAS) discovery, identification and risk assessment," *Polymers*, vol. 13, no. 13, pp. 6–9, 2021.

[13] L. Bengtström, A. K. Rosenmai, X. Trier et al., "Non-targeted screening for contaminants in paper and board food-contact materials using effect-directed analysis and accurate mass spectrometry," *Food Additives & Contaminants. Part A, Chemistry, Analysis, Control, Exposure & Risk Assessment*, vol. 33, no. 6, pp. 1080–1093, 2016.

[14] V. Heizhenzhen, *Application of Rapid Screening of Risk Substances in Food Safety Testing*, China Institute for Food and Drug Control, Beijing, China, 2019.

[15] J. Hollender, B. van Bavel, V. Dulio, and E. Farmen, "High resolution mass spectrometry-based non-target screening can support regulatory environmental monitoring and chemicals management," *Environmental Sciences Europe*, vol. 31, pp. 4–9, 2019.

[16] E. L. Schymanski, A. J. Williams, and J. Hollender, "Identifying complex mixtures in the environment with cheminformatics and non-targeted high resolution mass spectrometry," in *Proceedings of the SETAC FTM*, vol. 10, no. 5, pp. 11–13, Denver, CO, USA, September 2017.

[17] W. Wei, X. Xuyang, S. W. Lin, C. J. Dai, X. Xiuli, and X. Chu, "Application of high resolution mass spectrometry in screening and analysis of exogenous risk substances in dairy products," *Modern Food Technology*, vol. 34, no. 8, pp. 246–254+89, 2018.

[18] X. Xingguo, "Analysis of big data in food safety testing," *Food Safety Guide*, vol. 31, pp. 72-73, 2020.

[19] O. Horlacher, F. Lisacek, and M. Müller, "Mining large scale tandem mass spectrometry data for protein modifications using spectral libraries," *Journal of Proteome Research*, vol. 15, no. 3, pp. 721–731, 2016.

[20] European Commission Health & Consumer Protection Directorate-General, *Guidance Document on Analytical Quality Control and Validation Procedures for Pesticide, Residues Analysis in Food and Feed*, SANCO/12571/2013, European Commission Health & Consumer Protection Directorate-General, Ispra, Italy, 2013.

[21] Y. Zhou, "Implementation of general software platform for automatic test system based on Python language," *Electronic Design Engineering*, vol. 27, no. 5, pp. 81–85, 2019.

[22] A. M. Knolhoff and T. R. Croley, "Non-targeted screening approaches for contaminants and adulterants in food using liquid chromatography hyphenated to high resolution mass spectrometry," *Journal of Chromatography A*, vol. 1428, pp. 5-6, 2015.

[23] A. C. Chiaia-Hernández, B. F. Günthardt, M. P. Frey, and J. Hollender, "Unravelling contaminants in the anthropocene

using statistical analysis of liquid chromatography-high-resolution mass spectrometry nontarget screening data recorded in lake sediments," *Environmental Science & Technology*, vol. 51, no. 21, pp. 12547–12556, 2017.

[24] L. Hamers, Y. Hemeryck, G. Herweyers et al., "Similarity measures in scientometric research: the Jaccard index versus Salton's cosine formula," *Information Processing & Management*, vol. 25, no. 3, pp. 315–318, 1989.

[25] X. Xia, *Research on Improved C4.5 Algorithm Based on Cosine Similarity and Weighted Pruning Strategy*, Qingdao University of Science and Technology, Qingdao, China, 2017.

[26] Q. Zhu, J. Yu, and R. Zhang, "Improved spectral database retrieval algorithm based on combinatorial algorithm," *Acta Mass Spectrometry*, vol. 39, no. 3, pp. 337–341, 2018.

[27] Q. Chen and J. He, "Application analysis of Vue + springboot + mybatis technology," *Computer Programming Skills and Maintenance*, vol. 1, pp. 14-15+28, 2020.

[28] C. Wei and X. Ji, "Design of visual data display platform based on springmvc + ecarts," in *Proceedings of the 34th China (Tianjin) 2020 'IT, Network, Information Technology, Electronics, Instrumentation Innovation Academic Conference*, Tianjin, China, January 2021.

[29] R. Adusumilli and P. Mallick, "Data conversion with ProteoWizard msConvert," *Methods in Molecular Biology*, vol. 1550, pp. 339–368, 2017.

[30] M. Wang, *Research on Routing Protocol of Ultra-high-speed Wireless Personal Area Network*, Chongqing University of Posts and Telecommunications, Chongqing, China, 2016.

[31] B. Till, B. Johannes, N. Anna, M. Specht, M. Hippler, and C. Fufezan, "pymzML-Python module for high-throughput bioinformatics on mass spectrometry data," *Bioinformatics*, vol. 28, no. 7, pp. 1052-1053, 2012.

[32] X. Sun, "Study on detection methods of four isomers of butene," *Modern Chemical Engineering*, vol. 39, no. 5, pp. 237–239, 2019.

WILEY | Hindawi

Research Article

Multielement Principal Component Analysis and Origin Traceability of Rice Based on ICP-MS/MS

Yan Wang ⓘ**, Xiaoxuan Yuan** ⓘ**, Linan Liu** ⓘ**, Junmei Ma** ⓘ**, Sufang Fan** ⓘ**, Yan Zhang** ⓘ**, and Qiang Li** ⓘ

Hebei Food Safety Key Laboratory, Hebei Food Inspection and Research Institute, Shijiazhuang 050000, China

Correspondence should be addressed to Yan Zhang; snowwinglv@126.com and Qiang Li; liqiang@nepp.com.cn

In this experiment, inductively coupled plasma tandem mass spectrometry (ICP-MS/MS) was used to determine the content of 30 elements in rice from six places of production and to explore the relationship between the multielement content in rice and the producing area. The contents of Ca, P, S, Zn, Cu, Fe, Mn, K, Mg, Na, Ge, Sb, Ba, Ti, V, Se, As, Sr, Mo, Ni, Co, Cr, Al, Li, Cs, Pb, Cd, B, In, and Sn in rice were determined by ICP-MS/MS in the SQ and MS/MS mode. By passing H_2, O_2, He, and NH_3/He reaction gas into the ICP-MS/MS, respectively, the interference was eliminated by means of in situ mass spectrometry and mass transfer. The detection limit of each element was 0.0000662–0.144 mg/kg, and the limit of quantification was in the range of 0.000221–0.479 mg/kg, the linear correlation coefficient was greater or equal to 0.9987 ($R^2 \geq 0.9987$), and the detection results had low detection limit and great linear regression. Recovery of the method was in the range of 80.6% to 110.5% with spike levels of 0.10–100.00 mg/kg, and relative standard deviations were lower than 10%. For the multielement content of rice from different producing areas, the principal component factor analysis can get six principal component factors, 87.878% cumulative contribution rate, and the distribution of the principal component scores of each element and different producing areas. Based on the multielement content and cluster analysis, the samples were accurately divided into two major categories and six subcategories according to the places of production, which proved that there was a significant correlation between the multielement content in rice and the place of production, so that the place of rice origin can be traced.

1. Introduction

Rice is the main staple food of our country, which contains sugar, protein, fat and dietary fiber, and other main nutrition elements and also contains a lot of necessary trace elements, such as Ca, Fe, Zn, Se, and other mineral elements [1]. Heavy and toxic metals, especially As and Cd, present due to environmental pollution are taken up by the rice plant [2–5]. In China, rice varieties are rich and diverse, with large planting area span and large quality difference. China is a vast country with diverse climatic and geographical conditions, and the crops have different biological characteristics and physical and chemical indexes. Therefore, it is valuable to analyze and compare the differences of multielement contents in rice from south to north China and to provide theoretical basis and technical support for distinguishing rice from different places of origin.

At present, the origin traceability indexes in food mainly include stable isotope [6–11], multielement composition [12, 13], characteristic content of organic component [14, 15], DNA fingerprint [16], and near-infrared spectrum [17–21]. There are some common problems in multielement analysis, such as few element types, high detection limit of low content elements, and unquantifiable trace elements. The determination methods of poly element contents in rice include an electrochemical method, atomic absorption spectroscopy (AAS) [22], atomic fluorescence spectrometry (AFS) [23], inductively coupled plasma optical emission spectrometer (ICP-OES) [24], and inductively coupled plasma mass spectrometry (ICP-MS) [25, 26]. However, there are some common problems in these methods, which hamper the rapid determination of trace elements in rice, thus causing the reduction of the accuracy of traceability of multielement composition in rice. The advantage of the ICP-

MS/MS method is to reduce elemental interference [27]. Alexander Simpson et al. [28]. found that by using ICP-MS/MS and NH$_3$ reagent gas, isotope interference can be reduced and the sensitivity of ^{176}Lu and ^{176}Yb can be improved. In terms of multielement determination, ICP-MS/MS has higher accuracy and greater diversity of elements than ICP-MS [29]. Among them, when measuring P, S, Sr, and other specific elements, O$_2$ and other reaction gases were used to accurately determine the element content by mass transfer [30, 31]. The advantage of the ICP-MS/MS method lies in the determination of ultratrace elements [32]. It can reduce the detection limit, which cannot be achieved by general ICP-MS and other detection methods.

In this paper, ICP-MS/MS was first used to determine the 30 elements' contents in rice from six rice-production areas in Anhui, Guangxi, Guangdong, Jilin, Heilongjiang, and Inner Mongolia. Under SQ and MS/MS models [33], He, NH$_3$/He [34], O$_2$ [35], and H$_2$ [36] were selected as reactive gases for different elements to eliminate mass spectrum interference and reduce detection limit, and the relationship between the element content and the origin was studied by principal component analysis and cluster analysis, which provides technical support for quality control and origin traceability of rice.

2. Materials and Methods

2.1. Reagents and Solutions. Li, Na, Mg, Al, B, P, S, K, Ca, Ti, V, Cr, Mn, Fe, Co, Ni, Cu, Zn, Ge, As, Se, Sr, Mo, Cd, In, Sn, Sb, Cs, Ba, Pb, Sc, Bi, Rh, and Y element standard solution (1000 μg/mL, Guobiao Testing & Certification Co., Ltd., Beijing, China), GBW0043, GBW10044, and GBW10045 Rice reference materials (Institute of Geophysical and Geochemical Exploration IGGE, Langfang, China), 65% BV-III grade of HNO$_3$ (Beijing Institute of Chemical Reagents, Beijing, China), 30% H$_2$O$_2$ (Sinopharm Chemical Reagent Co., Ltd., Beijing, China), and deionized water (18.2 MΩ/cm), prepared by using the Milli-Q system (Millipore, Bedford, MA), were used.

2.2. Sample Collection and Preparation. The samples were collected from six rice-producing areas in Anhui Province, Guangxi Province, Guangdong Province, Jilin Province, Heilongjiang Province, and Inner Mongolia. We purchased common local rice samples with large planting areas in each rice market, a total of 18 batches. Three independent packages were purchased for each batch, and mixed samples were taken to ensure uniformity. The rice samples of each batch were hulled, ground, crushed, and stored in a sealed, low-temperature, and dark place.

In a PTFE digestion tank, each rice sample which weighs 0.3–0.5 g (accurate to 0.001 g) was added to 4 mL HNO$_3$ and 1 mL 30% H$_2$O$_2$ and soaked for 3–4 h or overnight, the upper cap was screwed, and it was digested with the microwave digestion instrument (CEM MARS6, CEM, Matthews, USA). The conditions of the microwave digestion instrument are shown in Table 1. Then, they were placed on the temperature-controlled electric

heating plate (BHW-09C, Shanghai Botong Chemical Technology Co., Ltd., Shanghai, China) and heated at 100°C for 20–30 min for degassing. After cooling, the samples were diluted to 50 mL with deionized water and shook well for later use. For each group of samples, blanks (deionized water and reagents) and reference materials were included throughout the entire sample preparation and analytical process.

2.3. Inductively Coupled Plasma Tandem Mass Spectrometry Analysis. This experiment was carried out by tandem mass spectrometry. The concentration of 30 isotopes (^{7}Li, ^{23}Na, ^{24}Mg, ^{27}Al, ^{11}B, ^{31}P, ^{32}S, ^{39}K, ^{44}Ca, ^{47}Ti, ^{51}V, ^{52}Cr, ^{55}Mn, ^{56}Fe, ^{59}Co, ^{60}Ni, ^{63}Cu, ^{66}Zn, ^{72}Ge, ^{75}As, ^{78}Se, ^{88}Sr, ^{95}Mo, ^{111}Cd, ^{115}In, ^{118}Sn, ^{121}Sb, ^{133}Cs, ^{137}Ba, and ^{208}Pb) in rice was determined by inductively coupled plasma tandem mass spectrometry (Agilent 8900 Series, Agilent, USA). 1 μg/mL mixed solution of Li, Y, Co, Tl, Ce, and Mg was used as the tuning solution, and 0.10 rps speed of the peristaltic pump was used to continuously feed the solution. Through the tuning program, the conditions of no gas, H$_2$, O$_2$, He, and NH$_3$/He multimode analysis methods were optimized. In the no-gas mode, the monitored ions were 7, 89, and 205. In the He mode, the monitored ions were 59, 89, and 205. In the H$_2$ mode, the monitored ions were $Q_1 = Q_2 = 59$, 89, and 205. In the O$_2$ mode, the monitored ions were $Q_1 = Q_2 = 59$, $Q_1 = 89/Q_2 = 105$, and $Q_1 = Q_2 = 205$. In the NH$_3$/He mode, the monitored ions were $Q_1 = Q_2 = 59$, $Q_1 = 89/Q_2 = 191$, and $Q_1 = Q_2 = 205$. Under different modes, RF power was 1550 W, auxiliary gas was 0.90 L/min, plasma gas was 15.0 L/min, sampling depth was 8.0 mm, and extraction lens was −7.6 V. The instrument's other conditions of ICP-MS/MS are shown in Table 2.

For the selection of element determination mode and reagent gas, this method involves two modes: the SQ (single quadrupole) standard mode and MS/MS tandem mode. There are He and no-gas reagent gas modes in the SQ mode and He, NH$_3$/He, H$_2$, O$_2$, and no-gas reagent gas modes in the MS/MS mode. The elements are measured in all modes, and the mode with the lowest detection limit of each element is determined as the best measurement mode.

Through the measured experimental conditions and methods, the elements Sc, Y, Rh, and Bi were used as the internal standard elements. Analyzing the experimental data can get a linear fitting standard curve with the *X*-axis as the concentration point and the *Y*-axis as the response value. Through this standard curve, the detection limit and background equivalent concentration of the analysis element can be obtained by calculating the element standard deviation. The linear correlation coefficient and range, internal standard elements, limit of detection (LOD), and limit of quantification (LOQ) are shown in Table 3.

At the same time, the content of each element in rice reference materials (GBW10043, GBW10044, and GBW10045) was determined, the standard value was compared, and the recovery rate was calculated to prove the accuracy and reliability of the method, and the recovery experiment was conducted.

TABLE 1: The condition of microwave digestion.

Step	Climbing time (min)	Hold time (min)	Temperature (°C)	Power (W)
1	06 : 00	03 : 00	120	1500
2	08 : 00	06 : 00	155	1500
3	08 : 00	15 : 00	180	1500

TABLE 2: Instrument parameters of ICP-MS/MS.

Instrument conditions	No-gas mode	H_2 mode	He mode	O_2 mode	NH_3/He mode
Q_1 deflection voltage(V)	−3.0	1.0	−3.0	1.0	1.0
Q_2 deflection voltage(V)	−3.0	−18.0	−15.0	−10.0	−12.0
Collision pool gas	—	H_2	He	O_2	NH_3/He
Gas flow rate of collision pool (L·min^{-1})	—	7.0	5.0	4.5	4.5/1.0
Deflection voltage of eight-stage pole (V)	−8.0	−18.0	−18.0	−3.0	−5.0

TABLE 3: Linear range and detection limit of isotopes.

	Calibration (μg/L)	R^2	Internal standard	LOD (mg/kg)	LOQ (mg/kg)
^{7}Li	0~100	0.9998	Sc	0.000659	0.0220
^{23}Na	0~1000	0.9999	Sc	0.144	0.479
^{24}Mg	0~1000	0.9999	Sc	0.00372	0.0124
^{27}Al	0~100	0.9987	Sc	0.0907	0.302
^{11}B	0~100	0.9995	Sc	0.0375	0.125
^{31}P	0~1000	0.9994	Sc	0.0204	0.0679
^{32}S	0~1000	0.9997	ScO	0.0614	0.205
^{39}K	0~1000	1.0000	Sc	0.0291	0.0970
^{44}Ca	0~1000	1.0000	Sc	0.105	0.351
^{47}Ti	0~100	0.9999	ScO	0.00219	0.00731
^{51}V	0~100	0.9999	ScO	0.000946	0.00315
^{52}Cr	0~100	0.9997	ScO	0.00521	0.0174
^{55}Mn	0~1000	1.0000	Sc	0.00148	0.00495
^{56}Fe	0~1000	1.0000	Sc(NH_3)$_2$	0.0170	0.0567
^{59}Co	0~100	1.0000	Sc(NH_3)$_2$	0.000510	0.00170
^{60}Ni	0~100	1.0000	Sc(NH_3)$_2$	0.00133	0.00444
^{63}Cu	0~1000	1.0000	Sc	0.00474	0.0158
^{66}Zn	0~1000	1.0000	Sc	0.0115	0.0383
^{72}Ge	0~100	1.0000	Y	0.000206	0.000686
^{75}As	0~100	1.0000	YO	0.00250	0.00832
^{78}Se	0~100	1.0000	Y	0.00152	0.00507
^{88}Sr	0~100	1.0000	Y	0.000929	0.00310
^{95}Mo	0~100	0.9999	YNH_3	0.000605	0.00202
^{111}Cd	0~100	1.0000	Rh	0.0000662	0.000221
^{115}In	0~100	0.9998	Rh	0.00123	0.00410
^{118}Sn	0~100	1.0000	Rh	0.00176	0.000588
^{121}Sb	0~100	1.0000	Rh	0.000196	0.000653
^{133}Cs	0~100	1.0000	Rh	0.000227	0.000756
^{137}Ba	0~100	1.0000	Rh	0.00158	0.00525
^{208}Pb	0~100	1.0000	Bi	0.000949	0.00317

2.4. Statistical Analysis. All analyses were conducted in triplicate. The results reported were the average of these three replicates. Each sample was considered as an assembly of 30 variables represented by the data of chemical information. The analysis data and the fitted linear regression curve were analyzed by Agilent Mass Hunter software (Agilent Inc., USA). A normal distribution test of multielements, principal component analysis, and clustering analysis were performed with SPSS 25.0 software (SPSS, IBM Corp., USA).

3. Results and Discussion

3.1. Mass Spectrometry Mode Selection and Interference Elimination. In this experiment, the SQ (single quadrupole) standard mode and MS/MS tandem mode were used to simultaneously determine the concentration of multielement. The elements were measured in different modes and different reaction gas modes, and the element detection limit was used as the criterion to determine the best measurement mode for each element. The results are shown in Table 4.

TABLE 4: Isotope mass spectrometry.

	Mode	Reaction gas	Mass number	Eliminate interference
^{7}Li	MS/MS	NH_3/He	$Q_1 = Q_2 = 7$	In situ mass spectrometry
^{23}Na	MS/MS	H_2	$Q_1 = Q_2 = 23$	In situ mass spectrometry
^{24}Mg	MS/MS	NH_3/He	$Q_1 = Q_2 = 24$	In situ mass spectrometry
^{27}Al	MS/MS	H_2	$Q_1 = Q_2 = 27$	In situ mass spectrometry
^{11}B	MS/MS	NH_3/He	$Q_1 = 11, Q_2 = 60$	Mass transfer
^{31}P	MS/MS	O_2	$Q_1 = 31, Q_2 = 47$	Mass transfer
^{32}S	MS/MS	O_2	$Q_1 = 32, Q_2 = 48$	Mass transfer
^{39}K	MS/MS	O_2	$Q_1 = Q_2 = 39$	In situ mass spectrometry
^{44}Ca	MS/MS	NH_3/He	$Q_1 = Q_2 = 44$	In situ mass spectrometry
^{47}Ti	MS/MS	O_2	$Q_1 = 47, Q_2 = 63$	Mass transfer
^{51}V	MS/MS	O_2	$Q_1 = 51, Q_2 = 67$	Mass transfer
^{52}Cr	MS/MS	O_2	$Q_1 = 52, Q_2 = 68$	Mass transfer
^{55}Mn	MS/MS	H_2	$Q_1 = Q_2 = 55$	In situ mass spectrometry
^{56}Fe	MS/MS	NH_3/He	$Q_1 = 56, Q_2 = 90$	Mass transfer
^{59}Co	MS/MS	NH_3/He	$Q_1 = 59, Q_2 = 93$	Mass transfer
^{60}Ni	MS/MS	NH_3/He	$Q_1 = Q_2 = 60$	In situ mass spectrometry
^{63}Cu	SQ	He	$Q_2 = 63$	—
^{66}Zn	MS/MS	H_2	$Q_1 = Q_2 = 66$	In situ mass spectrometry
^{72}Ge	MS/MS	H_2	$Q_1 = Q_2 = 72$	In situ mass spectrometry
^{75}As	MS/MS	O_2	$Q_1 = 75, Q_2 = 91$	Mass transfer
^{78}Se	MS/MS	H_2	$Q_1 = Q_2 = 78$	In situ mass spectrometry
^{88}Sr	MS/MS	H_2	$Q_1 = Q_2 = 88$	In situ mass spectrometry
^{95}Mo	MS/MS	NH_3/He	$Q_1 = Q_2 = 95$	In situ mass spectrometry
^{111}Cd	SQ	No gas	$Q_2 = 111$	—
^{115}In	MS/MS	H_2	$Q_1 = Q_2 = 115$	In situ mass spectrometry
^{118}Sn	SQ	He	$Q_2 = 118$	—
^{121}Sb	SQ	No gas	$Q_2 = 121$	—
^{133}Cs	MS/MS	O_2	$Q_1 = Q_2 = 133$	In situ mass spectrometry
^{137}Ba	MS/MS	NH_3/He	$Q_1 = Q_2 = 137$	In situ mass spectrometry
^{208}Pb	SQ	No gas	$Q_2 = 208$	—
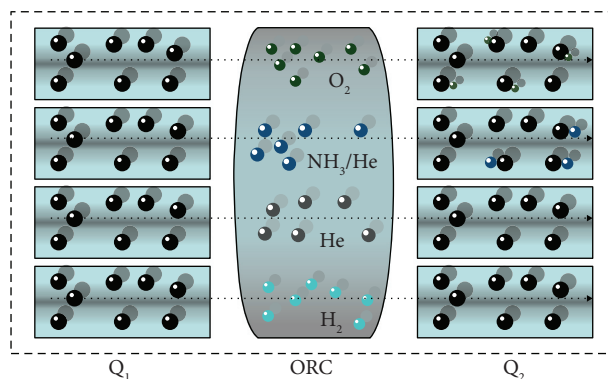
FIGURE 1: Interference cancellation model of the MS/MS mode. The ions collided with gas in the ORC.

The interference was eliminated by making full use of the collision mode between the element and the reaction gas. In the SQ mode, the mass ions of ^{63}Cu, ^{111}Cd, ^{118}Sn, ^{121}Sb, and ^{208}Pb had the characteristics of high abundance value and less interference. The corresponding Q_2 mass number was the only one that needs to be set during the determination.

In the MS/MS mode, the NH_3/He mixture gas collided with ^{7}Li, ^{24}Mg, ^{44}Ca, ^{60}Ni, ^{95}Mo, and ^{137}Ba ions in the reaction cell, H_2 collided with ^{23}Na, ^{27}Al, ^{55}Mn, ^{66}Zn, ^{72}Ge, ^{78}Se, ^{88}Sr, and ^{115}In ions, and O_2 collided with ^{39}K and ^{133}Cs ions, respectively. The interference was eliminated by in situ

mass spectrometry, which means the elements only collide with the reaction gas and do not combine with each other. Therefore, the mass number of the front and after tetrodes to be set remains unchanged ($Q_1 = Q_2$). However, the system will still have the same amount of heterotopic number signal superposition interference and double charge ion interference; for example, ions Ni^{++}, SiH, CO, and NO may interfere with ^{31}P; ions Zn^{++}, NO, and OO may interfere with ^{32}S; ions CAr and ArO interfere with ^{52}Cr; ions ArCl, CaCl, and CoO interfere with ^{75}As; ions ArO and MnH interfere with ^{56}Fe; and ions Sn^{++}, NiH, and MgCl interfere with ^{59}Co.

TABLE 5: Recovery rate of reference materials.

Recovery (%)	As	B	Ba	Ca	Cd	Co	Cr	Cs	Cu	Fe	Ge	K	Li	Mg	Mn	Mo	Na	Ni	P	Pb	S	Sb	Se	Sr	Sn	Ti	V	Al	Zn	In
GBW10043	92.6	91.6	92.6	95.2	109	89.4	91.7	103	92.2	104	106	96.5	92.8	105	96.5	88.6	95.3	90.6	102	89.5	95.3	106	105	95.6	ND	94.8	105	92.6	95.6	ND
GBW10044	95.1	93.8	104	105	108	90.2	93.5	107	85.6	108	109	94.8	107	103	91.5	85.7	92.1	105	106	115	90.7	108	109	96.1	ND	93.8	109	90.2	94.1	ND
GBW10045	96.3	103	105	93.8	102	96.5	107	87.5	93.8	95.6	112	95.9	111	96.5	90.3	82.9	94.8	92.8	103	106	93.1	110	103	92.8	ND	91.1	113	93.5	103	ND

*ND means not detected.

TABLE 6: The spike recovery and reproducibility of the spiked sample ($n = 6$).

Element	Background (mg/kg)	Added (mg/kg)	Recovery (%)	RSD (%)
As	0.127	10	105.3	3.5
		1	108.1	3.2
		0.1	104.6	1.1
B	0.506	10	98.6	0.6
		1	86.1	2.8
		0.1	105.8	1.6
Ba	0.351	10	94.3	2.8
		1	95.2	2.6
		0.1	82.8	8.9
Ca	41.6	100	93.6	0.9
		50	95.4	2.2
		10	102.5	1.6
Cd	0.0272	10	107.6	5.8
		1	92.5	0.9
		0.1	108.6	3.5
Co	0.00675	10	91.6	4.5
		1	95.3	4.1
		0.1	106.8	0.9
Cr	0.0138	10	84.3	5.0
		1	93.5	1.5
		0.1	89.6	1.1
Cs	0.00152	10	110.5	0.6
		1	92.3	2.8
		0.1	94.2	2.3
Cu	2.06	10	95.1	0.5
		1	96.7	4.1
		0.1	97.6	4.8
Fe	2.45	10	105.6	2.3
		1	103.9	6.8
		0.1	107.5	0.5
Ge	0.00261	10	85.3	2.4
		1	96.4	2.9
		0.1	95.8	6.3
K	510	100	84.3	2.5
		50	82.2	2.7
		10	93.6	4.1
Li	0.00365	10	109.5	0.9
		1	106.4	2.2
		0.1	93.6	5.4
Mg	105	100	104.3	3.6
		50	106.4	1.1
		10	83.2	1.8
Mn	7.46	10	92.6	2.0
		1	91.1	1.5
		0.1	93.7	2.9
Mo	0.496	10	94.5	0.4
		1	105.6	7.1
		0.1	93.2	3.8
Na	1.97	10	108.9	4.5
		1	103.7	4.8
		0.1	82.6	1.5
Ni	0.168	10	91.6	0.5
		1	106.3	0.8
		0.1	87.5	1.6

TABLE 6: Continued.

Element	Background (mg/kg)	Added (mg/kg)	Recovery (%)	RSD (%)
P	448	100	101.2	1.3
		50	104.5	2.9
		10	93.4	3.5
Pb	0.00152	10	89.9	6.6
		1	104.2	1.7
		0.1	106.6	0.9
S	552	100	80.6	1.1
		50	85.9	0.7
		10	93.8	2.5
Sb	0.000154	10	106.4	3.9
		1	95.3	3.3
		0.1	92.8	0.6
Se	0.0274	10	94.7	2.5
		1	95.9	2.1
		0.1	84.6	0.8
Sr	0.163	10	106.4	0.7
		1	108.5	0.9
		0.1	84.9	5.3
Sn	ND	10	104.3	1.4
		1	96.1	5.6
		0.1	95.6	2.0
Ti	0.0865	10	85.3	1.7
		1	91.8	0.8
		0.1	85.9	7.6
V	0.00594	10	92.7	1.6
		1	108.5	1.5
		0.1	106.9	0.8
Al	ND	10	94.5	2.6
		1	93.7	2.1
		0.1	105.2	1.0
Zn	10.9	100	92.3	6.8
		50	82.8	4.6
		10	94.6	3.7
In	ND	10	91.5	2.5
		1	85.4	8.9
		0.1	96.3	1.9

*ND means not detected.

Therefore, in the determination of some specific elements, if the reactant gas and the element collide with each other to generate ions with a new mass number, the abovementioned interferences can be better avoided. In addition, when the gas collided with the analysis element, new mass ions were formed in the reaction, that is, mass transfer (Figure 1). In the experiment, NH_3/He mixture gas can react with $^{11}B^+$ and $^{56}Fe^+$ to form $^{11}B^{49}NH(NH_3)_2^+$ and $^{56}Fe(^{14}NH_3)_2^+$ cluster ions. Also, the O_2 mode was more widely used, which can undergo mass transfer with $^{31}P^+$, $^{32}S^+$, $^{47}Ti^+$, $^{51}V^+$, $^{52}Cr^+$, $^{75}As^+$, and generated $^{31}P^{16}O^+$, $^{32}S^{16}O^+$, $^{47}Ti^{16}O^+$, $^{51}V^{16}O^+$, $^{52}Cr^{16}O^+$, and $^{75}As^{16}O^+$ cluster ions, respectively.

3.2. Standard Material Determination and Precision. Multielement determination was performed on the standard materials GBW10043, GBW10044, and GBW10045, and the

TABLE 7: Element content of rice.

	Li	B	Na	Mo	Al	As	Ca	P	S	Ti	V	Cr	Mn	Ni	Cu	Fe	Sb	Pb	Ge	In	Sr	K	Sn	Cd	Se	Mg	Co	Cs	Ba	Zn
A-1	3.47	0	1.91	0.546	0	0.124	41.5	436	569	77.6	5.17	13.6	7.05	0.122	2.11	2.37	0.135	0	2.62	0	0.148	513	0	26.8	21.5	96.6	6.68	1.57	0.316	10.9
A-2	0	0	1.35	0.484	0	0.106	40.5	466	581	75.3	3.68	19.7	7.60	0.114	2.55	1.95	0.0227	0	2.64	0	0.120	517	0	52.0	34.3	98.2	7.53	1.13	0.297	12.4
A-3	1.90	0	1.73	0.546	0	0.117	40.2	494	605	72.6	4.85	11.8	9.94	0.130	2.39	2.15	0.0625	0.368	2.75	0	0.139	524	0	201	28.2	89.9	7.49	1.20	0.304	12.3
X-1	9.56	0.506	4.80	0.502	0	0.134	48.3	540	630	45.6	8.33	5.22	8.43	0.130	2.31	2.79	0.350	16.6	1.91	0	0.121	701	0	5.59	38.9	172	5.94	1.79	0.187	11.8
X-2	4.84	0.333	4.44	0.485	0	0.112	49.3	528	624	51.7	7.81	0	9.54	0.129	3.15	2.32	0.245	2.76	2.44	0	0.132	739	0	28.9	27.9	200	6.29	1.91	0.190	11.9
X-3	1.39	0	3.63	0.474	0	0.115	48.1	499	611	82.2	7.98	7.99	9.45	0.117	3.04	2.53	0.116	1.15	2.31	0	0.128	716	0	150	26.8	167	6.35	1.24	0.178	11.6
D-1	1.52	0	1.04	0.459	0	0.126	37.1	456	599	42.6	5.17	11.5	8.63	0.136	2.06	1.77	0.159	0	1.13	0	0.137	593	0	39.7	59.4	52.6	6.94	9.94	0.194	11.6
D-2	1.57	0	1.03	0.317	0	0.0618	37.8	450	581	43.3	5.35	13.7	10.9	0.113	2.96	1.81	0.177	0	1.71	0	0.180	578	0	175	23.0	54.1	6.95	10.9	0.205	11.7
D-3	1.46	0	0.563	0.514	0	0.112	38.6	463	606	79.4	4.15	9.15	9.10	0.116	2.10	1.73	0.125	0.216	1.59	0	0.116	685	0	169	61.3	69.6	6.94	12.6	0.224	11.0
J-1	5.46	0.283	21.3	0.270	0	0.0930	50.0	409	448	21.8	7.34	34.5	10.1	0.0611	1.26	1.74	0.150	5.97	0.529	0	0.137	537	0	9.17	24.5	120	2.78	0.734	0.0479	10.4
J-2	6.45	0.233	19.5	0.201	0	0.0858	52.4	413	436	38.4	6.74	34.8	10.1	0.0508	1.12	2.91	0.136	0	0.630	0	0.156	514	0	3.49	14.3	124	2.84	0.695	0.0486	9.27
J-3	7.10	0.245	16.6	0.254	0	0.111	54.1	454	467	36.6	9.47	41.9	10.6	0.0597	1.15	2.22	0.984	0	0.520	0	0.131	526	0	3.10	34.1	128	2.64	0.624	0.0508	10.5
H-1	2.64	0.0219	5.66	0.470	0	0.106	47.9	448	514	36.2	7.68	55.2	10.4	0.126	1.72	2.34	0	8.65	0.969	0	0.103	549	0	5.73	24.7	124	4.84	1.05	0.0357	13.6
H-2	2.63	0	6.63	0.406	0	0.166	47.1	450	481	36.3	6.95	59.4	10.4	0.106	1.60	2.05	0.105	0	0.911	0	0.0802	516	0	15.5	53.0	114	4.95	1.56	0.0375	12.6
H-3	3.10	0.0311	4.05	0.414	0	0.0646	45.8	428	495	56.5	6.03	61.9	9.83	0.106	1.32	2.44	0.209	0	0.949	0	0.102	472	0	4.26	16.0	105	4.39	1.19	0.0343	12.8
N-1	5.97	0	13.0	0.363	0	0.110	41.0	499	525	19.9	5.22	65.8	7.12	0.0515	1.43	2.99	0.089	0	0.972	0	0.182	616	0	4.69	25.8	127	3.90	0.833	0.0247	11.2
N-2	5.19	0.0377	10.9	0.376	0	0.0900	45.1	519	537	23.1	5.72	61.4	7.25	0.0515	1.51	2.93	0.104	1.20	0.948	0	0.191	582	0	3.87	21.4	125	4.45	0.741	0.0292	10.4
N-3	4.65	0	11.9	0.340	0	0.0902	41.5	510	529	21.7	5.62	59.5	7.03	0.0791	1.60	2.52	0.100	0.302	0.808	0	0.189	591	0	3.00	26.6	119	4.50	0.637	0.0202	10.8

The data unit is mg(kg), among which the element data unit of Li, Ti, V, Cr, Co, Ge, Se, Cd, Sb, Cs, and Pb is μg(kg). A- Anhui Province, X- Guangxi Province, D- Guangdong Province, J- Jilin Province, H- Heilongjiang Province, N- Inner Mongolia.
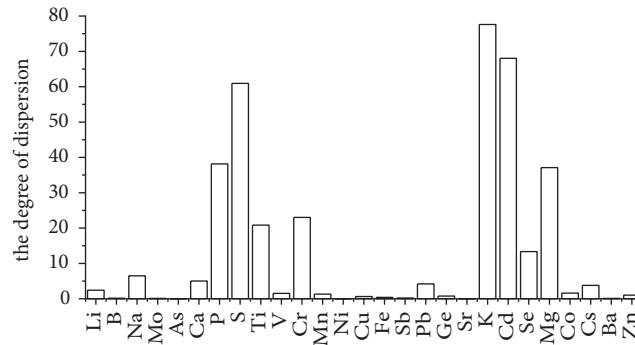
FIGURE 2: The degree of dispersion.

TABLE 8: Results of principal component analysis.

Component	Initial eigenvalue			Rotate the sum of squares loading		
	Total	Variance (%)	Accumulate (%)	Total	Variance (%)	Accumulate (%)
1	10.41	38.56	38.56	7.547	27.95	27.95
2	4.800	17.78	56.34	4.870	18.04	45.99
3	3.142	11.64	67.97	3.225	11.94	57.94
4	2.243	8.306	76.28	3.223	11.94	69.87
5	1.850	6.852	83.13	2.809	10.41	80.28
6	1.282	4.749	87.88	2.052	7.599	87.88

TABLE 9: Contribution value of the element's principal component.

Element	Component					
	1	2	3	4	5	6
Li	−0.697	0.551	−0.164	0.167	0.154	−0.115
B	−0.367	0.753	0.162	0.324	0.003	−0.068
Na	−0.927	−0.009	−0.038	0.184	−0.016	−0.114
Mg	−0.318	0.846	−0.124	−0.167	−0.185	0.045
K	0.324	0.644	−0.263	0.291	0.289	0.282
Ca	−0.684	0.515	0.360	0.011	−0.278	−0.083
P	0.236	0.617	−0.559	−0.079	0.253	0.182
S	0.855	0.381	−0.277	0.102	0.108	0.094
Ti	0.772	0.070	0.141	0.016	−0.375	−0.333
V	−0.512	0.660	0.405	0.087	−0.092	0.132
Cr	−0.693	−0.380	−0.096	−0.508	0.140	0.175
Mn	−0.091	−0.002	0.794	0.261	−0.281	0.353
Ni	0.847	0.248	0.297	−0.177	−0.010	0.113
Cu	0.809	0.346	−0.112	0.180	−0.213	0.212
Fe	−0.476	0.361	−0.587	−0.277	−0.133	−0.014
Co	0.984	0.033	−0.093	−0.020	−0.007	0.000
Zn	0.472	0.092	0.364	−0.633	−0.052	0.401
Ge	0.818	0.301	−0.192	−0.039	−0.363	−0.216
Se	0.432	−0.003	0.368	0.081	0.778	−0.154
Sr	−0.221	−0.212	−0.822	0.384	−0.008	0.107
As	0.244	0.383	0.273	−0.316	0.480	−0.448
Mo	0.822	0.277	−0.040	−0.395	0.056	−0.117
Cd	0.715	−0.172	0.034	0.380	−0.209	0.165
Sb	−0.368	0.308	0.329	0.438	0.062	−0.237
Cs	0.547	−0.332	0.152	0.521	0.399	0.247
Ba	0.860	0.097	−0.044	0.198	−0.203	−0.350
Pb	−0.087	0.706	0.132	−0.114	0.148	0.236
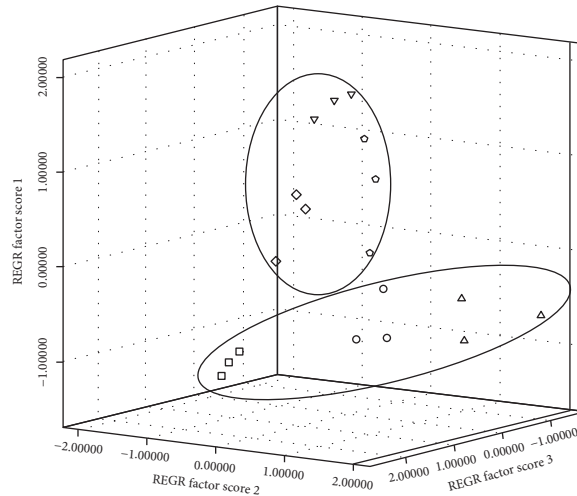
FIGURE 3: Score distribution of principal component analysis.
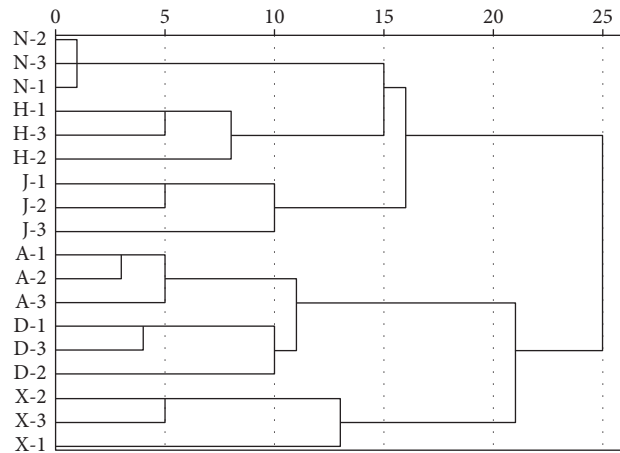
FIGURE 4: Systematic clustering of element content. A- Anhui Province, X- Guangxi Province, D- Guangdong Province, J- Jilin Province, H-Heilongjiang Province, and N- Inner Mongolia.

results are shown in Table 5. The average recoveries of element content of reference materials were in the range between 82.9% and 115%.

The recoveries of analytes were evaluated by adding the standard solutions with three different concentration levels to the known amounts of samples. The data of recovery and precision are given in Table 6, and the average recoveries of element content in rice were in the range between 80.6% and 110.5%. The RSDs were in the range of 0.4%–8.9%. The measurement results show that this method has high accuracy and meets the requirements of analysis and measurement.

3.3. Multielement Analysis of Samples. There are obvious differences in the content of Ba, Ge, Co, Cu, Cr, Ti, S, Ca, Mg, Na, Li, and other elements in rice from different producing areas in north and south China. In southern China, there are differences in the content of Na, Mg, K, Ca, V, Ge, Cs, Ba, and other elements in rice produced in Anhui Province, Guangxi Province, and Guangdong Province. However, in northern China, there are obvious differences in the content

of B, Na, Ca, P, Cr, Mn, Ni, Co, Zn, Sr, Mo, Cs, and other elements in batches of rice in Jilin Province, Heilongjiang Province, and Inner Mongolia (Table 7). The contents of Al, In, and Sn were not detected.

We conducted further statistical analysis on the abovementioned experimental data, by calculating the standard deviation of each element and judging the difference of each element in different regions according to the degree of dispersion of the value of each element. As shown in Figure 2, the standard deviations of S, P, K, Cd, Mg, and other elements were large, and the degree of dispersion was relatively higher than that of other elements, which can be initially used as indicative elements for traceability.

3.4. Multielement Normal Distribution Test. The Kolmogorov–Smirnov test was conducted on the content of 30 elements in rice from different origins. The asymptotic significance (bilateral) value was calculated. The content data of 24 elements obeyed normal distribution.

3.5. *Principal Component Analysis.* Principal component analysis (PCA) is a multivariate statistical analysis method that analyses a few variables which can reveal the internal structure sufficiently by studying the relationship between multiple original variables.

According to the rule that the characteristic value is greater than 1 and the cumulative variance contribution rate is greater than 80%, six principal component factors were obtained through rotation and extraction factors, and the total contribution rate was 87.878%, indicating that the experimental data can fully reflect the original information (Table 8).

The first principal component is mainly composed of S, Ti, Ni, Cu, Co, Ge, Mo, Cd, Cs, Ba, Zn, and Se elements. The second principal component is mainly composed of Li, B, Mg, K, Ca, P, V, Pb, Fe, and As elements. The third principal component is mainly composed of Mn and Sb elements (Table 9). The first principal component, the second principal component, and the third principal component were used to analyze the contribution of the principal components of samples from different origins (Figure 3). The contribution scores of the principal components of samples from the same origin were concentrated, while the distribution of different origins is scattered. On the whole, rice samples from the north and south of China have a large difference in the contribution scores of the principal components which can be clearly distinguished. This result has certain guiding significance for the distinction of rice from different production places.

3.6. *Cluster Analysis.* The contents of multielements in rice from different areas were analyzed by cluster analysis. The samples were successfully divided into two categories (the north and south of China) and six subcategories (six rice-producing areas) by the method of intergroup connection (Figure 4). The results show that there were obvious differences in the contents of multielements in rice from different producing areas, and they had certain regional characteristics. Therefore, by measuring the multielement content of rice, it is possible to accurately classify the samples according to the place of origin and finally realize the traceability of the production place of the rice.

4. Conclusions

In this experiment, the ICP-MS/MS method was developed to determine the content of 30 elements in rice from different production areas. The determination mode and reaction gas conditions were optimized, and the optimal determination conditions were selected for each element in five determination modes of no gas, H_2, O_2, He, and $NH_3/$ He. In addition, in situ mass spectrometry and mass transfer technology were used to eliminate the interference and reduce the detection limit. To achieve the determination of ultratrace elements, we established a complete detection method, which provided a method basis for rice origin traceability. Through the principal component analysis of the multielement content of 18 batches of samples from different origins, the distribution of the six principal components of the samples and the characteristic elements of each principal component were determined. Through cluster analysis, the samples were accurately classified according to the place of production based on the multielement content, which proved that there was a significant correlation between the content of multielement in rice and the place of production, providing technical support and research direction for the traceability of the origin of rice.

Data Availability

The data used to support the findings of this study are included within the article.

Conflicts of Interest

The authors declare no conflicts of interest regarding the publication of this article.

Authors' Contributions

YZ, QL, and YW conceived and designed the study. YW and LNL performed the experiments. YW and XXY wrote the paper. YZ, QL, JMM, and SFF reviewed and edited the manuscript. All authors read and approved the manuscript.

Acknowledgments

References

[1] V. Taleon, S. Gallego, J. C. Orozco, and C. Grenier, "Retention of Zn, Fe and phytic acid in parboiled bio fortified and non-biofortified rice," *Food Chemistry X*, vol. 8, Article ID 100105, 2020.

[2] M. Jaafar, A. Shrivastava, S. Rai Bose, M. Felipe-Sotelo, and N. I. Ward, "Transfer of arsenic, manganese and iron from water to soil and rice plants: an evaluation of changes in dietary intake caused by washing and cooking rice with groundwater from the Bengal Delta, India," *Journal of Food Composition and Analysis*, vol. 96, Article ID 103748, 2021.

[3] M. Tatahmentan, S. Nyachoti, L. Scott et al., "Toxic and essential elements in rice and other grains from the United States and other countries," *International Journal of Environmental Research and Public Health*, vol. 17, no. 21, p. 8128, 2020.

[4] Z. Y. Min, L. S. Si, L. B. Yu et al., "Enrichment of cadmium in rice (*Oryza sativa L.*) grown under different exogenous pollution sources," *Environmental Science and Pollution Research International*, vol. 27, pp. 44249–44256, 2020.

[5] F. Zhang, F. Gu, H. Yan et al., "Effects of soaking process on arsenic and other mineral elements in brown rice," *Food Science and Human Wellness*, vol. 9, no. 2, pp. 168–175, 2020.

[6] L. Wang and Y. Jin, "Possible application of stable isotope compositions for the identification of metal sources in soil," *Journal of Hazardous Materials*, vol. 407, p. 5, 2021.

[7] W. Jie, Z. Tengteng, and G. Yongbin, "C/N/H/O stable isotope analysis for determining the geographical origin of American ginseng (Panax quinquefolius)," *Journal of Food Composition and Analysis*, vol. 96, Article ID 103756, 2021.

[8] S. Yaeko, M. Shotaro, T. Tomoki et al., "Preliminary study for tracing the geographical origin of wheat flour in breads using stable isotope analysis of wheat proteins," *Food Analytical Methods*, vol. 14, p. 1, 2020.

[9] J. Wang, T. Chen, W. Zhang, Y. Zhao, S. Yang, and A. Chen, "Tracing the geographical origin of rice by stable isotopic analyses combined with chemometrics," *Food Chemistry*, vol. 313, Article ID 126093, 2020.

[10] P. Vera, G. Raquel, C. B. Dias, and M. Cabrita, "Combination of stable isotope analysis and chemo metrics to discriminate geoclimatically and temporally the virgin olive oils from three mediterranean countries," *Foods*, vol. 9, p. 12, 2020.

[11] Y.-Y. SU, J. Gao, Y. F. Zhao et al., "Geographical origin classification of Chinese wines based on carbon and oxygen stable isotopes and elemental profiles," *Journal of Food Protection*, vol. 83, p. 8, 2020.

[12] N. W. Ling, B. L. Jie, G. Gary et al., "Multivariate statistical analysis of stable isotope signatures and element concentrations to differentiate the geographical origin of retail milk sold in Singapore," *Food Control*, vol. 123, Article ID 107736, 2020.

[13] L. Qian, F. Zuo, H. Liu, C. Zhang, X. Chi, and D. Zhang, "Determination of geographical origin of wuchang rice with the geographical indicator by multielement analysis," *Journal of Food Quality*, vol. 2, pp. 1–7, 2019.

[14] J. Zhang, Z. Tian, Y. Ma et al., "Origin identification of the sauce-flavor Chinese baijiu by organic acids, trace elements, and the stable carbon isotope ratio," *Journal of Food Quality*, vol. 2019, Article ID 7525201, 7 pages, 2019.

[15] M. Du, Y. Fang, F. Shen et al., "Multiangle discrimination of geographical origin of rice based on analysis of mineral elements and characteristic volatile components," *International Journal of Food Science & Technology*, vol. 53, p. 9, 2018.

[16] P. Cheajesadagul, C. Arnaudguilhem, J. Shiowatana, A. Siripinyanond, and J. Szpunar, "Discrimination of geographical origin of rice based on multi-element fingerprinting by high resolution inductively coupled plasma mass spectrometry," *Food Chemistry*, vol. 141, p. 4, 2013.

[17] P. Wang, X. R. Ma, W. P. WANG et al., "Characterization of flavor fingerprinting of red sufu during fermentation and the comparison of volatiles of typical products," *Food Science and Human Wellness*, vol. 8, pp. 375–384, 2019.

[18] A. Maike, R. Marc, D. Alissa et al., "Food authentication: determination of the geographical origin of almonds (Prunus dulcis Mill.) via near-infrared spectroscopy," *Micro Chemical Journal*, vol. 160, 2021.

[19] C. Hui, T. Chao, and L. Hongjin, "Discrimination between wild-grown and cultivated Gastrodia elata by near-infrared spectroscopy and chemometrics," *Vibrational Spectroscopy*, vol. 113, Article ID 103203, 2021.

[20] G. L. Truong, T. P. Quoc, and Y. D. Hai, "Identification of rice varieties specialties in Vietnam using Raman spectroscopy," *Vietnam Journal of Chemistry*, vol. 58, p. 6, 2020.

[21] A. Maike, D. Alissa, A. Christian, and M. Fischer, "Determination of the geographical origin of walnuts (*juglans regia L.*) using near-infrared spectroscopy and chemometrics," *Foods*, vol. 9, p. 12, 2020.

[22] A. A. Wasim, S. Naz, M. N. Khan, and S. Fazalurrehman, "Assessment of heavy metals in rice using atomic absorption spectrophotometry–a study of different rice varieties in Pakistan," *Pakistan Journal of Analytical & Environmental Chemistry*, vol. 20, p. 1, 2019.

[23] X. Deng, R. Li, and S. Deng, "Determination of the total content of arsenic, antimony, selenium and mercury in Chinese herbal food by chemical vapor generation-four-channel non-dispersive atomic fluorescence spectrometry," *Journal of Fluorescence*, vol. 30, pp. 949–954, 2020.

[24] L. HongLin, Z. YiTao, Z. Xin, and H. Tong, "Improved geographical origin discrimination for tea using ICP-MS and ICP-OES techniques in combination with chemo metric approach," *Journal of the Science of Food and Agriculture*, vol. 100, p. 8, 2020.

[25] S. O. Yeon, I. M. Atikul, S. J. Hyeon et al., "Elemental composition of pork meat from conventional and animal welfare farms by inductively coupled plasma-optical emission spectrometry (ICP-OES) and ICP-mass spectrometry (ICP-MS) and their authentication via multivariate chemo metric analysis," *Meat Science*, vol. 172, Article ID 108344, 2021.

[26] B. M. Freire, V. D. S. Santos, P. D. C. F. Neves et al., "Elemental chemical composition and as speciation in rice varieties selected for bio fortification," *Analytical Methods*, vol. 12, p. 16, 2020.

[27] L. Emily, F. Juraj, G. Sarah, J. Hutson, and L. Mosley, "A simple and rapid ICP-MS/MS determination of sulfur isotope ratios (^{34}S/^{32}S) in complex natural waters: a new tool for tracing seawater intrusion in coastal systems," *Talanta*, vol. 235, Article ID 122708, 2021.

[28] S. Alexander, G. Sarah, T. Renee et al., "In-situ Lusingle bondHf geochronology of garnet, apatite and xenotime by LA ICP MS/MS," *Chemical Geology*, vol. 577, Article ID 120299, 2021.

[29] S. Yoshinari, M. Kirara, and Y. Yukiya, "Assignment of PM$_{2.5}$ sources in western Japan by non-negative matrix factorization of concentration-weighted trajectories of GED-ICP-MS/MS element concentrations," *Environmental Pollution*, vol. 207, Article ID 116054, 2021.

[30] L. Xiaoming, D. Shuofei, Y. Yahu et al., "^{87}Sr/^{86}Sr isotope ratios in rocks determined using inductively coupled plasma tandem mass spectrometry in O_2 mode without prior Sr purification," *Rapid Communications in Mass Spectrometry*, vol. 34, Article ID e8690, 2020.

[31] A. Akif, E. A. Pelin, and O. G. Eftade, "Chemical characterization of size-segregated particulate matter (PM) by inductively coupled plasma – tandem mass spectrometry (ICP-MS/MS)," *Talanta*, vol. 208, Article ID 120350, 2020.

[32] J. Hirata, D. Itabashi, and M. Aimoto, "Determination of ultra-trace tellurium in steel by ID-ICP-MS/MS with liquid-liquid extraction," *Analytical Sciences*, 2021.

[33] T. M. A. M. Tamer, I. H. E. Dalia, and S. S. Abdelsalam, "Determination of some common heavy metals and radio-nuclides in some medicinal herbs using ICP-MS/MS," *Journal of AOAC International*, vol. 102, p. 5, 2020.

[34] L. Fu and S. Shi, "A novel strategy to determine the compositions of inorganic elements in fruit wines using ICP-MS/MS," *Food Chemistry*, vol. 299, Article ID 125172, 2019.

[35] O. Pérez-Arvizu and J.-P. Bernal, "Measurement of sulfur in environmental samples using the Interference Standard Method with a O_2-pressurized reaction cell and a single quadrupole inductively coupled plasma mass spectrometer," *Rapid Communications in Mass Spectrometry : Rapid Communications in Mass Spectrometry*, vol. 35, p. 9034, 2020.

[36] F. Liang, X. Hualin, H. Jianhua, and L. Chen, "Determination of the non-metallic elements in herbal tea by inductively coupled plasma tandem mass spectrometry," *Biological Trace Element Research*, vol. 199, pp. 769–778, 2021.

Research Article

Application of Next-Generation Sequencing Technology Based on Single Gene Locus in Species Identification of Mixed Meat Products

Xinmei Liu,[1] Zhiyang Liu [ID],[2] Yiyu Cheng,[1] Haijing Wu,[1] Wei Shen,[1] Yan Liu,[1] Qiushi Feng,[1] and Jun Yang [ID][1]

[1]*Nanjing Institute for Food and Drug Control, Nanjing 211198, China*
[2]*Institute of Vegetable Crops, Jiangsu Academy of Agricultural Sciences, Nanjing 210014, China*

Correspondence should be addressed to Jun Yang; yj711003@sina.com

Polymerase chain reaction (PCR) detection is a commonly used method for species identification of meat products. However, this method is not suitable for the analysis of meat products containing multiple mixtures. This study aimed to test whether next-generation sequencing (NGS) technology could be used as a method for the certification of mixed meat products. In this study, five kinds of common meat (pigs, cattle, sheep, chickens, and ducks) were mixed as samples with different proportions. The primers designed from mitochondrial 16S rRNA and nuclear genome gene (growth hormone receptor, GHR), respectively, were used to detect these meats. The sequencing results of NGS were analyzed using a self-designed bioinformatics program. The fragments with similar sequences were classified and compared with the database to determine their species. The results showed that all five kinds of meat components could be correctly identified using these two primers. The meat composition could be detected as low as 0.5% in the mixed samples using the NGS technology targeting GHR gene fragments, which was superior to those targeting mitochondrial 16S rRNA. However, the quantitative detection of species in the mixture was not likely to be quite accurate due to the amplification bias of PCR amplification. These results showed that the NGS technology could be applied to identify meat species in mixtures.

1. Introduction

Low-cost meat is often used in the consumer market as high-quality meat or high value-added meat [1], which damages the economic interests of consumers and leads to social problems such as food safety and religious ethics [2]. DNA in meat contains species-specific genetic information; it is stable in terms of chemical properties and is not easily destroyed in food processing. It is especially suitable for identifying different species in meat [3, 4]. In the last two decades, many DNA-based methods have been developed to identify meat species. Most of them rely on PCR to amplify specific DNA fragments and analyze them by different methods [5]. Previously, indirect methods, such as restriction fragment length polymorphism or single-strand conformation polymorphism, were mainly used to distinguish the specific DNA sequences of different species [6]. Nowadays, the most commonly used technology is to amplify the complete specific gene sequence by PCR and then use the conventional Sanger sequencing method for sequencing analysis. The target genes usually detected are mitochondrial cytochrome b (cytb) or cytochrome oxidase I (cox1) genes [7]. However, these methods usually detect only one species at a time; also, the species in the sample needs to be known in advance so as to identify them using specific analysis steps. To overcome these limitations, the dot blot and gene chip methods have been developed in recent years, which can detect mixed meat samples [8] and analyze more than one species simultaneously. However, these methods rely on the species-specific gene probes prepared in advance, which makes it impossible to detect unknown species in mixed meat.

The emergence of next-generation sequencing (NGS) technology has greatly improved the speed and accuracy of DNA sequencing [9], overcoming the limitation that the conventional Sanger sequencing method can sequence only a single DNA fragment [10]; NGS can sequence different DNA fragments in parallel. It has become a standard DNA sequencing analysis method for whole-genome sequencing, metagenomics research, transcriptomics research, environmental microbial polymorphism research, and other applications requiring sequence data [11, 12]. NGS technology can be used to analyze meat products containing different species mixtures by parallel sequencing of different template molecules from a sample.

Recently, the application of high-throughput sequencing technology in food species identification is still in its infancy. In the species identification of tuna, two short cytochrome b gene (cytb) fragments were sequenced on Illumina MiSeq platform, which could identify the species whose content was less than 1% but not marked on the biological commodity label [6]. Besides, according to the genes of expanded 12S and 16S rRNA mitochondrial DNA, the library was constructed for NGS sequencing. The mixture of 13 kinds of common meat, such as pigs, cattle, and sheep, was detected, which proved that NGS sequencing could be applied to identifying meat species in the mixture [13].

The aforementioned studies were based on the sequencing analysis of mitochondrial DNA genes in meat, but the content of mitochondrial DNA in different species was very different. Therefore, the sequencing analysis could only be used for qualitative detection and not for the quantitative analysis of species in mixed meat. In this study, we used the single-copy gene GHR in the nuclear genome as the target gene site, designed primers to construct the library, compared the results of NGS sequencing with GHR gene and 16S rRNA gene as the target site, and verified the potential of high-throughput sequencing technology in the quantitative detection of different species in mixed meat.

2. Materials and Methods

2.1. Primers and Conventional Sanger Sequencing.
The GHR gene was used as the target gene because of the great difference in the mitochondrial DNA content in muscles of different species. GHR genes of pigs, cattle, sheep, chickens, and ducks were downloaded from the GeneBank database, and primers were designed according to the common conservative region; the mitochondrial DNA primer 16S_ki was used as control (Table 1) [14]. PCR reactions were performed in volumes of 20 μL containing about 20 ng extracted DNA, 10 pmol of forward and reverse primers, and 10 μL of PCR super mix (Bio-Rad, CA, USA). Temperature profiles were as follows: 10 min at 95°C followed by 30 cycles of 30 s at 94°C, 30 s at 60°C, and 30 s at 72°C. Reactions were completed with a final extension step of 7 min at 72°C. The DNA of pigs, cattle, sheep, chickens, and ducks were used as templates. The fragments were amplified using the primers GHR_1 and 16S_ki. The size of the fragments was verified by electrophoresis, followed by confirmation using conventional Sanger sequencing.

2.2. Sample Preparation.
Five samples containing muscle tissues were prepared. The samples were frozen at −70°C for 24 h and then lyophilized with a lyophilizer to remove moisture from the samples. The freeze-dried samples were ground into minced meat with a tissue grinder and then mixed according to different mass ratios to obtain artificially mixed samples, 10 g for each sample. Sample S1 was an equal mixture of pigs, cattle, sheep, chickens, and ducks. The pork content in sample S2a–S2h was 80%, 50%, 20%, 10%, 5%, 1%, 0.5%, and 0.1%, respectively; the remaining was equally mixed with four other kinds of muscle tissues. Samples S3a–S3h, S4a–S4h, S5a–S5h, and S6a–S6h contained tissues from cattle, sheep, chickens, and ducks with different mass ratios, respectively; the preparation method was the same as that for pork samples (S2A–S2h).

2.3. DNA Isolation and NGS on the Illumina MiSeq Platform.
DNA of samples was extracted using a Qiagen's meat DNA extraction kit (Qiagen, Germany). A microspectrophotometer was used to determine DNA concentration to ensure that the A260/A280 value was between 1.8 and 2.0. Fragments were amplified in separate PCRs with the primers GHR_1 and 16S_ki. The primers featured additional Illumina adapter sequences at the 5'-end, including binding sites for the hybridization of PCR products, binding sites for sequencing primers, and poly(N)-regions for unique sample identification. The quality of PCR amplicons was analyzed with agarose gel electrophoresis and/or spectrophotometric analysis (NanoDrop spectrophotometer, Thermo Scientific, MA, USA). Amplicons were applied in equimolar ratios to bridge amplification and sequencing by synthesis on the Illumina MiSeq platform (Illumina, CA, USA). The samples were submitted to two independent NGS runs to assess the reaction's repeatability.

2.4. Data Analysis.
The reads were obtained by NGS sequencing. Then, the same reads were given the same order number and collected in a FastA document. A basic local alignment search tool (BLAST) was used in the mentioned FastA document to remove the primer sequences in the reads. The reads were collected later in another FastA document, which were then taken to BLAST in the document containing the sequences from tissues of pigs, cattle, sheep, chickens, and ducks. The reads matching the different kinds of meats were counted.

3. Results

3.1. Mixed Samples and Sequence Variability.
All the sequences could be amplified by the primers GHR_1 and 16S_ki. The two primers amplified fragments of the expected size for pigs, cattle, sheep, chickens, and ducks under the same PCR conditions. No nonspecific products were detected by agarose gel electrophoresis. The amplified fragments were confirmed by Sanger sequencing. The results showed that all the sequences were correct as expected.

TABLE 1: Primer pairs used for DNA amplification.

Name	Primers (5' to 3'): forward and reverse	Amplified fragment (bp)
16S_ki	GCCTGTTTACCAAAAACATCACCTCCATAGGGTCTTCTCGTCTT	243
GHR_1	CACCACAGAAAGCCTTACCACTACTGTGCTCACATAGCCAC	191

3.2. Analysis of NGS Sequencing Results of Mixed Samples.
Sample S1 was a mixture of pigs, cattle, sheep, chickens, and ducks, and each meat accounted for 20% of the total mass. Sample S1 was sequenced using the primer 16S_ki, and 14,977 reads were obtained. The results of BLAST showed 60,008 reads (40.21%) in sheep, 59,762 reads (40.05%) in pigs, 27,217 reads (18.24%) in cattle, 1735 reads (1.16%) in ducks, and 478 reads (0.32%) in chickens. Using the primer GHR_1, the results of NGS sequencing showed 105,942 reads in total. These included 59,639 reads (56.65%) in ducks, 17,839 reads (16.94%) in sheep, 15,434 reads (14.66%) in cattle, 7525 reads (7.94%) in pigs, and 4804 reads (4.65%) in chickens (Figure 1). A small number of reads for geese and horses were also identified, which might be due to the contamination of the sample or the mismatch in the sequencing.

The results showed a significant difference between the number ratio and the mass ratio of reads obtained by sequencing with these two primers, which could not be directly used for quantitative analysis. The reason might be the difference in DNA content or PCR amplification efficiency in different kinds of meat. The amplification efficiency of the 16S_Ki primer was lower than that of the GHR_1 primer in birds such as chickens and ducks, but had high amplification efficiency in mammals (pigs, cattle, and sheep). The amplification efficiency of the GHR_1 primer was the highest in ducks, but not different in mammals, and the lowest in chickens.

3.3. NGS Sequencing Results of Mixed Samples with Different Proportions. NGS sequencing was carried out on five common meat samples with different mass ratios (80%–0.1%), and the results of the sequencing of two primers were compared (Tables 2 and 3). The results showed that the number of reads obtained by NGS sequencing changed with the change in the content in the mixed samples of five kinds of common meat with different proportions. The change trend was consistent, but the absolute number was not proportional; therefore, it could not be used for quantitative detection. The amplification efficiency of the 16S_Ki primer was higher in mammals (pigs, cattle, and sheep), and the number of reads was significantly more than that of the GHR_1 primer (more than 100 reads could be detected with 0.1% content). However, the amplification efficiency of birds (chickens and ducks) was low in the 16S_Ki primer. When the content of chickens and ducks was less than 10%, only a small number of reads could be obtained, which was easily confused with foreign pollutants and could not be detected effectively. The GHR_1 primer could get higher reads in mammals and birds. When the content was more than 0.5%, more than 1000 reads could be obtained, which could be used for the qualitative detection of these 5 kinds of common

meat. To distinguish false positives such as sample contamination or mismatching during sequencing, we regarded the results with >100 reads as positive and those with <100 reads as false positive. The 16S_Ki primer could detect mammalian components as low as 0.1%, but could only detect more than 10% of poultry components. The GHR_1 primer could detect 0.1% of the four components except chickens, and the detection rate of chicken components was 0.5%. The results indicated that GHR_1 primer was more suitable for the detection in these five kinds of common meat.

4. Discussion

NGS sequencing has great application potential in species identification. The mitochondrial gene 16S rRNA was used as the target gene, and the NGS method was used to identify mammalian samples in mixed samples, with a detection limit of less than 1% [15]. Illumina sequencing was used to detect species DNA from mammals (pigs, cattle, horses, and sheep) and birds (chickens and turkeys) in sausages, which could distinguish species at the 1% level [16].

In this study, we tested the possibility of using Illumina second-generation sequencing technology to identify common meats (pigs, cattle, sheep, chickens, and ducks) in meat products. Adulteration identification of meat products is a hot topic in society. The low value meat, such as chickens, ducks, and pigs, is often impersonated as high value meat such as cattle and sheep, leading to a high concern worldwide [17]. Besides, many kinds of meat may produce different kinds of harmful substances in the process of deep processing [18]. At the same time, the sales scale of artificial plant meat products is growing rapidly in the global food market, and the taste and color are more and more close to the traditional meat products [1, 19]. All these put forward new demands for species identification of meat products. The advantage of NGS in species identification is that it can identify multiple species simultaneously from mixed samples without any prior information [20]. Species information can be obtained by matching the sequencing results with the existing sequence data in the database using bioinformatics methods. In this study, we did not consider the sequence differences among individuals because the sequence differences within species were less than that among species. Using the program algorithm, we can combine the sequences with individual differences into one class for analysis. According to the literature review [13], the target genes used in the existing NGS identification methods are mostly concentrated in mitochondrial DNA. Its main advantage is that mtDNA is rich in animal cells, is easy to extract, and contains multiple DNA sequences with both highly variable regions (differences between species) and conserved regions (highly similar between species), which
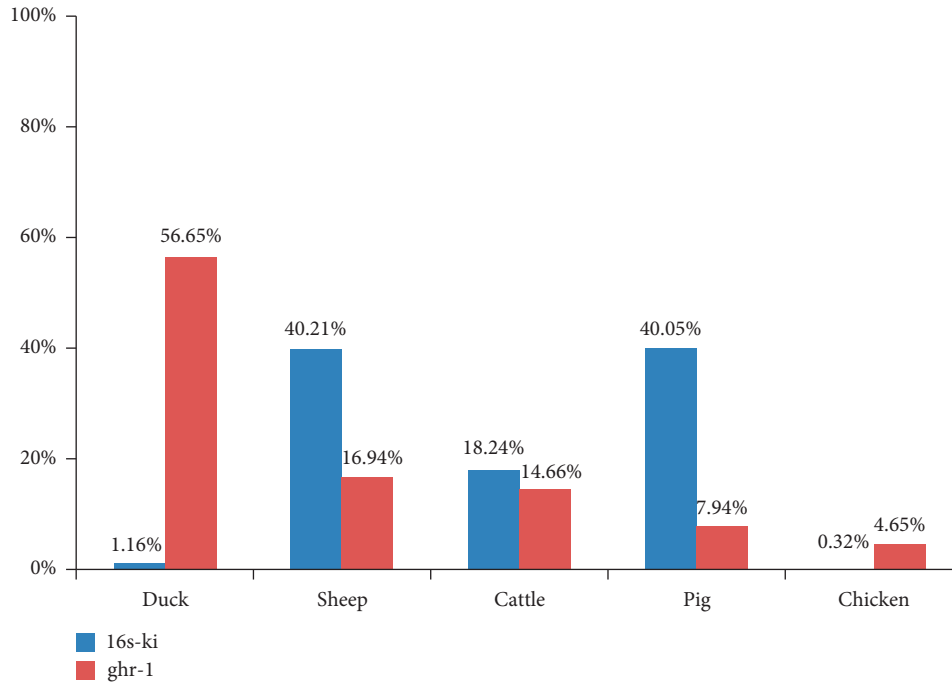
FIGURE 1: NGS sequencing results of mixed samples with an equal mass ratio.

TABLE 2: NGS sequencing results by 16S_Ki primer.

Content (%)	Number of reads for each species				
	Pigs	Cattle	Sheep	Chickens	Ducks
80	127913	104762	189945	5143	17271
50	100808	40736	102967	2013	8933
20	59762	27217	60008	213	1735
10	31030	22441	30514	128	459
5	8925	4931	12858	4	21
1	1918	2587	4366	4	8
0.5	440	1443	3832	7	6
0.1	279	396	1957	1	4

TABLE 3: NGS sequencing results by GHR_1 primer.

Content (%)	Number of reads for each species				
	Pigs	Cattle	Sheep	Chickens	Ducks
80	82930	96455	113943	80336	135320
50	30518	50870	76538	53362	81978
20	7551	15537	17831	4819	59849
10	5425	8989	13558	4217	37926
5	3387	5386	8555	1397	19547
1	2041	2485	3876	1863	2141
0.5	1740	1073	1399	1012	5841
0.1	162	1287	854	8	1253

are suitable for species identification, such as 16S RNA gene. However, the mtDNA content in mammals is higher than that in birds due to the significant difference in the mtDNA content in different species, which makes the detection efficiency of the original detection method for birds low. False negatives may be detected for a low content of bird components in mixed samples. The content of nuclear genome monoclonal genes is the same in different species of cells, and their number can directly reflect the number of cells. In recent years, it has been widely used in droplet digital PCR (DDPCR) quantitative detection of species [21–23] and has strong application potential in NGS.

We designed the primer GHR_1 based on the auxin receptor gene GHR; the mitochondrial DNA primer 16S_Ki was also used in NGS. The results showed that it was feasible to use the Illumina MiSeq NGS method to identify two short fragments of mitochondrial 16S RNA gene and nuclear genome GHR gene. The 16S_Ki primer can help detect as low as 0.1% of mammalian components (pigs, cattle, and sheep) in the samples, but the detection effect on poultry was not good. However, GHR_1 primer could detect as low as

0.5% of the components in all the samples. The limit of detection depends largely on species composition. Due to the amplification bias of PCR amplification, it is unlikely that the quantification of species in the mixture will have considerable accuracy. The target site of the primer GHR_1 is the nuclear genome monoclonal gene, which has a certain quantitative detection potential. However, the present study found that the number of reads detected by different species had a certain correlation with the species content, but it was not linear. Therefore, an accurate quantitative analysis could not be carried out, and hence further research is needed.

A small number of other species are detected, probably due to experimental pollution. Therefore, it is necessary to distinguish the positive results from possible pollution. The 16S_Ki primer had poor detection effect on poultry samples, and the number of reads obtained was very low, which might be confused with the background pollution. The GHR_1 primer was better, and thousands of reads could be obtained for 0.5% species, which was significantly different from the background pollution. For NGS technology, DNA residues detected in the sequencer may pollute the next detection;

therefore, appropriate monitoring methods should be used. In addition, DNA extraction, PCR, and NGS sequencing should be carried out in different rooms to avoid accidental contamination between samples.

In conclusion, NGS sequencing is a promising tool for detecting possible species mixing in meat products. With the decreasing cost of NGS detection equipment and services, the advantages of NGS sequencing, such as high throughput and nontargeting, have become more prominent. It may become a routine method for species identification in food.

Data Availability

The data are available from the corresponding author upon request.

Conflicts of Interest

The authors declare that they have no conflicts of interest.

Authors' Contributions

Xinmei Liu and Zhiyang Liu contributed equally to this study.

Acknowledgments

References

[1] M. Flores, L. Mora, M. Reig, and F. Toldrá, "Risk assessment of chemical substances of safety concern generated in processed meats," *Food Science and Human Wellness*, vol. 8, no. 3, pp. 244–251, 2019.

[2] N. Z. Ballin, "Authentication of meat and meat products," *Meat Science*, vol. 86, no. 3, pp. 577–587, 2010.

[3] D. C. Carvalho, R. M. Palhares, M. G. Drummond, and T. B. Frigo, "DNA barcoding identification of commercialized seafood in South Brazil: a governmental regulatory forensic program," *Food Control*, vol. 50, pp. 784–788, 2015.

[4] S.-Y. Chen, Y.-G. Yao, and Y.-P. Liu, "Species identification of ten common farm animals based on mitochondrial 12S rRNA gene polymorphisms," *Animal Biotechnology*, vol. 23, no. 3, pp. 213–220, 2012.

[5] I. Mafra, I. M. P. L. V. O. Ferreira, and M. B. P. P. Oliveira, "Food authentication by PCR-based methods," *European Food Research and Technology*, vol. 227, no. 3, pp. 649–665, 2008.

[6] K. Kappel, I. Haase, C. Käppel, C. G. Sotelo, and U. Schröder, "Species identification in mixed tuna samples with next-generation sequencing targeting two short cytochrome b gene fragments," *Food Chemistry*, vol. 234, pp. 212–219, 2017.

[7] A. M. Griffiths, C. G. Sotelo, R. Mendes et al., "Current methods for seafood authenticity testing in Europe: is there a need for harmonisation?" *Food Control*, vol. 45, pp. 95–100, 2014.

[8] C. C. Lin, L. L. Fung, P. K. Chan, C. M. Lee, K. F. Chow, and S. H. Cheng, "A rapid low-cost high-density DNA-based multi-detection test for routine inspection of meat species," *Meat Science*, vol. 96, no. 2, pp. 922–929, 2014.

[9] M. L. Metzker, "Sequencing technologies—the next generation," *Nature Reviews Genetics*, vol. 11, no. 1, pp. 31–46, 2010.

[10] N. Nagarajan and M. Pop, "Sequencing and genome assembly using next-generation technologies," *Methods in Molecular Biology*, vol. 673, pp. 1–17, 2010.

[11] B. M. Forde and P. W. O'Toole, "Next-generation sequencing technologies and their impact on microbial genomics," *Briefings in Functional Genomics*, vol. 12, no. 5, pp. 440–453, 2013.

[12] S. Shokralla, J. L. Spall, J. F. Gibson, and M. Hajibabaei, "Next-generation sequencing technologies for environmental DNA research," *Molecular Ecology*, vol. 21, no. 8, pp. 1794–1805, 2012.

[13] F. Bertolini, M. C. Ghionda, E. D'Alessandro, C. Geraci, V. Chiofalo, and L. Fontanesi, "A next generation semiconductor based sequencing approach for the identification of meat species in DNA mixtures," *PLoS One*, vol. 10, no. 4, Article ID e0121701, 2015.

[14] T. Kitano, K. Umetsu, W. Tian, and M. Osawa, "Two universal primer sets for species identification among vertebrates," *International Journal of Legal Medicine*, vol. 121, no. 5, pp. 423–427, 2007.

[15] A. O. Tillmar, B. Dell'Amico, J. Welander, and G. Holmlund, "A universal method for species identification of mammals utilizing next generation sequencing for the analysis of DNA mixtures," *PLoS One*, vol. 8, no. 12, Article ID e83761, 2013.

[16] F. Ripp, C. Krombholz, Y. Liu et al., "All-food-seq (AFS): a quantifiable screen for species in biological samples by deep DNA sequencing," *BMC Genomics*, vol. 15, no. 1, p. 639, 2014.

[17] B. Çapan and A. Bağdatli, "Investigation of physicochemical, microbiological and sensorial properties for organic and conventional retail chicken meat," *Food Science and Human Wellness*, vol. 10, no. 2, pp. 183–190, 2021.

[18] S. Iwatani and N. Yamamoto, "Functional food products in Japan: a review," *Food Science and Human Wellness*, vol. 8, no. 2, pp. 96–101, 2019.

[19] B. M. Bohrer, "An investigation of the formulation and nutritional composition of modern meat analogue products," *Food Science and Human Wellness*, vol. 8, no. 4, pp. 320–329, 2019.

[20] F. Ripp, C. F. Krombholz, Y. Liu et al., "All-Food-Seq (AFS): a quantifiable screen for species in biological samples by deep DNA sequencing," *BMC Genomics*, vol. 15, p. 639, 2014.

[21] Y. Cai, L. I. Xiang, and R. Lv, "Quantitative analysis of pork and chicken products by droplet digital PCR," *Journal of Biomedicine and Biotechnology*, vol. 2014, Article ID 810209, 2014.

[22] C. Floren, I. Wiedemann, B. Brenig, E. Schütz, and J. Beck, "Species identification and quantification in meat and meat products using droplet digital PCR (ddPCR)," *Food Chemistry*, vol. 173, pp. 1054–1058, 2015.

[23] E. S. Noh, Y. J. Park, E. M. Kim et al., "Quantitative analysis of Alaska pollock in seafood products by droplet digital PCR," *Food Chemistry*, vol. 275, pp. 638–643, 2019.

WILEY | Hindawi

Research Article

Disperse Solid-Phase Extraction Cleanup for the Determination of 1-Deoxynojirimycin in Mulberry Leaves with Ultraperformance Liquid Chromatography-Tandem Mass Spectrometry

Lei Zhang [1,2] **Yiran Zhou** [3] **Jing Meng** [3] **and Jia Li** [2]

[1]*Taishan University, Tai'an, China*
[2]*College of Pharmaceutical, Shandong University of Traditional Chinese Medicine, Jinan, China*
[3]*Jining Institute for Food and Drug Control, Jining, China*

Correspondence should be addressed to Yiran Zhou; sfdazyr@163.com and Jia Li; 05000045@sdutcm.edu.cn

A new determination method of 1-deoxynojirimycin (1-DNJ) in mulberry leaves based on ultraperformance liquid chromatography-tandem mass spectrometry (UPLC-MS/MS) has been developed. Dried and crushed mulberry leaves' sample was extracted by MeCN-water solvent, purified by graphitized carbon black (GCB) and primary secondary amine (PSA) to remove organic acids and pigments, and then analyzed after attenuation and filtration. The calibration curve showed linearity in the concentration range of 10–500 ng/mL, with the correlation coefficient of 0.998. Recoveries of spiked 1-DNJ at three fortification levels ranged from 94.6% to 96.4%, with relative standard derivation below 1.2%. Additionally, the matrix effect was assessed as negligible. Compared with methods by gas chromatography (GC) and liquid chromatography (LC) via real sample detection, the proposed method acquired better stability and detection efficiency. These results proved that this method has advantages of simple operation, complete purification, small pretreatment loss, good precision and accuracy, and high determination specificity, which is suitable for massive monitoring and precise quantitation of 1-DNJ in mulberry leaves.

1. Introduction

Mulberry branch (*Ramulus mori*) is a traditional Chinese medicinal herb, and its leaves are the main food of silkworm. It has been demonstrated that the intake of mulberry leaves or their extracts could treat diabetes, and the main active component is 1-deoxynojirimycin (1-DNJ) [1, 2], which is a kind of alkaloid compound with nitrogen atoms. It was found to be a potential α-glucosidase inhibitor by effectively suppressing the transformation of carbohydrate in the human body, reducing the sugar content in blood, and inhibiting the rapid rise of blood glucose and insulin secretion after eating [3].

At present, the detection methods of 1-DNJ are mainly based on gas chromatography (GC) and high-performance liquid chromatography (HPLC) [4–6]. It is reported that 1-DNJ concentrations in mature leaves varied from 0.1341 to 1.472 mg/g of dry leaves among 132 mulberry varieties [7]. However, due to the characteristics of high water solubility and weak absorbance, the methods based on GC and HPLC need suitable derivatization processes [4–9], as well as the method employed gas chromatography-tandem mass spectrometry (GC-MS) [10]. Therefore, the complex pretreatment operation will lead to a long preprocessing time and poor stability.

In recent years, ultraperformance liquid chromatography-tandem mass spectrometry (UPLC-MS/MS) has been widely used in the determination of trace amounts, such as pesticides, veterinary drugs, and mycotoxins [11, 12]. It has also been employed for the determination of 1-DNJ in mulberry leaves, which can overcome the problem of derivatization in the methods based on GC or HPLC and could acquire lower detection limits [13–15]. However, considering the accuracy and repeatability of the method, how to

effectively remove pigments such as chlorophyll, organic acids, and other interfering substances which lead to the matrix effect and instrument pollution is an important problem for the detection of pesticide residues in vegetables with dark green color [16], which is also applied to the pretreatment process of mulberry leaves. Some materials for purification were synthesized and found to be effective in removing these matrix interferences. Organic acids could be removed by silica microspheres bonded with amidogen, which was upgraded and replaced by primary secondary amine (PSA), while graphitized carbon black (GCB) has better adsorbing capacity on chlorophyll [16]. Some solid-phase extraction (SPE) methods based on these materials have been widely used in the analysis of pesticide residues and pollutants in vegetables and herbal plants [17–19], especially the quick, easy, cheap, efficient, rugged, and safe (QuEChERS) method which was the most popular in this field in recent years [20–22].

In this study, a massive monitoring and precise quantitation method of 1-DNJ in mulberry leaves based on LC-MS/MS was established, including (1) determining a suitable column and mobile phase proportion and acquiring optimal instrument parameters for the LC-MS system; (2) determining the optimal extraction, purification, and other pretreatment processes; (3) carrying out the methodology validation and comparing with the existing GC and HPLC methods. It is the first development for the determination of 1-DNJ in mulberry leaves with both LC-MS/MS system and matrix interference purification.

2. Materials and Methods

2.1. Chemicals and Solvents. Mulberry leaves were collected from Tai'an (Shandong Province, China). The leaves were harvested, cleaned, air-dried at 80°C for 12 hours, ground into powder, and then passed through a 100-mesh sieve and stored in a drying dish until used.

The reference material of 1-deoxynojirimycin (1-DNJ) was purchased from DASF Biological Co., Ltd. (Nanjing, China) with the purity of 98%. Acetonitrile (MeCN) and methanol (HPLC grade) were obtained from Merck (Darmstadt, Germany), while graphitized carbon black (GCB) and primary secondary amine (PSA) purification powder were purchased from Agela Technologies (Tianjin, China).

2.2. Standard and Sample Pretreatment. Stock standard solutions (100 μg/mL): 10 mg of 1-deoxynojirimycin standard was accurately weighted (accurate to 0.1 mg) into a 100 mL brown volumetric flask and diluted to volume with methanol. The working solution was prepared in the initial mobile phase (MeCN : water = 1 : 1) and diluted to prepare the calibration curves at six concentration points of 500, 200, 100, 50, 20, and 10 ng/mL. The stock solution was kept at 4°C before being used.

200 milligrams of the dried mulberry leaf powder was weighed and put into a 50 mL centrifuge tube. After 50 mL of 30% MeCN/water solution was added, the sample was sonicated in an ultrasonic bath for 5 min, following centrifugation at 7000 r/min for 5 min at 4°C. Subsequently, 5 mL of the supernatant was collected into a centrifuge tube with 45 mg PSA and 30 mg GCB added and then centrifuged at 10,000 r/min for 5 min after being vortexed for 1 min. Finally, 1.0 mL of purified supernatant was transferred to a 50 mL volumetric flask and then diluted to volume with the initial mobile phase solvent. The solution was filtered using a nylon syringe filter (0.2 μm) before being injected into the LC-MS system.

It should be mentioned that because negative samples with no 1-DNJ were unavailable, in the tests for pretreatment discussion, samples detected by the published method [6] were employed as quality control (QC) samples; therefore, the parameter "accuracy" was selected to exhibit the relative detection accuracy in the comparing groups. We thought it was a reasonable solution for this test.

2.3. LC-MS/MS Instrumentation. Samples were analyzed by a set of liquid chromatography-tandem mass spectrometry, equipped with the electrospray ionization source (ESI) and triple quadrupole mass analyzer (ExionLC-Triple Quad 3500, USA). The chromatographic separation was performed with the SunShell C18 (4.6 × 100 mm, 2.6 μm) (ChromaNik, Japan) column using a flow rate of 0.35 mL/min at 40°C. Mobile phases A and B of HPLC were deionized water and MeCN, respectively, and a 5 min gradient program was employed: proportion of B was kept at 50% for 2 min, then increased to 90% within 0.8 min and kept for 1.1 min, then suddenly decreased to 50% within 0.01 min, and kept to the end. The injection volume was 2 μl. ESI was performed in the positive ion mode with the 550°C interface temperature. The gas of curtain and ion sources 1 and 2 was set at 10, 50, and 50 psi, respectively. The capillary voltage was set at 5,500 V and the declustering potential of the parent ion (m/z = 164) as 40 eV. Four ions with m/z as 146.0, 109.9, 128.0, and 69.0 were adopted as product ions, in which the first one was employed as a quantitative ion, and their collision voltages were 19, 22, 19, and 26 eV, respectively, while the dwell time of each ion was set as 200 ms.

3. Results and Discussion

3.1. Optimization for Instrument Analysis

3.1.1. Comparison of the Separation Column. Theoretically, 1-DNJ would be better separated by a column bonded with amidogen because it was employed for the separation of monosaccharides such as glucose and fructose with similar structures in the HPLC system [23, 24], while it was used for 1-DNJ analysis and showed a good result in the previous study [13]. In this study, some types of column were employed and tested, including SunShell C18 (4.6 × 100 mm, 2.6 μm), ZORBAX Eclipse Plus C18 (2.1 × 50 mm, 1.8 μm), ACQUITY UPLC® BEH HILIC (2.1 × 50 mm, 1.7 μm), and Pinnacle II Amino (4.6 × 150 mm, 3 μm). As shown in Figure 1, it was found that the SunShell C18 column can lead to the retention time near 2 min, earlier than the Pinnacle II Amino column but later than other columns, while it could
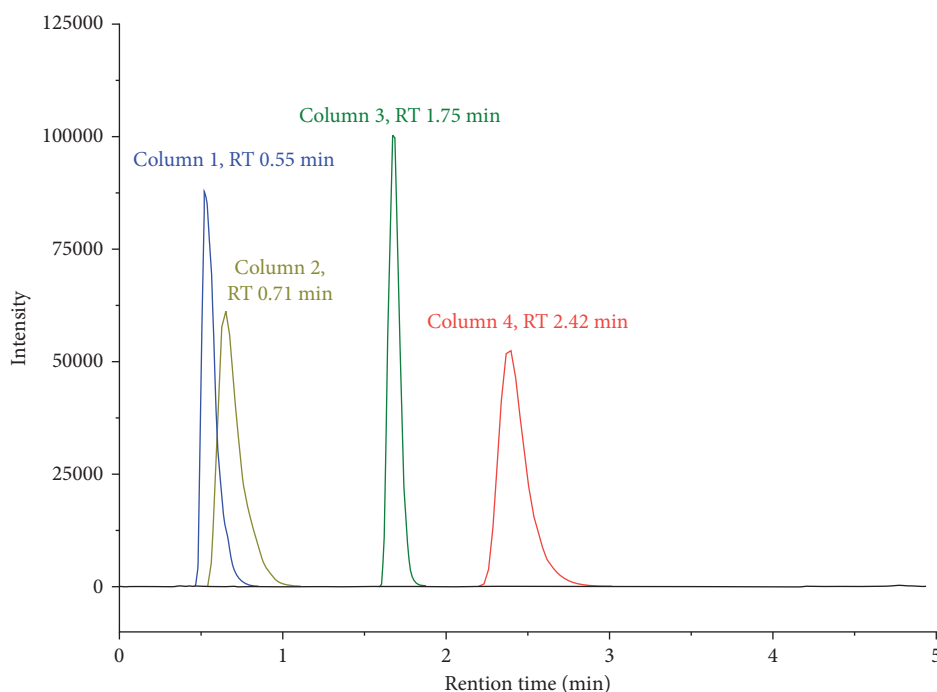
FIGURE 1: Real sample test chromatograms for the quantitation ion of 1-DNJ with the four types of column ($c = 500$ ng/mL). Column 1: Agilent ZORBAX Eclipse Plus C18, 2.1×50 mm $1.8\,\mu$m, column 2: Waters ACQUITY UPLC® BEH HILIC, 2.1×50 mm $1.7\,\mu$m, column 3: SunShell C18, 4.6×100 mm $2.6\,\mu$m, and column 4: Pinnacle II Amino, 4.6×150 mm, $3\,\mu$m.

acquire a satisfactory peak shape and separation. Thus, SunShell C18 was chosen for the HPLC system in this study.

3.1.2. Mobile Phase and Solvents. Good separation performance and perfect distribution status of target compounds between the stationary and mobile phase would be achieved by appropriate mobile phase and solvents, as well as influence on peak width [25, 26]. Due to the strong water solubility of 1-DNJ, water would help eluting, while the organic solvent would lead to 1-DNJ retaining on the stationary phase, which differ from distribution characters of other substances. Therefore, the mobile phase proportion and gradient elution procedures must be considered. For the organic solvent, methanol and MeCN were chosen for the test, and we found that using MeCN would acquire a better peak shape, smaller column pressure, and better stability of injection. Thus, MeCN was selected.

Furthermore, the proportion of the initial mobile phase and gradient elution procedure were optimized. It was found that a higher proportion of water at initial would lead to retention time earlier than 1 min and tend to bring matrix effect, which was unsatisfactory. However, higher ratio of the organic solvent would make matrix interferences be eluted more earlier. Thus, we set up several combinations of them to test the same samples, employing retention time, peak area, and full width at half maximum (FWHM) as parameters. It is shown in Table S1 that, with the increase of the proportion of the organic phase, the retention time decreased, and the peak area value of the target increased, while the FWHM that is closely related to column efficiency showed a gradual decrease. Considering these factors, the

mobile phase of water and MeCN with equal proportion was selected for this method. Moreover, the imino group in the 1-DNJ structure would lead to the cationic characteristic, so it is necessary to provide hydrogen ions for the ionization process by adding formic acid. We also verified the performance while adding 0.1% formic acid, finding that the response (peak area) increased by 22.6%, and the stability difference was also obvious. Finally, optimal initial of the mobile phase, elution gradient, and solvent for determination were confirmed.

3.1.3. Optimization of Instrument Parameters. Standard solution of 1-DNJ was injected directly into mass spectrometry by using the syringe pump and detected by the ESI source, acquiring a higher response in the positive mode than the negative mode. Strong response of the precursor ion appeared with m/z of 164.0, while product ions of m/z 146.0, 109.9, 128.0, and 69.0 showed relatively higher response. Thus, in the multiple reaction mode (MRM), based on the difference of response, m/z 146.0 was reasonable to be applied as the quantitation ion, while the other 3 ions were employed as qualification ions. From the overlaid ion chromatogram shown in Figure 2, we can see that the monitoring parameters can achieve an ideal absolute response value and relative response ratio.

3.2. Optimization on the Pretreatment Process and Parameters

3.2.1. Extraction Efficiency of Different Solvents. Mixed MeCN-water was employed as the extraction solvent in this study. We compared the extraction effect of different
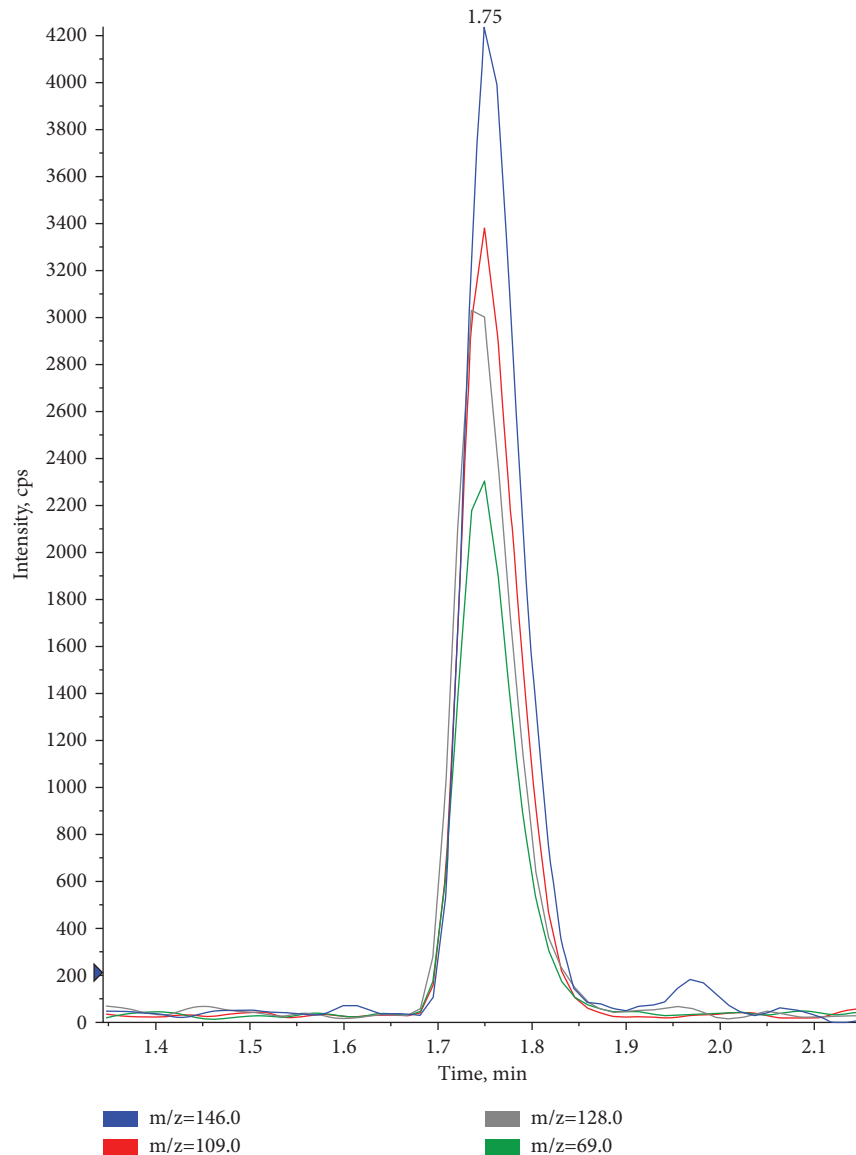
FIGURE 2: Overlaid chromatogram of four selective ions ($c = 50$ ng/mL).

proportions of MeCN in the extraction solvent (0%, 10%, 30%, 50%, 80%, and 100%), as shown in Figure 3. The highest extraction efficiency was achieved, while the MeCN content was 30%. Because of the strong water solubility of 1-DNJ, a higher proportion of water in the extraction solvent was needed, but it still needs some organic solvent to assist extraction.

3.2.2. Research on Purification. There are many coextracts in plant foods, including organic acids and chlorophyll [16]. These substances brought into the LC-MS system will not only cause the contamination of the HPLC system, ion source, and quadrupole mass analyzer but also lead to matrix effect and matrix interference, which will affect the accuracy of determination [27, 28]. Thus, purification for the extraction solvent was set as a key point of this study. Some processes applied in pesticide residue determination were

referred [29, 30], including disperse solid-phase extraction (d-SPE) based on GCB and PSA, as well as solid-phase extraction (SPE) based on cation exchange, and comparison was also taken among different cleanup procedures about the performance and efficiency. From Figure 4, we can see that average accuracies by d-SPE, SPE, and no cleanup process were 89.6%, 62.4%, and 106.3%, respectively. Although the accuracy of the no cleanup group seems higher, there was an interference peak that did not completely separate with the target peak, which seriously affected quantitation. For the group of SPE, strong water solubility of 1-DNJ leads to considerable loss in the eluting process, and the repeatability was not satisfactory.

Furthermore, dosages of GCB and PSA were discussed. We set the adding amount of both as 10 mg, 20 mg, 40 mg, and 80 mg in the orthogonal test to compare the parameters of accuracy, stability, and visual purification effect. It was found that accuracy of 1-DNJ improved with increasing
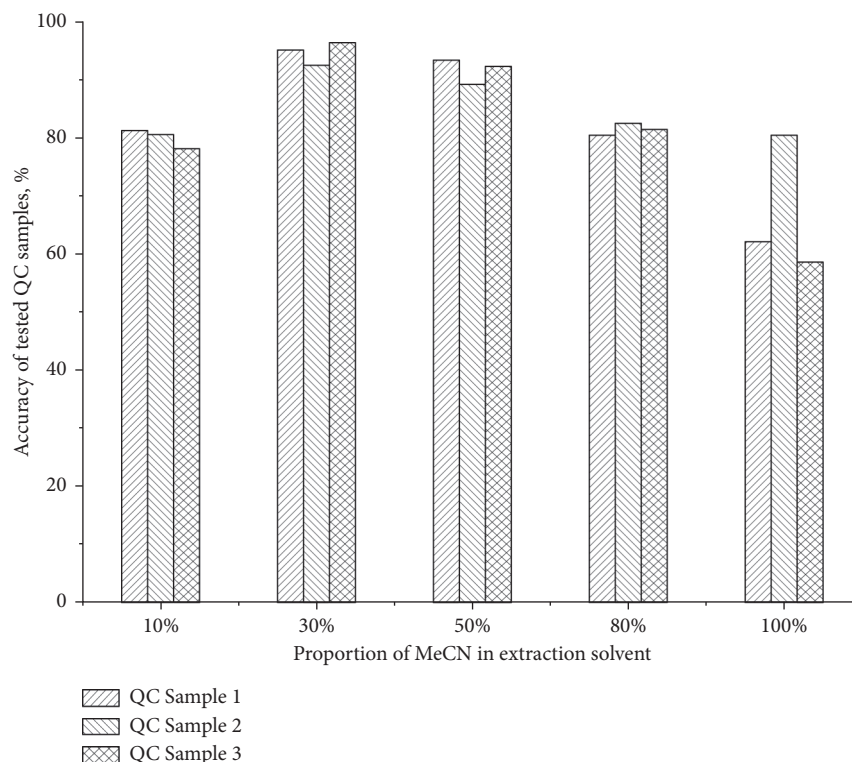
FIGURE 3: Influence of acetonitrile proportion in the solvent on 1-DNJ extraction efficiency.
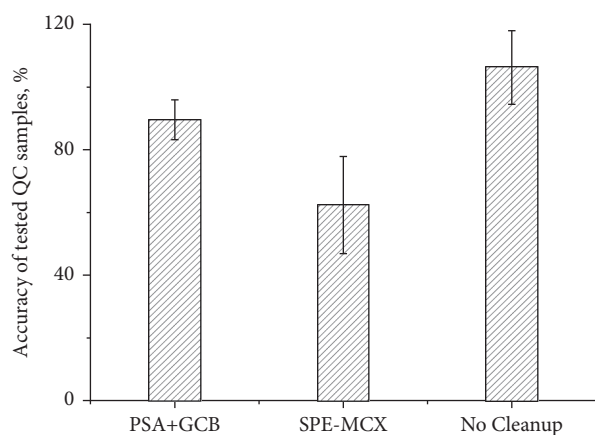
FIGURE 4: Influence of different purification processes on 1-DNJ detection accuracy.

adding amount of PSA, yet it showed little decrease when the adding amount of PSA was more than 40 mg. This may be because PSA could effectively adsorb interfering organic acids rather than alkaline compounds such as 1-DNJ, thus reducing matrix interference in mass spectrometry analysis. For GCB, similar regularity was found, but the accuracy significantly decreased while adding more than 40 mg. Due to the cyclic planar structure in 1-DNJ molecules, the target would be more or less adsorbed by GCB though there is no conjugated double bond. In terms of visible color, it is shown in Figure 5 that adding more than 20 mg GCB had little effect, indicating that 20–30 mg GCB added could adsorb most chlorophyll in the matrix extraction solvent.

Combining with the accuracy reference of the orthogonal test data in Table S2 and Figure 6, the amount of 45 mg PSA and 30 mg GCB was determined.

Purification for the extraction solvent will lead to results, the obvious one of which is the change of the acquired ion chromatogram. The extraction ion chromatograms are shown in Figure 7, including purified sample extraction solvent and unpurified one for two samples. It can be seen that the signal of interferences following the peak of 1-DNJ is markedly improved, which would help for the accuracy of quantitation. This is the important reason for employing the purification process.

3.2.3. Dilution Ratio. The contents of 1-DNJ in mulberry leaves were at the level of thousandth (w/w) [13, 31]. For LC-MS analysis, the optimal linear range was 10–500 ng/mL in this study. Thus, the dilution ratio of the extraction process was set at about 100 times, which means 0.5 g mulberry leaves were extracted with 50 mL extraction solvent and diluted by 50 times during purification and dilution.

3.3. Method Validation. Although the content of 1-DNJ in mulberry leaves was relatively high, the validation for limits of detection and quantitation (LOD and LOQ) was carried out completely in this study. Based on 3 times and 10 times of signal-to-noise ratio, they were acquired as 4 ng/mL and 10 ng/mL, respectively, and the corresponding method detection limit (MDL) and method quantitation limit (MQL) were 20 mg/kg and 50 mg/kg, respectively. For standard solvents with concentration higher than 500 ng/mL,
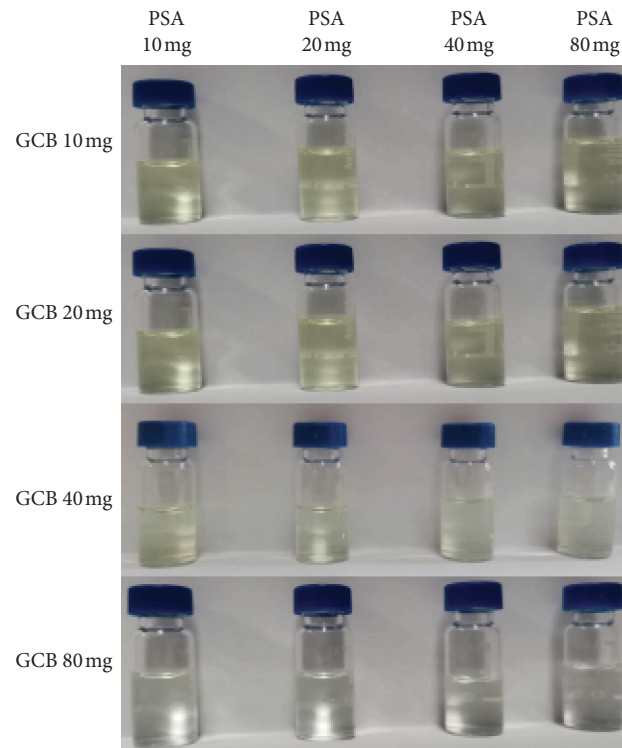
FIGURE 5: Visual color comparison of the orthogonal test for the adding amount of GCB and PSA.
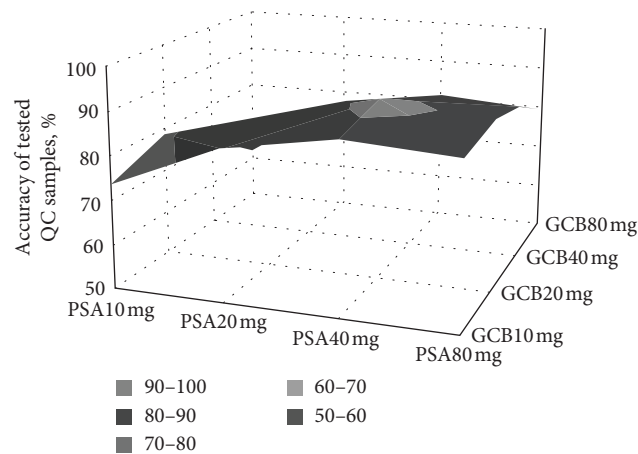
FIGURE 6: Response surface diagram of the data in Table S2.

considerable response attenuation was found, which may be because of competitive soft ionization of 1-DNJ in the ESI source, so the linear range of 10–500 ng/mL was determined. Six concentration points of 10, 20, 50, 100, 200, and 500 ng/mL were chosen for the calibration curve, and the linear equation was calculated as $Y = 1.3342e5X$, with correlation coefficient as 0.998. Precision and accuracy were also investigated by spiking in the positive QC sample, the 1-DNJ concentration of which was detected by this method as 0.78 mg/g. Spiked concentrations of 1-DNJ were 0.1, 0.5, and 2 mg/g, respectively, with six parallel samples for each concentration. Recoveries for the three levels were 96.4%, 95.7%, and 94.6%, respectively, while the relative standard

derivations (RSDs) were 0.9%, 1.2%, and 0.9%, respectively. The above validation data were satisfactory, indicating good method applicability.

Considering that negative samples of the mulberry leaf were hard to acquire, much less to prepare matrix standard solution, we investigated the matrix effect. 100 and 500 ng/mL levels of 1-DNJ were spiked into the test solution of positive samples that had already acquired response peak area to prepare matrix standard solution. The difference value of peak area before spiking and after spiking was employed as the peak area of spiked matrix standard solution. The matrix effect (ME) value was calculated by the equation $ME = A_{Matrix}/A_s$, where A_{Matrix} is the peak area of
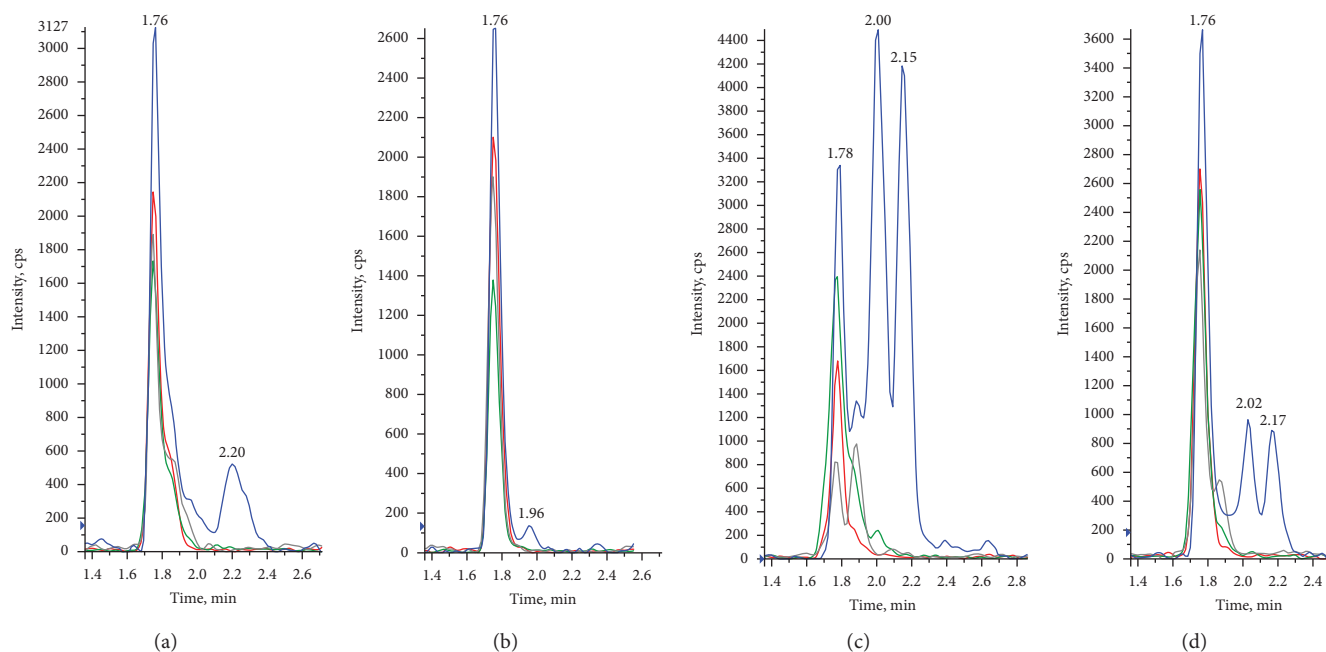
FIGURE 7: Comparison of chromatograms for purified and unpurified samples ($c = 50$ ng/mL). (a) Sample 1, unpurified. (b) Sample 1, purified. (c) Sample 2, unpurified. (d) Sample 2, purified.

spiked matrix standard solution and A_s is the peak area of pure solvent standard solution [19].

The ME was 0.91 and 0.93, respectively, at the concentration level of 100 and 500 ng/g, which shows little difference. The matrix effect value was considered to be negligible effect at the range of 0.9–1.1 in the previous study [32]. So, preparing standard solution by initial mobile phase solvent is suitable for this method.

3.4. Investigation of Method Applicability. In this study, thirteen mulberry leaf samples were collected from eight areas of China, and the information is shown in Table S3. All the samples were detected by this method and other two methods based on GC and HPLC, respectively [4, 5]. Every sample was set three parallel tests. The results are also listed in Table S3. There are some different analysis results between the three detection methods. Data of the GC group seem generally lower, and data of the HPLC group seem partially higher and with bad repeatability. The analysis results by this method showed best repeatability and most of them distributed fall in between the other two groups. This is mainly because both methods based on GC and HPLC required derivatization of 1-DNJ; thus, the uncertain efficiency and stability of derivatization lead to the test performance worse than the present study method. For this method, the RSDs of 13 samples ranged from 0.5% to 1.5%, indicating that this method is relatively mature and stable.

4. Conclusion

In this study, a new analysis method for the determination of 1-DNJ in mulberry leaves based on LC-MS was developed. Optimal parameters were determined by testing the

instrument analysis condition, while matrix interference was effectively reduced and satisfactory cleanup performance was acquired by studying the procedure process, especially disperse purification based on GCB and PSA. MDL and MQL were verified at 20 and 50 mg/kg, respectively, and this method exhibited good accuracy and precision based on different levels of spiked recovery test, while the matrix effect was found to be negligible. Comparing with the published methods detected by GC or HPLC, this developed method has solved the problems such as poor repeatability and quantitative inaccuracy brought by derivatization and improved the detection efficiency obviously. Furthermore, the developed approach can be used for massive monitoring and precise quantitation of 1-DNJ in mulberry leaves, and it has important application value and innovation significance.

Data Availability

The data used to support the findings of this study are included within the supplementary information file.

Conflicts of Interest

The authors declare that they have no conflicts of interest.

Acknowledgments

Health Service Special Subsidy in 2019, the National Traditional Chinese Medicine Resources Survey Project.

Supplementary Materials

Table S1: effect of different mobile phase compositions on the chromatographic peak ($c = 100$ ng/mL). Table S2: data of the orthogonal test for the adding amount of GCB and PSA ($n = 6$). Table S3: detection results of 1-DNJ from different kinds of mulberry leaf samples via three analysis methods. (*Supplementary Materials*)

References

[1] Q. Ge, L. Chen, M. Tang et al., "Analysis of mulberry leaf components in the treatment of diabetes using network pharmacology," *European Journal of Pharmacology*, vol. 833, pp. 50–62, 2018.

[2] T. Kimura, K. Nakagawa, H. Kubota et al., "Food-grade mulberry powder enriched with 1-deoxynojirimycin suppresses the elevation of postprandial blood glucose in humans," *Journal of Agricultural and Food Chemistry*, vol. 55, no. 14, pp. 5869–5874, 2007.

[3] K. Gao, C. Zheng, T. Wang et al., "1-Deoxynojirimycin: occurrence, extraction, chemistry, oral pharmacokinetics, biological activities and in silico target fishing," *Molecules*, vol. 21, no. 11, p. 1600, 2016.

[4] X. C. Zhang, "The study on determination of 1-deoxynojirimycin in mulberry leaves by gas chromatography," MA Dissertation, Northwest A & F University, Yangling, Xianyang, China, 2007.

[5] X. Zheng, J. Wu, J. He, and Y. Gao, "Determination of DNJ from mulberry leaves by RP-HPLC," *Journal of Chinese Institute of Food Science and Technology*, vol. 13, no. 1, pp. 188–194, 2013.

[6] J. Tang, Y. Chai, J. Peng et al., "Determination of 1-deoxynojirimycin in mulberry leaf using HPLC-UV with pre-column derivatization," *Lishizhen Medicine and Materia Medica Research*, vol. 27, pp. 1096–1098, 2016.

[7] X.-Q. Hu, L. Jiang, J.-G. Zhang, W. Deng, H.-L. Wang, and Z.-J. Wei, "Quantitative determination of 1-deoxynojirimycin in mulberry leaves from 132 varieties," *Industrial Crops and Products*, vol. 49, pp. 782–784, 2013.

[8] J.-W. Kim, S.-U. Kim, H. S. Lee, I. Kim, M. Y. Ahn, and K. S. Ryu, "Determination of 1-deoxynojirimycin in *Morus alba* L. leaves by derivatization with 9-fluorenylmethyl chloroformate followed by reversed-phase high-performance liquid chromatography," *Journal of Chromatography A*, vol. 1002, no. 1-2, pp. 93–99, 2003.

[9] E. Nuraniye and D. Emrah, "Determination of 1-Deoxynojirimycin by a developed and validated HPLC-FLD method and assessment of *In-vitro* antioxidant, α-Amylase and α-Glucosidase inhibitory activity in mulberry varieties from Turkey," *Phytomedicine*, vol. 53, pp. 234–242, 2019.

[10] S. Rodríguez-Sánchez, O. Hernández-Hernández, A. I. Ruiz-Matute, and M. L. Sanz, "A derivatization procedure for the simultaneous analysis of iminosugars and other low molecular weight carbohydrates by GC-MS in mulberry (*Morus* sp.)," *Food Chemistry*, vol. 126, no. 1, pp. 353–359, 2011.

[11] A. Masiá, M. M. Suarez-Varela, A. Llopis-Gonzalez, and Y. Picó, "Determination of pesticides and veterinary drug residues in food by liquid chromatography-mass spectrometry: a review," *Analytica Chimica Acta*, vol. 936, pp. 40–61, 2016.

[12] G. Balizs and A. Hewitt, "Determination of veterinary drug residues by liquid chromatography and tandem mass spectrometry," *Analytica Chimica Acta*, vol. 492, no. 1-2, pp. 105–131, 2003.

[13] N. Nuengchamnong, K. Ingkaninan, W. Kaewruang, S. Wongareonwanakij, and B. Hongthongdaeng, "Quantitative determination of 1-deoxynojirimycin in mulberry leaves using liquid chromatography-tandem mass spectrometry," *Journal of Pharmaceutical and Biomedical Analysis*, vol. 44, no. 4, pp. 853–858, 2007.

[14] X. Wang, H. Ouyang, Y. Feng, T. Dou, F. Bo, and J. He, "Method of LC-MS/MS for determination of 1-deoxynojirimycin from mulberry leaves of different habitats," *Journal of Liaoning University of TCM*, vol. 16, no. 12, pp. 60–62, 2014.

[15] B. Xu, D.-Y. Zhang, Z.-Y. Liu et al., "Rapid determination of 1-deoxynojirimycin in *Morus alba* L. leaves by direct analysis in real time (DART) mass spectrometry," *Journal of Pharmaceutical and Biomedical Analysis*, vol. 114, pp. 447–454, 2015.

[16] Y.-F. Li, L.-Q. Qiao, F.-W. Li, Y. Ding, Z.-J. Yang, and M.-L. Wang, "Determination of multiple pesticides in fruits and vegetables using a modified quick, easy, cheap, effective, rugged and safe method with magnetic nanoparticles and gas chromatography tandem mass spectrometry," *Journal of Chromatography A*, vol. 1361, pp. 77–87, 2014.

[17] A. G. Santos, A. C. D. Regis, G. O. Da Rocha, M. D. A. Bezerra, R. M. De Jesus, and J. B. De Andrade, "A simple, comprehensive, and miniaturized solvent extraction method for determination of particulate-phase polycyclic aromatic compounds in air," *Journal of Chromatography A*, vol. 1435, pp. 6–17, 2016.

[18] Y. Zhou, Y. Lian, X. Sun et al., "Determination of 20 perfluoroalkyl substances in greenhouse vegetables with a modified one-step pretreatment approach coupled with ultra performance liquid chromatography tandem mass spectrometry (UPLC-MS-MS)," *Chemosphere*, vol. 227, pp. 470–479, 2019.

[19] J.-N. Chen, Y.-J. Lian, Y.-R. Zhou et al., "Determination of 107 pesticide residues in wolfberry with acetate-buffered salt extraction and Sin-QuEChERS nano column purification coupled with ultra performance liquid chromatography tandem mass spectrometry," *Molecules*, vol. 24, no. 16, p. 2918, 2019.

[20] M. Á. González-Curbelo, B. Socas-Rodríguez, A. V. Herrera-Herrera et al., "Evolution and applications of the QuEChERS method," *TrAC Trends in Analytical Chemistry*, vol. 71, pp. 169–185, 2015.

[21] M. C. Bruzzoniti, L. Checchini, R. M. De Carlo, S. Orlandini, L. Rivoira, and M. Del Bubba, "QuEChERS sample preparation for the determination of pesticides and other organic residues in environmental matrices: a critical review," *Analytical and Bioanalytical Chemistry*, vol. 406, no. 17, pp. 4089–4116, 2014.

[22] S. J. Lehotay, K. Maštovská, and S. J. Yun, "Evaluation of two fast and easy methods for pesticide residue analysis in fatty food matrixes," *Journal of AOAC International*, vol. 88, no. 2, pp. 630–638, 2005.

[23] K. Mustafa, E. Mustafa, K. U. Mustafa, and A. Mehmet, "Comparison of different extraction and detection methods for sugars using amino-bonded phase HPLC," *Journal of Chromatographic Science*, vol. 41, no. 6, pp. 331–333, 2003.

[24] National Health and Family Planning Commission of the People's Republic of China (NHFPC), *GB 5009.8-2016 National Standard of Food Safety: Determination of Fructose, Glucose, Sucrose, Maltose and Lactose in Food*, China Standard Press, Beijing, China, 2016.

[25] L. A. Riddle and G. Guiochon, "Influence of mobile phase gradients on the retention and separation of peptides from a cytochrome-C digest by reversed-phase liquid chromatography," *Chromatographia*, vol. 64, no. 3-4, pp. 1–7, 2006.

[26] E. Cabo-Calvet, C. Ortiz-Bolsico, J. Baeza-Baeza, and M. C. García-Alvarez-Coque, "Description of the retention and peak profile for chromolith columns in isocratic and gradient elution using mobile phase composition and flow rate as factors," *Chromatography*, vol. 1, no. 4, pp. 194–210, 2014.

[27] S. Uclés, A. Lozano, A. Sosa, P. Parrilla Vázquez, A. Valverde, and A. R. Fernández-Alba, "Matrix interference evaluation employing GC and LC coupled to triple quadrupole tandem mass spectrometry," *Talanta*, vol. 174, pp. 72–81, 2017.

[28] H. Stahnke, T. Reemtsma, and L. Alder, "Compensation of matrix effects by postcolumn infusion of a monitor substance in multiresidue analysis with LC–MS/MS," *Analytical Chemistry*, vol. 81, no. 6, pp. 2185–2192, 2009.

[29] X. Liu, W. Guan, X. Hao, X. Wu, Y. Ma, and C. Pan, "Pesticide multi-residue analysis in tea using d-SPE sample cleanup with graphene mixed with primary secondary amine and graphitized carbon black prior to LC-MS/MS," *Chromatographia*, vol. 77, no. 1-2, pp. 31–37, 2014.

[30] G. Stubbings, J. Tarbin, A. Cooper, M. Sharman, T. Bigwood, and P. Robb, "A multi-residue cation-exchange clean up procedure for basic drugs in produce of animal origin," *Analytica Chimica Acta*, vol. 547, no. 2, pp. 262–268, 2005.

[31] X. Q. Shi, C. J. Chen, F. Li et al., "Determination of 1-deoxynojimycin content in leaves of mulberry cultivars in Shandong Province," *Science of Sericulture*, vol. 39, no. 1, pp. 177–182, 2013.

[32] L. Xiang, L. Chen, T. Xiao et al., "Determination of trace perfluoroalkyl carboxylic acids in edible crop matrices: matrix effect and method development," *Journal of Agricultural and Food Chemistry*, vol. 65, no. 39, pp. 8763–8772, 2017.

WILEY | Hindawi

Research Article

The Residues and Risk Assessment of Sulfonamides in Animal Products

Xiao-lei Zuo [ID] [1] **and Han Ai-yun** [ID] [2]

[1]*Shijiazhuang Animal Products and Veterinary Drug Feed Quality Testing Center, Shijiazhuang 050000, China*
[2]*Shijiazhuang University, Shijiazhuang 050000, China*

Correspondence should be addressed to Han Ai-yun; irene0001@126.com

Objective. To investigate and assess the risk of sulfonamide residues in livestock and poultry products in Shijiazhuang and determine the risk level of the dietary intake of sulfonamides, in order to provide the basis for the safety production, consumption, and safety supervision of livestock products. *Methods.* Totally, 1200 samples of livestock products were collected, and the samples were detected by high-performance liquid chromatography-tandem mass spectrometry. Combined with the data of Chinese residents' dietary survey in 2015, a nonparametric probability assessment model was constructed to assess the risk of sulfonamides in the livestock and poultry products of Shijiazhuang residents by using the professional risk assessment software @Risk. Risk assessment of the consumption of sulfonamide veterinary drugs in livestock and poultry products of Shijiazhuang residents was conducted. *Results.* Of the 1200 main livestock products tested, 8 were found to have sulfonamide residues, which were mainly sulfadiazine residue, sulfadiazine, and sulfadimethoxy, with the detection rates of 0.17%, 0.25%, and 0.25%, respectively. The average residual concentrations were 0.66, 0.50, and 0.50 g/kg, respectively, which were lower than the national residue limit of China (100 μg/kg). The food safety index was 2.95×10^{-4}, which was far less than 1. *Conclusion.* The risk of residual exposure to sulfonamides in livestock and poultry meat in Shijiazhuang is very low and is at a very safe level. However, it is still necessary to strengthen the supervision of animal products in order to reduce the residues of veterinary drugs in the human body.

1. Introduction

In recent years, livestock and poultry products, such as meat, eggs, and milk, are taking an increasing proportion in the diet of Chinese consumers, and food quality has received extensive concern throughout the society. Among others, sulfonamide residue is a critical influencing factor of livestock and poultry product quality. Sulfonamides are a type of synthetic drugs mainly used in livestock production and veterinarian clinical practices and are very effective to cure and prevent bacterial diseases and parasitic diseases [1]. Sulfonamides have made remarkable contribution to the development of stock farming industries ever since their extensive application, are especially featured by affordable cost, easy application, wide antimicrobial spectrum, and stable properties, and provide improved antimicrobial activity and bactericidal effect when used together with synergists [2]. Sulfonamides have a peculiar p-aminobenzenesulfonamide structure and compete with para-aminobenzoic acid for dihydrofolate synthetase in the body metabolism, preventing the synthesis of folic acid in the bacteria [3]. However, sulfonamides have a slow metabolism and long stay in the body, which result in excess residues in the livestock and poultry. Long-term intake of the animal products with excess sulfonamide residues may cause the building up of sulfonamide residues in the human body and cause a variety of toxic effects, such as hemopoietic system disorder, allergy, and cancer [4]. In the US and EU, laws and standards require that the maximum residue limit of sulfonamides in animal source foods is 100 μg/kg [4, 5], and in China, the maximum residue limit of sulfonamides in the animal muscle and liver is also 100 μg/kg (MOA Announcement No. 235) [6].

Currently, many research studies are focused on the risk assessment of pesticide residues in vegetables and fruits [7, 8], but the research on animal-based livestock and poultry products is mainly focused on the detection methods. There are also many research studies on the livestock and poultry product quality assurance and tracing systems as well as the detection methods [9, 10]; however, only a small number of the research studies are aimed to report and study the risk assessment of sulfonamide residues in livestock and poultry products. This research studies the sulfonamide residues and risk levels in livestock and poultry products available and marketed in Shijiazhuang, by taking 1,200 random samples of pork, beef, mutton, and chicken in Shijiazhuang, on the basis of livestock and poultry product quality monitoring findings in Shijiazhuang between 2015 and 2017 and by taking the 2015 Report on Chinese Resident's Chronic Disease and Nutrition and dietary guidelines into overall consideration and aims to provide data reference and scientific basis for resident's consumption and scientific supervision.

2. Materials and Methods

2.1. Sampling. Totally, 1,200 samples, in 600 g each, of pork, beef, mutton, and chicken products were collected from the markets of Shijiazhuang. The samples collected are products available in various markets: supermarkets, open fair, and slaughter companies, throughout the 18 counties and 6 districts in Shijiazhuang. After samples were collected, they are homogenized and stored in a refrigerator at −20°C. All samples were collected in accordance with *Sampling Criterion for the Monitoring of Veterinary Drug Residues in Animals and Animal Products* (NY/T 1897–2010) [11].

2.2. Reagents and Instruments

2.2.1. Reagents and Consumables. Methyl alcohol and acetonitrile (chromatographically pure, Fisher Scientific); n-hexane and n-propyl alcohol (analytically pure, Tianjin No.1 Chemical Reagent Factory), methanoic acid, acetic acid, ethyl acetate, sodium dihydrogen phosphate, and anhydrous sodium sulfate (analytically pure, Shenyang No. 1 Reagent Factory); solid-phase column extractor (Alumina-B SPE extractor, Waters); etc. were used. Experiment water is the ultrapure water produced by the Milli ultrapure water system.

2.2.2. Reference Material. The reference materials in this research are sulfonamides, which mainly and specifically include sulfadiazine (SD), sulfamerazine (SM1), sulfamethazine (SM2), sulfamonomethoxine (SMM), sulfadimethoxine (SDM), sulfamoxol, sulfamethoxazole (SMZ), sulfisoxazole (SIZ), sulfaquinoxaline (SQX), and sulfachloropyridazine (SCP) (purity ≥99.0%, China Institute of Veterinary Drug Control).

2.2.3. Instruments. A 5982–9110 solid-phase extraction device, 1290–6410B high-performance liquid chromatography-tandem mass spectrum analyzer (Agilent); 3K30 high-speed freezing centrifuge (SIGMA); RE-52AA rotary evaporator

(Shanghai Yarong), N-EVAP112 Termovap sample concentrator (Organomation); ultrapure water system (Millipore); SK-1 vortex mixer (Jiangsu Jintan); and BSA2202S electronic balance (Sartorius) were used.

2.3. Testing Method. Samples are tested in accordance with *Determination of Sulfonamide Residues in Edible Tissues of Animal, Liquid Chromatography-Tandem Mass Spectrometry* [12] (MOA Announcement No. 1025-23-2008) and reference resources of *Rapid analysis of fifteen sulfonamide residues in pork and fish samples by automated online solid phase extraction coupled to liquid chromatography-tandem mass spectrometry* [13] for the sulfonamide levels, and the results obtained from the tests are evaluated in accordance with the methods provided in the standard.

For all results reported as nondetectable, the data are processed in accordance with the principles provided in Session 2 of GEMS/FOOD regarding "reliable evaluation of contamination in food": data of the nondetectable samples should be substituted by the Limit of Detection (LOD) when more than 60% data are "not detected" or substituted by 1/2LOD when 60% and less data are "not detected" [14–16].

2.4. Average Intake of Livestock and Poultry Products by Consumer Groups in Shijiazhuang. As for the intake of animal source food, the Joint FAO/WHO Expert Committee on Food Additives (JECFA) is currently using a very conservative artificial estimation method against reference food, which assumes that a person of 60 kg body weight consumes 300 g animal/poultry muscle, equivalent to the upper limit of daily intake of animal tissue and products [17]. However, in this research, as shown in Table 1, the mean intake of animal products by consumers in Shijiazhuang is based on the *2015 Report on Chinese Resident's Chronic Disease and Nutrition* [18], according to which the mean daily intake of animal/poultry food by each Chinese resident is 89.7 g, including 64.3 g pork, 8.2 g other animal products, 2.5 g internal organs, and 14.7 g poultry food.

2.5. Mean Body Weight of Populations in Shijiazhuang. The mean body weight of populations in Shijiazhuang is based on the *2015 Report on Chinese Resident's Chronic Disease and Nutrition*, and this research only studies and evaluates the sulfonamide residues in animal/poultry food of adult consumers aged 18 or above and groups the research objects by age, place (urban or rural), and gender, on the basis of the reference intake of Chinese residents and food consumption models [19]. The body weight data of these target consumers are shown in Table 2.

2.6. Risk Assessment Methods. In accordance with the definition and procedures provided by the Codex Alimentarius Commission (CAC) for risk assessment of contaminants in foods, this research assesses the safety of animal/poultry products using the mean value of Index of Food Safety (IFS) [20]. The research is conducted on the basis of the Acceptable Daily Intake (ADI, in $\mu g/(kg \cdot bw \cdot d)$) provided by the Ministry

TABLE 1: Main food intake of Chinese residents in 2012 (g/d●person).

Group	Nationwide	City	Countryside
Pork	64.3	68.8	59.9
Cattle/sheep	8.2	10.5	6.0
Gut	2.5	2.9	2.2
Chicken	14.7	16.3	13.1
Sum	89.7	98.5	81.2

TABLE 2: Average weight of Chinese residents (kg).

Group (age)	Nationwide			City			Countryside		
	Male + female	Male	Female	Male + female	Male	Female	Male + female	Male	Female
18~44	62.00	67.00	56.70	63.10	68.70	57.20	61.00	65.30	56.30
45~59	63.10	66.60	59.50	64.50	68.50	60.40	61.50	64.40	58.40
≥60	58.90	62.40	55.60	61.00	61.00	57.40	56.70	60.00	53.60
Sum	61.80	66.20	57.30	63.20	68.00	58.20	60.40	64.30	56.30

of Agriculture and Rural Affairs for sulfonamides, adopts the internationally adopted probability assessment methods, i.e., a Monte Carlo simulation-based @Risk7.5 risk assessment software system in random simulations, by which the daily sulfonamide intake is obtained as the product of the daily intake of animal/poultry products multiplied by the sulfonamide residues, and estimates the exposure of main population groups in Shijiazhuang, both urban and rural, to the veterinary antibiotics through diet [21].

The evaluation and calculation formula is [22]

$$
\begin{aligned}
\text{EDI}_c &= \sum (R_i \times F_i), \\
\text{IFS}_c &= \sum \frac{R_i \times F_i \times f}{\text{SI}_c \times bw},
\end{aligned}
\tag{1}
$$

where IFS_C is the food safety index of sulfonamide C; EDI_C is the estimated daily intake of sulfonamide C; i is the type of livestock and poultry product; R_i is the residue level of sulfonamide C in product i, expressed as μg/kg; F_i is the per-capita daily intake of livestock and poultry product i, expressed as kg/person·day; bw is the body weight, expressed as kg; and f is a correction factor. $f = 1$, if the ADI, RFD, and PTDI are adopted as the safe intake data. SI_C is the safe intake and obtained from the ADI, PTWI, or RFD data depending on the chemicals concerned. In this research, the evaluation is based on the Acceptable Daily Intake (ADI, in μg/(kg·bw·d)) provided by the Ministry of Agriculture and Rural Affairs for veterinary drugs [6, 23]. According to related standards, the ADI for sulfonamides is, respectively, 10, 20, and 50 μg/(kg·d), among which the ADI for sulfadimidine is 50 μg/(kg·d). Some internationally adopted ADI values are also taken into consideration; specifically, the ADI for sulfadimethoxine is set as 6 μg/(kg·d) by referring to the internationally adopted 6 μg/(kg·d) ADI of sulfamonomethoxine.

The IFS value, if smaller than 1, means that the sulfonamides detected may cause insignificant harm to human health and the risks are acceptable, and if the IFS value is larger than 1, it means that the harm of sulfonamides detected to human health is unacceptable and the risk control procedures should be activated [24].

3. Analysis and Results

3.1. Sulfonamide Residues in Livestock and Poultry Products.
As shown in the Table 3, sulfonamide residues were detected in 8 out of 1,200 livestock and poultry meat samples collected from markets in Shijiazhuang, and the residues mainly include sulfamethazine, sulfamonomethoxine, and sulfadimethoxine, with detection rate being 0.17%, 0.25%, and 0.25%, and on the other hand, sulfadiazine, sulfamerazine, sulfamoxol, sulfamethoxazole, sulfisoxazole, sulfaquinoxaline, and sulfachloropyridazine were not detected. The mean residue concentration of sulfadimidine, sulfamonomethoxine, and sulfadimethoxine detected in the animal/poultry products is 0.66, 0.50, and 0.50 μg/kg, respectively, which are much lower than the maximum residue limit of 100 μg/kg as stipulated by national standards.

3.2. Risk Assessment on Sulfonamide Residues in Livestock and Poultry Products.
The risks of exposure to sulfonamides by residents in Shijiazhuang are assessed in accordance with the data of mean body weight and intake of main food by Chinese residents in 2012 as provided in the *2015 Report on Chinese Resident's Chronic Disease and Nutrition*. As shown in the Table 4, it is found through calculation that based on the intake of main food by Chinese residents, the per-capita daily exposure of Shijiazhuang residents to sulfonamide residues in food is 0.4459 μg, specifically 0.4897 μg for urban residents and 0.4037 μg for rural residents; and on the other hand, if calculated on the basis of per-capita daily consumption of 300 g animal/poultry muscle as provided by JECFA, the per-capita daily exposure of Shijiazhuang residents to sulfonamide residues in animal/poultry products is 1.4915 μg. The results obtained by both methods are far below the maximum acceptable daily intake of 30 μg. According to the second calculation method, the IFS is 2.95×10^{-4} and 1.02×10^{-3}, respectively, which are much lower than 1. The results show that the sulfonamide residues in animal/poultry products available in Shijiazhuang market are at very low level and are fairly safe. The index of food safety of sulfonamides in animal products of Shijiazhuang is shown in Table 5.

TABLE 3: Monitoring result of sulfonamide residues in animal products.

Sulfonamides	Sample numbers	Detectable numbers	Detectable rate/%	Excessive numbers	Excessive rate/%	Min/ (μg/kg)	Max/ (μg/kg)	Average/ (μg/kg)	SD/ (μg/kg)
Sulfamethazine	1200	2	0.17	0	0	ND	26.30	0.66	0.40
Sulfamonomethoxine	1200	3	0.25	0	0	ND	4.65	0.50	0.12
Sulfadimethoxine	1200	3	0.25	0	0	ND	3.93	0.50	0.10

TABLE 4: The exposure of sulfonamides in animal products (μg/d·person).

Group	Nationwide	City	Countryside
Min	0.0897	0.0985	0.0812
Middle	0.4459	0.4897	0.4037
Max	7.2146	7.9224	6.5309
JECFA		1.4915	

TABLE 5: The index of food safety of sulfonamides in animal products of Shijiazhuang.

Group	Age	Nationwide			City			Countryside		
		Male + female	Male	Female	Male + female	Male	Female	Male + female	Male	Female
Min	18~44	1.35×10^{-4}	1.26×10^{-4}	1.46×10^{-4}	1.45×10^{-4}	1.35×10^{-4}	1.58×10^{-4}	1.25×10^{-4}	1.18×10^{-4}	1.35×10^{-4}
	45~59	1.35×10^{-4}	1.25×10^{-4}	1.48×10^{-4}	1.46×10^{-4}	1.34×10^{-4}	1.61×10^{-4}	1.24×10^{-4}	1.16×10^{-4}	1.35×10^{-4}
	≥60	1.33×10^{-4}	1.26×10^{-4}	1.41×10^{-4}	1.43×10^{-4}	1.34×10^{-4}	1.52×10^{-4}	1.23×10^{-4}	1.18×10^{-4}	1.30×10^{-4}
	Sum	1.42×10^{-4}	1.34×10^{-4}	1.51×10^{-4}	1.51×10^{-4}	1.42×10^{-4}	1.60×10^{-4}	1.34×10^{-4}	1.26×10^{-4}	1.41×10^{-4}
	JECFA					1.40×10^{-4}				
Middle	18~44	2.94×10^{-4}	2.72×10^{-4}	3.21×10^{-4}	3.17×10^{-4}	2.91×10^{-4}	3.50×10^{-4}	2.70×10^{-4}	2.53×10^{-4}	2.93×10^{-4}
	45~59	2.89×10^{-4}	2.74×10^{-4}	3.06×10^{-4}	3.10×10^{-4}	2.92×10^{-4}	3.31×10^{-4}	2.68×10^{-4}	2.56×10^{-4}	2.83×10^{-4}
	≥60	3.09×10^{-4}	2.92×10^{-4}	3.28×10^{-4}	3.28×10^{-4}	3.28×10^{-4}	3.49×10^{-4}	2.91×10^{-4}	2.75×10^{-4}	30.8×10^{-4}
	Sum	2.95×10^{-4}	2.75×10^{-4}	3.18×10^{-4}	3.17×10^{-4}	2.94×10^{-4}	3.44×10^{-4}	2.73×10^{-4}	2.57×10^{-4}	2.93×10^{-4}
	JECFA					1.02×10^{-3}				
Max	18~44	3.31×10^{-3}	3.07×10^{-3}	3.62×10^{-3}	3.58×10^{-3}	3.28×10^{-3}	3.94×10^{-3}	3.05×10^{-3}	2.85×10^{-3}	3.30×10^{-3}
	45~59	3.26×10^{-3}	3.09×10^{-3}	3.45×10^{-3}	3.50×10^{-3}	3.29×10^{-3}	3.74×10^{-3}	3.02×10^{-3}	2.89×10^{-3}	3.18×10^{-3}
	≥60	3.49×10^{-3}	3.29×10^{-3}	3.70×10^{-3}	3.70×10^{-3}	3.49×10^{-3}	3.93×10^{-3}	3.28×10^{-3}	3.10×10^{-3}	3.47×10^{-3}
	Sum	3.32×10^{-3}	3.10×10^{-3}	3.59×10^{-3}	3.57×10^{-3}	3.32×10^{-3}	3.88×10^{-3}	3.08×10^{-3}	2.89×10^{-3}	3.30×10^{-3}
	JECFA					3.42×10^{-3}				

4. Discussion

It is found in the research that the toxic reaction of chemical contaminants is highly related to the absolute amount into the human body [25], and therefore, the actual intake of certain chemical contaminants into the body and its comparison with the safe intake amount is used to assess whether the food is safe or not, the Index of Food Safety (IFS) is used to describe whether the chemical contaminants taken into human body from food can cause harm to the human body, and the calculated results are used to assess the safety influence after consuming the food, so that the results are used to guide the risk control practice and actions are taken accordingly to lower the risks [26]. IFS takes the food consumption into overall consideration and reflects the level of food contamination and the harm to consumers by the contaminated food. Through the residue monitoring and dietary exposure assessment, we can effectively assess the level of harm to human health by certain contaminants in the food.

In this research, the IFS is used to compare the EDI of sulfonamide residues in animal/poultry products with the ADI values provided by the Chinese Ministry of Agriculture and Rural Affairs for sulfonamides [27], in order to assess the

potential risk level and food safety. In this research, there are some uncertainties in the calculation of exposure levels of sulfonamides; for example, a small amount of plucks are also included as animal/poultry meat in the diet of Chinese residents, besides the detection is mainly targeted at the sulfonamides as required by the testing method, while no detection and analysis are made for other sulfonamide-type veterinary drugs available in the market. The research mainly studies and assesses the exposure and risks of adults aged 18 and above; however, infants, children, and teenagers are not considered in the research. Given that the Chinese regulations on ADI of sulfamonomethoxine and sulfadimethoxine are not yet available, the evaluation is based on the internationally adopted ADI [23] of 6 μg/(kg·d), in order to ensure the stringency of the risk assessment.

Guan et al. [2] reported that, in the risk assessment on sulfonamide residues in pork in Heilongjiang, sulfamethazine residue is detected in only 1 of the 100 samples, with a detection rate of 1%, but the result is still below the maximum residue limit allowed by related national standards. Zhang et al. [3] reported that, in the studies on cumulative exposure to sulfonamides in chicken products by 10 typical populations in a Guangdong city, residues of sulfaquinoxaline, sulfamethazine, sulfamonomethoxine, and

sulfadiazine were detected in 9 out of 100 chicken samples; however, none of the residues detected are above the maximum allowed limit and that the IFS is far lower than 1. The abovementioned research shows that sulfonamide veterinary drugs are still widely used in the Chinese livestock and poultry farming industry and the use of sulfonamide veterinary drugs varies from region to region. This research finds that no animal/poultry products were detected with sulfonamide residues higher than the national maximum limit in recent years, besides the IFS obtained, respectively, on the basis of either the main food intake data and body weight data of Chinese residents and on the basis of the JECFA standard food consumption data is much smaller than 1, which indicates that the sulfonamide residues in animal/poultry products in Shijiazhuang will not cause harm to human health and are acceptable. However, it is found in the research that sulfamethazine, sulfamonomethoxine, and sulfadimethoxine residues were detected in the animal/poultry products, despite that the residue concentration remain much lower than the national maximum limit and will not cause any harm to human health, and these residues remain potential risks that may influence the food products from pork. As such, the governmental authorities should pay sufficient attention to such potential risks and strengthen the food safety supervision, to ensure the quality and safety of the animal/poultry products.

Data Availability

The data used to support the findings of this study are currently under embargo, while the research findings are commercialized. Requests for data, 12 months after publication of this article, will be considered by the corresponding author.

Conflicts of Interest

The authors declare no conflicts of interest.

Acknowledgments

References

[1] X. Z. Zhao and M. Y. Li, "Development of sulfonamides residues detection in edible animal products," *Chinese Journal of Food Hygiene*, vol. 24, no. 3, pp. 292–296, 2012.

[2] S. H. Guan, R. Li, H. R. Jin et al., "Detection and risk assessment of sulfonamide residues in pork from Heilongjiang province," *Heilongjiang Animal Science and Veterinary Medicine*, vol. 4, no. 1, pp. 288–260, 2017.

[3] W. J. Zhang, M. Y. Wang, H. X. Gui et al., "Residues and cumulative exposure estimate of sulfonamide in chickens," *Journal of Food Science*, vol. 34, no. 19, pp. 298–301, 2013.

[4] Z. L. Chen, *Veterinary Pharmacology*, China Agriculture Press, Beijing, China, 2002.

[5] S. X. Xu, *EU Regulations on Food Safety of Animal Origin*, China Agriculture Press, Beijing, China, 2003.

[6] Announcement 235th of the Ministry of Agriculture of People's Republic of China, "Maximum limit of veterinary drug residues in animal food [EB/OL]," 2002, http://jiuban.moa.gov.cn/zwllm/tzgg/gg/200302/%20t20030226_59300.%20htm.

[7] Y. F. Song, X. Lv, F. S. Ren et al., "Risk assessment of cypermethrin residues in vegetables," *Journal of Agro-Environment Science*, vol. 29, no. 12, pp. 2293–2298, 2010.

[8] J. Y. Nie, Z. X. Li, and C. D. Liu, "Risk assessment of pesticide residues in apples," *Sci. Agric. sin.* vol. 47, no. 18, pp. 3655–3667, 2014.

[9] Y. P. Tan, Y. N. Hu, C. H. Lu, and Y. D. Wei, "Application of big data technology in the quality and safety management innovation system of animal-derived food products," *Journal of Food Safety and Food Quality*, vol. 7, no. 7, pp. 2973–2981, 2016.

[10] S. J. Gu, H. Li, X. J. Niu et al., "Practice and enlightenment of the construction of traceability system of livestock products in developed countries and regions," *World Agriculture*, vol. 4, no. 12, pp. 4–10, 2016.

[11] *NY/T 1897–2010 Sampling Criterion for the Monitoring of Veterinary Drug Residues in Animals and Animal Products*, People's Publishing House, Beijing, China, 2010.

[12] Announcement of the Ministry of Agriculture of the People's Republic of China, "Determination of sulfonamides residues in edible tissues of animal liquid chromatography-tandem mass spectrometry [EB/OL]," 2008, http://jiuban.moa.gov.cn/zwllm/tzgg/gg/200805/t20080509_%201036076.%20htm.

[13] J. M. Ma, S. F. Fan, L. Sun, L. He, Y. Zhang, and Q. Li, "Rapid analysis of fifteen sulfonamide residues in pork and fish samples by automated on-line solid phase extraction coupled to liquid chromatography-tandem mass spectrometry," *Food Science and Human Wellness*, vol. 9, no. 4, pp. 363–369, 2020.

[14] X. Q. Wang, Y. N. Wu, and J. S. Chen, "Discussion on common problems in statistical processing of food safety risk monitoring data," *Chinese Journal of Preventive Medicine*, vol. 36, no. 4, pp. 63-64, 2002.

[15] C. B. Gong, Z. X. Wang, Y. L. Sun et al., "Application of statistic analysis processing on food safety risk surveillance date," *Chinese Journal of Food Hygiene*, vol. 25, no. 6, pp. 575–578, 2013.

[16] Z. H. Zhang, T. Tang, H. Xu et al., "Dietary intake risk assessment of forchlorfenuron residue in fruits and vegetables," *Sci. Agric. sin.* vol. 45, no. 10, pp. 1982–1991, 2012.

[17] Y. H. Li, W. P. Li, H. Li et al., "Overview of international risk assessment of veterinary drug residue in food of animal origin," *Chinese Journal of Veterinary Medicine*, vol. 42, no. 8, pp. 38–42, 2008.

[18] Bureau of Disease Prevention and Control of the National Health Planning Commission, *Report on the Status of Chinese Residents' Nutrition and Chronic Diseases (2015)*, People's Medical Publishing House, Beijing, China, 2015.

[19] Chinese Nutrition Society, *Dietary Guidelines of Chinese Residents (2016)*, People's Medical Publishing House, Beijing, China, 2016.

[20] Y. Chai, Y. J. Ying, Y. Li, L. J. Zhen, K. Y. Qiong, and X. Ying, "Risk estimate of vegetables based on food safety indexes methods in Chongqing," *Southwest China Journal of Agricultural Sciences*, vol. 23, no. 1, pp. 98–102, 2010.

[21] M. J. Gibney and V. H. Van-der, "Introduction to the monte carlo project and the approach to the validation of

probabilistic models of dietary exposure to selected food chemicals," *Food Additives & Contaminants*, vol. 20, no. S1, pp. 1–7, 2003.

[22] United States Environmental Protection Agency and OSWER Directive 9285, "6-03 human health evaluation manual supplemental guidance: standard default exposure factors," *Risk Assessment Guidance for Superfund (RAGS)*, USEPA Office of Emergency and Remedial Response, Washington, DC, USA, 1991.

[23] W. Zhang and C. Pan, "Acceptable daily intakes for agricultural and veterinary chemicals," *Chinese Journal of Veterinary Medicine*, vol. 39, no. 3, pp. 39–45, 2005.

[24] Institute of Quality Standards and Testing Technology for Agro-Products and Chinese Academy of Agricultural Science, *Risk Assessment for Quality and Safety of Agro-Foods: Principles, Methodologies and Applications*, Standards Press of China, Beijing, China, 2007.

[25] S. S. Lan, T. Lin, X. Lin et al., "Risk assessment of pesticide residues in edible mushrooms in southwest China based on food safety indexes," *Jiangsu Journal of Agricultural Sciences*, vol. 30, no. 1, pp. 199–204, 2014.

[26] L. P. Ma, S. M. Wang, S. Jiang et al., "Evaluation of safety risk of local vegetables by food safty index method," *Chinese Journal of Health Laboratory Technology*, vol. 24, no. 2, pp. 247–249, 2014.

[27] Y. Z. Qian and Y. Li, *Risk Assessment for Quality and Safety of Agro-Foods: Principles, Methodologies and Applications*, Standards Press of China, Beijing, China, 2007.

WILEY | Hindawi

Research Article

Identification of Secondary Metabolites in *Flammulina velutipes* by UPLC-Q-Exactive-Orbitrap MS

Ying Ding [iD],[1] **Sitan Chen** [iD],[1] **Honglin Wang** [iD],[1,2] **Shanlei Li** [iD],[1,2] **Changyang Ma** [iD],[1] **Jinmei Wang** [iD],[1] **and Lili Cui** [iD][1,3]

[1]*National R & D Center for Edible Fungus Processing Technology, Henan University, Kaifeng 475004, Henan, China*
[2]*Henan Longfeng Edible Fungi Industry Research Institute Co.,Ltd, Puyang 457300, China*
[3]*Functional Food Engineering Technology Research Center, Kaifeng 475004, Henan, China*

Correspondence should be addressed to Lili Cui; cuill@vip.henu.edu.cn

Flammulina velutipes is the fourth largest edible fungus in China with high nutritional value. In this paper, ultrahigh-performance liquid chromatography tandem hybrid quadrupole-Orbitrap mass spectrometry (UPLC-Q-Exactive-Orbitrap MS) was used to identify the secondary metabolites of *F. velutipes*. The metabolites were identified by comparing the retention time, accurate molecular weight, and MS^2 data with standard databases of mzVault and mzCloud (compound: 17,000$^+$) and BGI high-resolution accurate mass plant metabolome database (plant metabolite: 2500$^+$). Finally, 26 secondary metabolites were preliminarily identified, including flavonoids, phenylpropanoids, organic acids, and steroids.

1. Introduction

Flammulina velutipes is also known as golden needle mushroom and winter mushroom with high nutritional value and medicinal value. According to "Analysis of the National Statistical Survey Results of Edible Fungi in 2019," *F. velutipes* is the fourth largest edible fungus in China with an output of 2.589,600 tons in 2019. *F. velutipes* contains a variety of nutrients, including proteins, carbohydrates, mineral elements, vitamins, and crude fibers [1]. *F. velutipes* contains eighteen amino acids, including eight essential amino acids, of which lysine content is 1.09%. It has been proved that lysine and its derivatives can promote children's growth and development and enhance memory. Therefore, *F. velutipes* is also known as "Zengzhi mushroom" [2, 3]. It can not only be used as functional food but also has great potential in the development of medical and health products [4]. *F. velutipes* contains many active components, including polysaccharides, proteins, terpenoids, phenolic acids, and flavonoids [4–10]. Ishikawa et al. isolated and identified

sesquiterpenoids enokipodins A-D with the cyathane skeleton from *F. velutipes* [7, 8]. Five flavonoids were isolated and identified from *F. velutipes* by Hu et al. [10], named epicatechin, phillyrin, apigenin, kaempferol, and formononetin. *F. velutipes* has many pharmacological effects, such as antitumor [4], regulating immunity [4, 11], improving memory [5], antibacterial [8], antioxidation [12, 13], protecting the kidney [12], protecting the liver [14], neuroprotection [15], regulating intestinal flora [16], and improving constipation [17].

Ultrahigh-performance liquid chromatography tandem hybrid quadrupole-Orbitrap mass spectrometry (UPLC-Q-Exactive-Orbitrap MS) is a new type of liquid chromatography-mass spectrometry developed in recent years; it is also one of the techniques commonly used in metabolomics with the characteristics of high resolution, good quality and precision, and strong qualitative and quantitative abilities. It is used for the qualitative analysis of Chinese medicinal materials and can realize the rapid identification of various components [18]. At present,

there are few systematic studies on the secondary metabolites of *F. velutipes*. Therefore, in this paper, the secondary metabolites of *F. velutipes* were investigated to provide a reference for research on the chemical composition of *F. velutipes*.

2. Materials and Methods

2.1. Materials. Fruiting bodies of *F. velutipes* were obtained from Henan Longfeng Industrial Co., Ltd. The specimens (no. 2020-09-09) were saved at the National Research and Development Center of Edible Fungi Processing Technology, Henan University.

2.2. Reagent. d_3-Leucine, $^{13}C_9$-phenylalanine, d_5-tryptophan, and $^{13}C_3$-progesterone were used as the internal standard. Both methanol (A454-4) and acetonitrile (A996-4) were of mass spectral grade, which were purchased from Thermo Fisher Scientific, USA. Ammonium formate (17843-250G) was obtained from Honeywell Fluka, USA. Formic acid (50144-50 mL) was obtained from DIMKA, USA.

2.3. Preparation of the Sample. Dried fruiting bodies of *F. velutipes* were crushed by using the grinding machine. 200 g of *F. velutipes* powder was immersed with 50% ethanol (2000 mL) for 2 times at room temperature, each time for 3 days. The filtrate was lyophilized to obtain 87.2 g extract. The yield was 43.6%. 50 mg extract of *F. velutipes* was weighed, and then the sample was managed according to Yang et al. [19].

2.4. Chromatographic Conditions. The type of column was C18 Hypersil GOLD aQ (100 mm ∗ 2.1 mm, 1.9 μm). The mobile phases were 0.1% formic acid-water (liquid A) and 0.1% formic acid-acetonitrile (liquid B) with the elution gradient of 0–2 min 5% B; 2–22 min 5%–95% B; 22–27 min 95% B; 27.1–30 min 5% B. 0.3 mL/min, 40°C, and 5 μL were used as the flow rate, column temperature, and injection volume, respectively.

2.5. Mass Spectrometry Conditions. Ultraperformance liquid chromatography (Waters 2D UPLC, USA) tandem Q-Exactive high-resolution mass spectrometer (Thermo Fisher Scientific, USA) was used to separate and detect the metabolites. The mass spectrometry parameters were set according to Yang et al. [19]. In brief, 150–1500 and 70,000 were used as the mass range and MS resolution, respectively. 35,000 was used as MS^2 resolution. The fragmentation energy was 20, 40, and 60 eV. Sheath gas flow rate and aux gas flow rate were 40 and 10, respectively. Spray voltage ($|KV|$) of the positive ion mode and negative ion mode was 3.80 and 3.20, respectively. Ion capillary temperature and aux gas heater temperature were 320°C and 350°C, respectively.

2.6. Data Analysis. BGI high-resolution accurate mass plant metabolome database (plant metabolite: 2500⁺), mzCloud database (compound: 17000⁺), and mzVault database were used to identify the metabolites.

3. Results

3.1. Total Ion Chromatogram. The total ion current chromatogram of *F. velutipes* is shown in Figure 1.

3.2. Results of Metabolites' Identification. The metabolites of *F. velutipes* were analyzed by UPLC-Q-Exactive-Orbitrap MS, the structural identification of compounds in *F. velutipes* was based on the retention time, MS data, and MS^2 data compared with the BGI high-resolution accurate mass plant metabolome database (plant metabolite: 2500⁺), mzCloud database (compound: 17000⁺), and mzVault database. The identified metabolites were classified into three grades (level 1, level 2, and level 3) according to the comparison results. The credibility sequence is as follows: level 1 > level 2 > level 3. The detailed results are shown in Table 1. 26 compounds were preliminarily identified in *F. velutipes*, including 3 phenylpropanoids, 7 flavonoids, 1 steroid, and 15 organic acids.

3.2.1. Structural Analysis of Flavonoids. Flavonoids are easily deprotonated in the negative ion mode to produce ion $[M - H]^-$. Some flavonoids are protonated in the positive ion mode to produce ion $[M + H]^+$. Methylated flavonoids are prone to losing methyl to obtain ion $[M - H-CH_3]^-$ or $[M + H-CH_3]^+$. Flavone O-glycoside mainly lost the sugar group by glycosidic bond fracturing. The parent nucleus of flavonoids is prone to RDA cracking and lost the CO group [20, 21].

Compound 1 had a weak quasi-molecular ion in the positive ion mode, the ion of $[M + H]^+$ was *m/z* 593, and then it continuously lost rhamnosyl and glucosyl groups to obtain two fragment ions *m/z* 447 $[M + H\text{-rhamnosyl}]^+$ and *m/z* 285 $[M + H\text{-rhamnosyl-glucosyl}]^+$. The ion $[M + H\text{-rhamnosyl-glucosyl}]^+$ further lost methyl to obtain *m/z* 270 and then further lost the CO group to produce *m/z* 242 $[M + H\text{-rhamnosyl-glucosyl-}CH_3\text{-CO}]^+$. It was speculated that compound 1 was linarin. Possible MS fragmentation pathway of linarin is shown in Figure 2. The cracking process of compound 3 is similar to that of compound 1 with fragment ions of *m/z* 447 $[M + H]^+$, *m/z* 285 $[M + H\text{-glucosyl}]^+$, *m/z* 270 $[M + H\text{-glucosyl-}CH_3]^+$, and *m/z* 242 $[M + H\text{-glucosyl-}CH_3\text{-CO}]^+$. It was speculated that compound 3 may be glycitin.

Compound 2 was deprotonated in the negative ion mode to produce ion *m/z* 285 $[M - H]^-$ and then underwent RDA cracking to obtain two fragment ions *m/z* 133 $[M - H\text{-}C_7H_4O_4]^-$ and *m/z* 151 $[M - H\text{-}C_8H_6O_2]^-$. It was speculated that compound 2 may be luteolin. Possible MS fragmentation pathway of luteolin is shown in Figure 3. The cracking process of compound 4 is similar to that of compound 2 with fragment ions of *m/z* 269 $[M - H]^-$, *m/z* 117 $[M - H\text{-}C_7H_4O_4]^-$, and *m/z* 151 $[M - H\text{-}C_8H_6O]^-$. It was speculated that compound 4 may be apigenin.

Compound 5 was protonated in the positive ion mode to produce the ion *m/z* 301 $[M + H]^+$, then lost methyl to obtain *m/z* 286, and further lost the CO group to obtain *m/z* 258 $[M + H–CH_3–CO]^+$. It was speculated that compound 5 may be diosmetin.
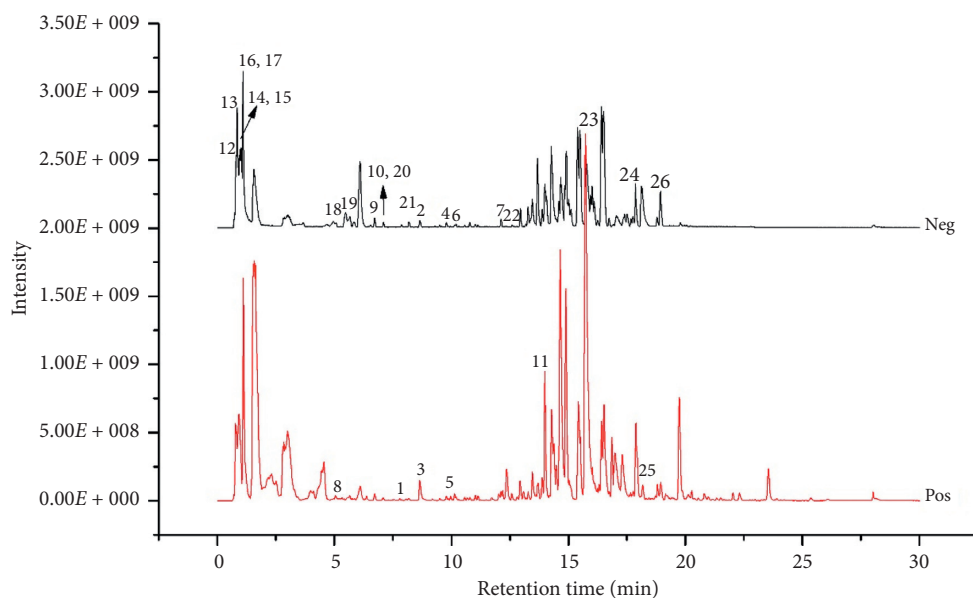
FIGURE 1: Total ion current chromatogram of *F. velutipes* in the positive ion mode (pos) and negative ion mode (neg).

Both compounds 6 and **7** contain a methoxy group, the quasi-molecular ion was m/z 299 $[M - H]^-$ and m/z 283 $[M - H]^-$, respectively, and then they lost the methyl unit to produce the ion $[M - H\text{-}CH_3]^-$ of m/z 284 and m/z 268, respectively. It was speculated that compounds 6 and **7** were hispidulin and acacetin, respectively.

3.2.2. Structural Analysis of Phenylpropanoids.

Compound 8 was protonated in the positive ion mode to produce ion m/z 193 $[M + H]^+$ and then produced two fragment ions m/z 165 and m/z 137; they may be $[M + H\text{-}CO]^+$ and $[M + H\text{-}2CO]^+$; the cracking process of compound 8 is consistent with that of coumarins [22]. It was speculated that compound 8 may be 5,7-dihydroxy-4-methylcoumarin.

Compounds 9 and 10 had the same quasi-molecular ion m/z 515 $[M - H]^-$, and both had characteristic fragment ions m/z 191 [quininic acid-H]$^-$ and m/z 173 [quininic acid-H-H_2O]$^-$. It was speculated that they were chlorogenic acids. The replacement position of caffeic acid can be determined according to the strength of the fragment ions [18]. Combined with the retention time, it was speculated that compounds 9 and 10 may be isochlorogenic acid B and isochlorogenic acid C, respectively. MS^2 spectrum of compounds 9 and 10 is shown in Figures 4 and 5, respectively.

3.2.3. Structural Analysis of Steroids.

Compound 11 was protonated in the positive ion mode to obtain the ion m/z 387 $[M + H]^+$ and then continuously lost the H_2O group to obtain fragment ions m/z 369 $[M + H\text{-}H_2O]^+$ and 351 $[M + H\text{-}2H_2O]^+$ [23]; combined with the retention time and accurate molecular weight, it was speculated that compound 11 may be bufalin.

3.2.4. Structural Analysis of Organic Acids.

Organic acids generally respond in the negative ion mode to produce ion $[M - H]^-$. The organic acids in *F. velutipes* were mostly fatty acids. They were prone to break apart and lose groups such as $(CH_2)_n$ and COOH [24]. In this paper, organic acids in *F. velutipes* mainly produce fragments that lose H_2O and CO_2. The structural analysis of some organic acid compounds is as follows.

Compound 12 responded in the negative ion mode to produce ion m/z 133 $[M - H]^-$, then lost the group H_2O to produce ion m/z 115 $[M - H\text{-}H_2O]^-$, and further lost the group CO_2 to produce ion m/z 71$[M - H\text{-}H_2O\text{-}CO_2]^-$. Combined with the retention time, accurate molecular weight, and the data of [25], it was speculated that compound 12 may be DL-malic acid. The structural analysis of other organic acids is similar to that of compound 12.

4. Discussion and Conclusion

Most of the compounds in *F. velutipes* have good biological activities. Hu et al. [15] investigated neuroprotective effects of six compounds from *F. velutipes* on H_2O_2-induced oxidative damage in PC12 cells, including arbutin, epicatechin, phillyrin, apigenin, kaempferol, and formononetin, and the results revealed that all components except apigenin mediate the apoptosis of PC12 cells via the endogenous pathway. In this paper, 7 flavonoids were identified by UPLC-Q-Exactive-Orbitrap MS, including linarin, luteolin, glycitin, apigenin, diosmetin, hispidulin, and acacetin. These flavonoids have many pharmacological effects such as antitumor, anti-inflammatory, and antioxidation. Luteolin has been showing numerous therapeutic activities such as anticancer, anti-inflammatory, antioxidation, and antimicrobial [26]. Apigenin has the cytostatic and cytotoxic effects on various cancer cells, prevents atherogenesis, hypertension, cardiac hypertrophy, ischemia/reperfusion-induced heart injury,

TABLE 1: Identification results of secondary metabolites in *F. velutipes*.

Number	RT (min)	Formula	Adducts	Measured values (m/z)	Theoretical value (Da)	Error (ppm)	MS²	Identification level	Name	Compound class
1	8.41	$C_{28}H_{32}O_{14}$	$[M+H]^+$	593.18524	593.18514	0.17	593 $[M+H]^+$, 447 $[M+H-rhamnosyl]^+$, 285 $[M+H-rhamnosyl-glucosyl]^+$, 270 $[M+H-rhamnosyl-glucosyl-CH_3]^+$, 242 $[M+H-rhamnosyl-glucosy-CH_3-CO]^+$	Level 1	Linarin	Flavonoids
2	8.509	$C_{15}H_{10}O_6$	$[M-H]^-$	285.03983	285.04053	−2.44	285 $[M-H]^-$, 151 $[M-H-C_8H_6O_2]^-$, 133 $[M-H-C_7H_4O_4]^-$	Level 2	Luteolin	Flavonoids
3	8.804	$C_{22}H_{22}O_{10}$	$[M+H]^+$	447.12946	447.12992	−1.03	447 $[M+H]^+$, 285 $[M+H-glucosyl]^+$, 270 $[M+H-glucosyl-CH_3]^+$, 242 $[M+H-glucosyl-CH_3-CO]^+$	Level 2	Glycitin	Flavonoids
4	9.46	$C_{15}H_{10}O_5$	$[M-H]^-$	269.04501	269.04573	−2.66	269 $[M-H]^-$, 151 $[M-H-C_8H_6O]^-$, 117 $[M-H-C_7H_4O_4]^-$	Level 1	Apigenin	Flavonoids
5	9.759	$C_{16}H_{12}O_6$	$[M+H]^+$	301.07047	301.07061	−0.46	301 $[M+H]^+$, 286 $[M+H-CH_3]^+$, 258 $[M+H-CH_3-CO]^+$	Level 2	Diosmetin	Flavonoids
6	9.764	$C_{16}H_{12}O_6$	$[M-H]^-$	299.05548	299.0562	−2.41	299 $[M-H]^-$, 284 $[M-H-CH_3]^-$	Level 1	Hispidulin	Flavonoids
7	11.787	$C_{16}H_{12}O_5$	$[M-H]^-$	283.06076	283.06135	−2.08	283 $[M-H]^-$, 268 $[M-H-CH_3]^-$	Level 1	Acacetin	Flavonoids
8	5.14	$C_{10}H_8O_4$	$[M+H]^+$	193.04933	193.04927	0.29	193 $[M+H]^+$, 165 $[M+H-CO]^+$, 137 $[M+H-2CO]^+$	Level 2	5,7-Dihydroxy-4-methylcoumarin	Phenylpropanoids
9	6.712	$C_{25}H_{24}O_{12}$	$[M-H]^-$	515.11823	515.1195	−2.47	515 $[M-H]^-$, 353, 335, 191 [quininic acid-H]$^-$, 179, 173 [quininic acid-H-H$_2$O]$^-$, 155, 135	Level 1	Isochlorogenic acid B	Phenylpropanoids
10	7.221	$C_{25}H_{24}O_{12}$	$[M-H]^-$	515.11835	515.11962	−2.47	515 $[M-H]^-$, 353, 191 [quininic acid-H]$^-$, 179, 173 [quininic acid-H-H$_2$O]$^-$, 135, 93	Level 1	Isochlorogenic acid C	Phenylpropanoids
11	14.001	$C_{24}H_{34}O_4$	$[M+H]^+$	387.2532	387.25326	−0.15	387 $[M+H]^+$, 369 $[M+H-H_2O]^+$, 351 $[M+H-2H_2O]^+$, 341, 143, 131, 105, 91, 81	Level 2	Bufalin	Steroids
12	1.006	$C_4H_6O_5$	$[M-H]^-$	133.01421	133.01437	−1.22	133 $[M-H]^-$, 115 $[M-H-H_2O]^-$, 71 $[M-H-H_2O-CO_2]^-$	Level 2	DL-malic acid	Organic acids
13	1.086	$C_5H_8O_5$	$[M-H]^-$	147.03015	147.03022	−0.48	147 $[M-H]^-$, 129 $[M-H-H_2O]^-$, 103 $[M-H-CO_2]^-$, 101, 87, 85, 57	Level 2	D-α-Hydroxyglutaric acid	Organic acids
14	1.093	$C_6H_5N\,O_2$	$[M-H]^-$	122.02499	122.02503	−0.33	122 $[M-H]^-$, 94 $[M-H-CO]^-$	Level 1	Picolinic acid	Organic acids
15	1.095	$C_6H_8O_7$	$[M-H]^-$	191.01964	191.01986	−1.17	191 $[M-H]^-$, 111[M-H-CO$_2$-2H$_2$O]$^-$, 111[M-H-CO$_2$-2H$_2$O]$^-$ 87	Level 1	Citric acid	Organic acids
16	1.141	$C_4H_6O_4$	$[M-H]^-$	117.01933	117.01931	0.21	117 $[M-H]^-$, 99 $[M-H-H_2O]^-$, 73 $[M-H-CO_2]^-$	Level 1	Succinic acid	Organic acids
17	1.161	$C_4H_4O_4$	$[M-H]^-$	115.00361	115.00362	−0.10	115 $[M-H]^-$, 71 $[M-H-CO_2]^-$	Level 1	Fumaric acid	Organic acids
18	4.225	$C_7H_{12}O_4$	$[M-H]^-$	159.0661	159.06625	−0.95	159 $[M-H]^-$, 115 $[M-H-CO_2]^-$, 97 $[M-H-CO_2-H_2O]^-$	Level 2	3-Methyladipic acid	Organic acids
19	5.199	$C_9H_{14}O_4$	$[M-H]^-$	185.08171	185.0819	−1.03	185 $[M-H]^-$, 141 $[M-H-CO_2]^-$, 123 $[M-H-CO_2-H_2O]^-$	Level 2	1-(Carboxymethyl) cyclohexanecarboxylic acid	Organic acids

TABLE 1: Continued.

Number	RT (min)	Formula	Adducts	Measured values (m/z)	Theoretical value (Da)	Error (ppm)	MS^2	Identification level	Name	Compound class
20	7.109	$C_9H_{16}O_4$	$[M-H]^-$	187.09744	187.09764	−1.05	187 $[M-H]^-$, 169 $[M-H-H_2O]^-$, 125 $[M-H-H_2O-CO_2]^-$, 97 $[M-H-H_2O-CO_2-CO]^-$	Level 1	Azelaic acid	Organic acids
21	8.302	$C_{10}H_{18}O_4$	$[M-H]^-$	201.11302	201.11329	−1.35	201 $[M-H]^-$, 183 $[M-H-H_2O]^-$, 139 $[M-H-H_2O-CO_2]^-$	Level 2	3-*tert*-Butyladipic acid	Organic acids
22	12.434	$C_{14}H_{26}O_4$	$[M-H]^-$	257.17542	257.17584	−1.62	257 $[M-H]^-$, 239 $[M-H-H_2O]^-$, 195 $[M-H-H_2O-CO_2]^-$	Level 2	Tetradecanedioic acid	Organic acids
23	16.105	$C_{14}H_{28}O_3$	$[M-H]^-$	243.1965	243.19673	−0.96	243 $[M-H]^-$, 197 $[M-H-HCOOH]^-$	Level 2	2-Hydroxymyristic acid	Organic acids
24	18.147	$C_{16}H_{32}O_3$	$[M-H]^-$	271.22733	271.22782	−1.80	271 $[M-H]^-$, 225 $[M-H-HCOOH]^-$	Level 2	16-Hydroxyhexadecanoic acid	Organic acids
25	18.531	$C_{16}H_{30}O_2$	$[M+H]^+$	255.23093	255.2311	−0.66	255 $[M+H]^+$, 237 $[M+H-H_2O]^+$, 219 $[M+H-2H_2O]^+$, 149, 135, 121, 97, 83, 81, 69	Level 2	Palmitoleic acid	Organic acids
26	18.934	$C_{18}H_{32}O_2$	$[M-H]^-$	279.23245	279.23298	−1.91	279 $[M-H]^-$, 261 $[M-H-H_2O]^-$, 59	Level 2	Linoleic acid	Organic acids
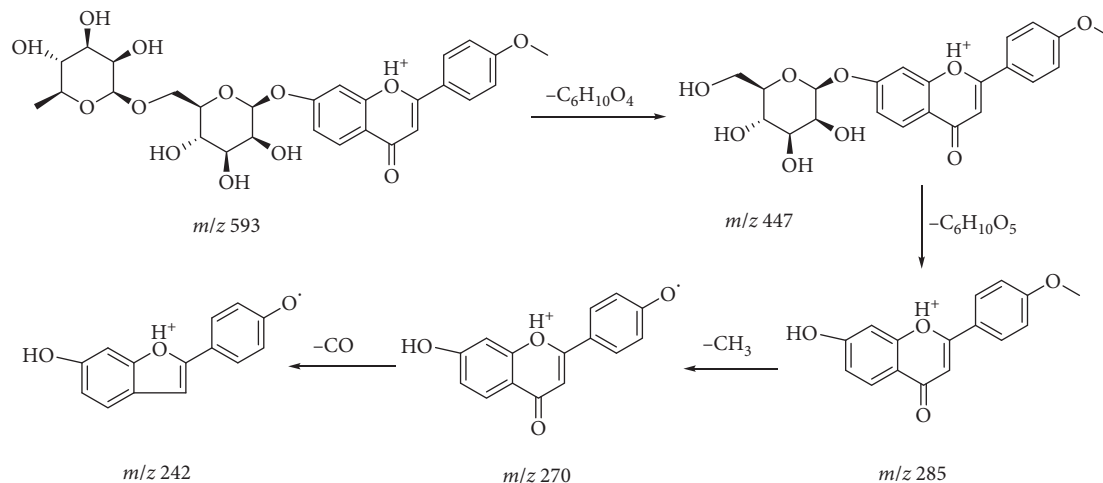
Figure 2: Possible MS fragmentation pathway of linarin.
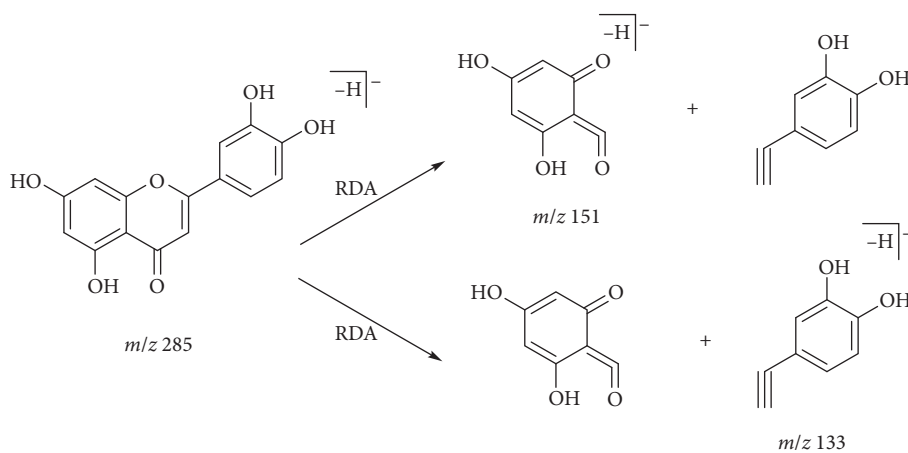
Figure 3: Possible MS fragmentation pathway of luteolin.
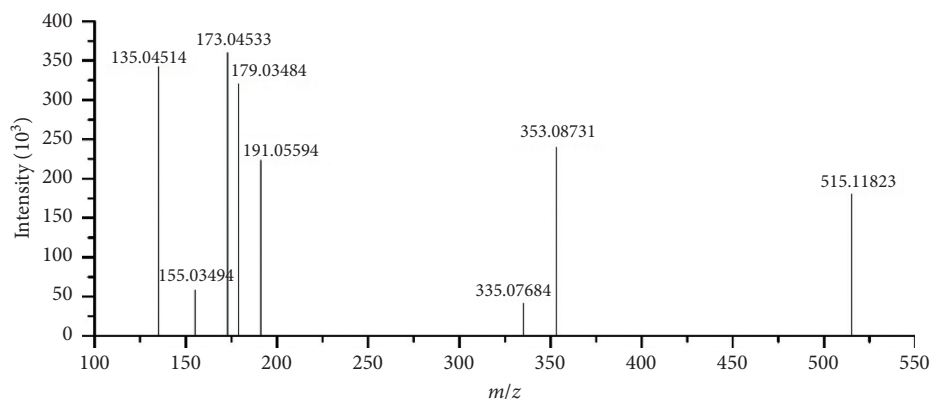
Figure 4: MS^2 spectrum of compound 9.

and autoimmune myocarditis, protects the chemical- and ischemia/reperfusion-induced liver injury, inhibits asthma, bleomycin-induced pulmonary fibrosis, abnormal behavior, and oxygen and glucose deprivation/reperfusion-induced neural cell apoptosis, and improves pancreatitis, type 2 diabetes and its complications, osteoporosis, and collagen-induced arthritis [27]. Acacetin has neuroprotective, cardioprotective, anticancer, anti-inflammatory, antidiabetic, and antimicrobial activities [28]. Hispidulin has diverse pharmacological effects such as anticancer, anti-
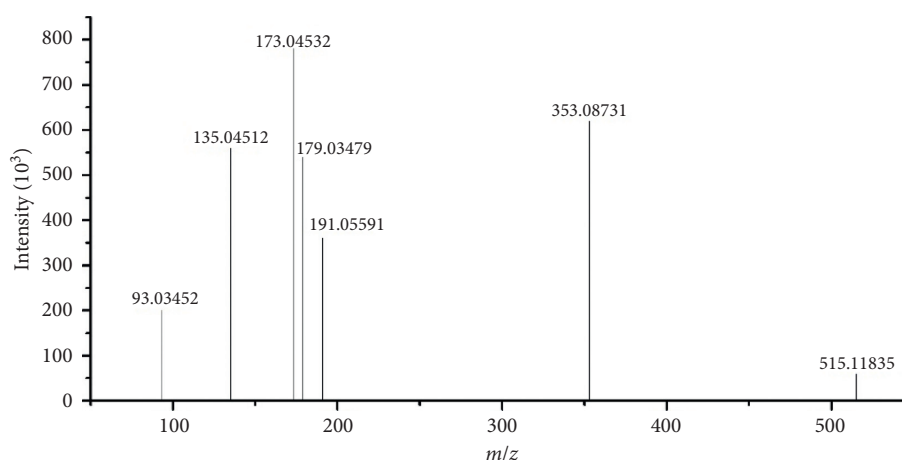
FIGURE 5: MS^2 spectrum of compound 10.

inflammatory, antifungal, antiplatelet, anticonvulsant, and antiosteoporotic [29]. Linarin could suppress glioma through inhibition of NF-κB/p65 and upregulating p53 expression *in vitro* and *in vivo* [30]. Glycitin has effects of alleviating lipopolysaccharide-induced acute lung injury via inhibiting NF-κB and MAPK pathway activation in mice [31]. Diosmetin has anti-inflammatory effects on IL-4- and LPS-induced macrophage activation and the atopic dermatitis model [32]. Therefore, it is beneficial to develop flavonoids in *F. velutipes*.

One steroid (bufalin) was identified in *F. velutipes* in this paper. Bufalin is one of the main pharmacological and toxicological components of Venenum Bufonis and many traditional Chinese medicine preparations [33]. Currently, there is no report of bufalin in *F. velutipes*. Whether *F. velutipes* contains bufalin needs more research to determine.

Chen et al. [25] investigated chemical compositions in the stipe and pileus of *F. filiformis* by UPLC-Q/TOF-MS, 130 compounds were identified, including 33 amino acids and derivatives, 34 nucleotides and derivatives, 37 organic acids and lipids, 9 carbohydrate alcohols, 8 alkaloids, and 9 other compounds, and most of them were primary metabolites. Han et al. [34] investigated chemical compositions of *F. velutipes*, 11 compounds were isolated and identified, including arabinitol, ergosterol, *cis*-9-tricosene, uracil, nicotinamide, xanthine, glycerol, adenosine, trehalose, mannitol, and tyrosine, and most of them were primary metabolites. In this paper, 26 secondary metabolites were preliminarily identified by UPLC-Q-Exactive-Orbitrap MS in *F. velutipes* from Henan province, including 3 phenylpropanoids, 7 flavonoids, 1 steroid, and 15 organic acids. It provides a reference for the future separation of chemical components of *F. velutipes*.

Data Availability

The data used to support the findings of this study are included within the article.

Conflicts of Interest

All authors declare that there are no conflicts of interest.

Acknowledgments

References

[1] Y. Zheng, C. Li, and N. X. Wang, "Research progress in polysaccharides from *Flammulina velutipes*," *Food Science*, vol. 31, no. 17, pp. 425–428, 2010.

[2] H. Wei, J. J. Xie, L. W. Wu et al., "Trients of the *Flammulina velutipes* and its functions," *Natural Product Research and Development*, vol. 9, no. 2, pp. 92–97, 1997.

[3] J. Y. Liu, *Separation and Exploitation of Bioactive Components from Flammulina velutipes*, Northwest A & F University, Xianyang, China, 2017.

[4] H. H. Chang, K. Y. Hsieh, C. H. Yeh, Y. P Tu, and F Sheu, "Oral administration of an Enoki mushroom protein FVE activates innate and adaptive immunity and induces anti-tumor activity against murine hepatocellular carcinoma," *International Immunopharmacology*, vol. 10, no. 2, pp. 239–246, 2010.

[5] W. Yang, J. Yu, L. Zhao et al., "Polysaccharides from *Flammulina velutipes* improve scopolamine-induced impairment of learning and memory of rats," *Journal of Functional Foods*, vol. 18, pp. 411–422, 2015.

[6] G. E. Pelin, A. Ilgaz, K. Fatih et al., "Fatty acid compositions of six wild edible mushroom species," *The Scientific World Journal*, vol. 2013, Article ID 163964, 4 pages, 2013.

[7] N. K. Ishikawa, K. Yamaji, S. Tahara, Y Fukushi, and K Takahashi, "Highly oxidized cuparene-type sesquiterpenes from a mycelial culture of *Flammulina velutipes*," *Phytochemistry*, vol. 54, no. 8, pp. 777–782, 2000.

[8] N. K. Ishikawa, Y. Fukushi, K. Yamaji, S Tahara, and K Takahashi, "Antimicrobial cuparene-type sesquiterpenes, Enokipodins C and D, from a mycelial culture of *Flammulina velutipes*," *Journal of Natural Products*, vol. 64, no. 7, pp. 932–934, 2001.

[9] M. A. Rahman, N. Abdullah, and N. Aminudin, "Antioxidative effects and inhibition of human low density lipoprotein oxidation in vitro of polyphenolic compounds in

Flammulina velutipes (Golden Needle Mushroom)," *Oxidative Medicine and Cellular Longevity*, vol. 2015, Article ID 403023, 10 pages, 2015.

[10] Q. Hu, J. Yu, W. Yang et al., "Identification of flavonoids from *Flammulina velutipes* and its neuroprotective effect on pheochromocytoma-12 cells," *Food Chemistry*, vol. 204, pp. 274–282, 2016.

[11] Z. Yin, Z. Liang, C. Li et al., "Immunomodulatory effects of polysaccharides from edible fungus: a review," *Food Science and Human Wellness*, vol. 10, no. 4, pp. 393–400, 2021.

[12] L. Lin, F. Cui, J. Zhang et al., "Antioxidative and renoprotective effects of residue polysaccharides from *Flammulina velutipes*," *Carbohydrate Polymers*, vol. 146, pp. 388–395, 2016.

[13] Y. Zhang, D. Wang, Y. Chen et al., "Healthy function and high valued utilization of edible fungi," *Food Science and Human Wellness*, vol. 10, no. 4, pp. 408–420, 2021.

[14] Y. Zhang, H. Li, T. Hu et al., "Metabonomic profiling in study hepatoprotective effect of polysaccharides from *Flammulina velutipes* on carbon tetrachloride-induced acute liver injury rats using GC-MS," *International Journal of Biological Macromolecules*, vol. 110, pp. 285–293, 2018.

[15] Q. Hu, D. Wang, J. Yu et al., "Neuroprotective effects of six components from *Flammulina velutipes* on H_2O_2-induced oxidative damage in PC12 cells," *Journal of Functional Foods*, vol. 37, pp. 586–593, 2017.

[16] J. Ye, X. Wang, K. Wang et al., "A novel polysaccharide isolated from *Flammulina velutipes*, characterization, macrophage immunomodulatory activities and its impact on gut microbiota in rats," *Journal of Animal Physiology and Animal Nutrition*, vol. 104, no. 2, pp. 735–748, 2020.

[17] X. Xin, K. W. Zheng, Y. Y. Niu et al., "Effect of *Flammulina velutipes* (golden needle mushroom, eno-kitake) polysaccharides on constipation," *Open Chemistry*, vol. 16, no. 1, pp. 155–162, 2018.

[18] B. Zeng, H. M. Liu, X. M. Liu et al., "Application of UPLC-Q-exactive orbitrap MS Technology in analysis of traditional Chinese medicine," *Journal of Chinese Medicinal Materials*, vol. 43, no. 9, pp. 2313–2319, 2020.

[19] F. Yang, H. L. Wang, G. Q. Feng et al., "Rapid identification of chemical constituents in *Hericium erinaceus* based on LC-MS/MS metabolomics," *Journal of Food Quality*, vol. 2021, Article ID 5560626, 10 pages, 2021.

[20] D. D. Luo, H. S. Peng, Y. Zhang et al., "Comparison of chemical components between Artemisia stolonifera and *Artemisia argyi* using UPLC-Q-TOF-MS," *China Journal of Chinese Materia Medica*, vol. 45, no. 17, pp. 4057–4064, 2020.

[21] G. H. Chang, Y. Y. Bo, J. Cui et al., "Identification on chemical constituents of aerial parts of *Glycyrrhiza uralensis* by UPLC-Q-Exactive Orbitrap-MS," *China Journal of Chinese Materia Medica*, vol. 46, no. 6, pp. 1449–1459, 2021.

[22] X. Li, H. Shi, J. X. Ding et al., "Analysis of chemical constituents as flavonoids and coumarins in radix ardisiae from different sources," *China Pharmacy*, vol. 32, no. 4, pp. 443–452, 2014.

[23] J. He, Y. Li, N. Si et al., "Comparison of the chemical composition between fresh and dried Venenum Bufonis by UPLC-Orbitrap MS," *Acta Pharmaceutica Sinica*, vol. 49, no. 10, pp. 1446–1450, 2014.

[24] Q. L. Kang, Z. Z. Li, S. S. Fan et al., "Qualitative analysis on *Perilla frutescens* leaves and stalks by UPLC-Q-exactive-orbitrap-MS," *Chinese Journal of Experimental Traditional Medical Formulae*, vol. 26, no. 13, pp. 156–162, 2020.

[25] Y. L. Chen, Q. Li, S. J. Chen et al., "UHPLC- Q/TOF-MS Analysis on chemical compounds in stipe and pileus of *Flammulina filiformis*," *Acta Edulis Fungi*, vol. 28, no. 1, pp. 75–90, 2021.

[26] M. F. Manzoor, N. Ahmad, Z. Ahmed et al., "Novel extraction techniques and pharmaceutical activities of luteolin and its derivatives," *Journal of Food Biochemistry*, vol. 43, no. 9, Article ID e12974, 2019.

[27] X. Zhou, F. wang, R. J. Zhou et al., "Apigenin: a current review on its beneficial biological activities," *Journal of Food Biochemistry*, vol. 41, no. 4, Article ID e12376, 2017.

[28] R. B. Semwal, D. K. Semwal, S. Combrinck et al., "Acacetin-A simple flavone exhibiting diverse pharmacological activities," *Phytochemistry Letters*, vol. 32, pp. 56–65, 2019.

[29] K. L. Liu, F. Zhao, J. J. Yan et al., "Hispidulin: a promising flavonoid with diverse anti-cancer properties," *Life Sciences*, vol. 259, Article ID 118395, 2020.

[30] Z.-G. Zhen, S.-H. Ren, H.-M. Ji et al., "Linarin suppresses glioma through inhibition of NF-κB/p65 and up-regulating p53 expression in vitro and in vivo," *Biomedicine & Pharmacotherapy*, vol. 95, no. 1, pp. 363–374, 2017.

[31] Y. Chen, S. Guo, K. Jiang et al., "Glycitin alleviates lipopolysaccharide-induced acute lung injury via inhibiting NF-κB and MAPKs pathway activation in mice," *International Immunopharmacology*, vol. 75, Article ID 105749, 2019.

[32] D. H. Lee, J. K. Park, J. Choi, H Jang, and J. W Seol, "Anti-inflammatory effects of natural flavonoid diosmetin in IL-4 and LPS-induced macrophage activation and atopic dermatitis model," *International Immunopharmacology*, vol. 89, Article ID 107046, 2020.

[33] M. Li, X.-J. Wang, Q. Zhao et al., "Bufalin-induced cardiotoxicity: new findings into mechanisms," *Chinese Journal of Natural Medicines*, vol. 18, no. 7, pp. 550–560, 2020.

[34] L. Han, N. Feng, and W. Han, "Chemical components of *Flammulina velutipes* fruiting bodies," *Acta Edulis Fungi*, vol. 22, no. 4, pp. 53–57, 2015.

WILEY | Hindawi

Research Article

Rapid Identification of Chemical Constituents in *Artemisia argyi* Lévi. et Vant by UPLC-Q-Exactive-MS/MS

Lili Cui [ID],[1,2] **Xianzhong Wang** [ID],[1,3] **Jie Lu** [ID],[1] **Jing Tian** [ID],[1] **Li Wang** [ID],[1] **Jiaojiao Qu** [ID],[1] **Zhenhua Liu** [ID],[1] **and Jinfeng Wei** [ID][1,4]

[1]*National R and D Center for Edible Fungus Processing Technology, Henan University, Kaifeng 475004, Henan, China*
[2]*Kaifeng Key Laboratory of Functional Components,Health Food, Henan Province, Kaifeng 475004, China*
[3]*Zhumadian Xusheng Agricultural Technology Co.,Ltd., Zhumadian 463800, China*
[4]*Minsheng College, Henan University, Kaifeng 475004, Henan, China*

Correspondence should be addressed to Zhenhua Liu; liuzhenhua623@163.com and Jinfeng Wei; weijinfeng20112011@ hotmail.com

Artemisia argyi Lévi. et Vant is a traditional Chinese medicine with a long history, and its buds and seedlings can be used as vegetables. However, the investigations on the chemical constituents of *A. argyi* are not sufficient. In this paper, ultra-high performance liquid chromatography tandem hybrid quadrupole-orbitrap mass spectrometry (UPLC-Q-Exactive-MS/MS) was used to identify the chemical constituents of *A. argyi*. The Q Exactive mass spectrometer was used to collect MS and MS^2 data. Finally, 125 compounds were preliminarily identified in *A. argyi* by comparing the retention time and accurate molecular weight with standard databases such as MZVault, MZCloud, and BGI Library (self-built standard Library by BGI Co., Ltd), including flavonoids, phenylpropanoids, terpenoids, and organic acids.

1. Introduction

Artemisia argyi Lévi. et Vant belongs to Asteraceae family, widely distributed in China. *A. argyi* is a traditional Chinese medicine with a long history, and its buds and seedlings can be used as vegetables. According to flora of China, *A. argyi* has functions of warming menstrual cycle, removing dampness, dispersing cold, hemostasis, anti-inflammation, relieving asthma, relieving cough, calming fetus and anti-allergy with whole grass as medicine [1, 2]. According to Chinese Pharmacopoeia (2020), Artemisiae argyi folium (*A. argyi* leaves) has minor poison, its nature and flavour are warm, pungent, and bitter, and its channel tropism is in liver, spleen, and kidney. *A. argyi* leaves have warm meridian to stop bleeding, disperse cold, and relieve pain and external clearing damp antipruritic effect [3].

At present, research about chemical constituents of *A. argyi* was focused on *A. argyi* leaves. Research showed that the chemical constituents of *A. argyi* leaves include volatile oil, flavonoids, terpenoids, phenylpropanoids, organic acids, and steroids. Among them, more than 200 volatile oils from *A. argyi* leaves have been identified, and 182 nonvolatile components have been isolated and identified [2, 4]. Pharmacological studies have shown that *A. argyi* leaves have many pharmacological effects, such as antibacterial, antiviral, hemostatic, anti-tumor, protecting liver and gallbladder, and anti-oxidation, relieving cough and asthma, analgesia, anti-inflammatory, and immune regulation. Moxibustion has the effect of warming and dispersing cold and treating all diseases [2, 4–6]. With the development of the health industry, more and more attention has been paid to the study of *A. argyi* leaves and moxa [6]. In recent years, systematic studies on the chemical constituents of *A. argyi* leaves or *A. argyi* have gradually increased [7, 8]. With the mature application of LC-MS/MS technology in the rapid identification of plant and food stuff ingredients [9–11], research studies on the rapid analysis of nonvolatile components of *A. argyi* leaves or *A. argyi* are gradually increasing

[12–15], but there are few identified compounds. Ultra-high performance liquid chromatography tandem hybrid quadru-pole-orbitrap mass spectrometry (UPLC-Q-Exactive-MS/MS) is a new type of liquid chromatography-mass spectrometry developed in recent years, which has the characteristics of high resolution, good quality and precision, and strong qualitative and quantitative ability [16, 17]. Samples can be separated quickly by ultra-high performance liquid chromatography, and accurate molecular weight can be determined by high-reso-lution mass spectrometry to obtain molecular formula of compounds. Zhumadian region is abundant with *A. argyi*; however, research about chemical components of *A. argyi* from Zhumadian region was less. Therefore, in this study, UPLC-Q-Exactive-MS/MS combined with standard substance database was used to rapidly identify the nonvolatile chemical components of *A. argyi* from Zhumadian region.

2. Materials and Methods

2.1. Instrument. Rotary evaporator (N-1300) was purchased from EYELA. Ultra-performance liquid chromatograph (Waters 2D UPLC) was purchased from Waters, USA. High-resolution mass spectrometer (Q Exactive) was purchased from Thermo Fisher Scientific, USA. Hypersil GOLD aQ column (100 mm × 2.1 mm, 1.9 μm) was purchased from Thermo Fisher Scientific, USA. Low temperature high speed centrifuge (Centrifuge 5430) was purchased from Eppendorf. Vortex finder (QL-901) was purchased from Qilinbeier In-strument Manufacturing Co., Ltd. Pure water meter (Milli-Q) was purchased from Integral Millipore Corporation, USA.

2.2. Reagent. d$_3$-Leucine, ^{13}C$_9$-Phenylalanine, d$_5$-Trypto-phan, and ^{13}C$_3$-Progesterone were used as internal standard. Methanol (A454-4) and acetonitrile (A996-4) were both in mass grade, which were purchased from Thermo Fisher Scientific, USA. Ammonium formate (17843–250G) was ob-tained from Honeywell Fluka, USA. Formic acid (50144–50 mL) was obtained from DIMKA, USA. 95% ethanol (20190320) was obtained from Tianjin Fuyu Fine Chemicals Co., Ltd. Water was supplied by a pure water meter.

2.3. Plants. *A. argyi* was collected in July 2020 in Wanhei Village, Shangcai County, Zhumadian City, and identified as the aerial part of *A. argyi* by professor Li Changqin of Henan University. The specimens (No. 2020-08-10) were saved in National Research and Development Center of Edible Fungi Processing Technology, Henan University.

2.4. Preparation of Sample. 10 g of *A. argyi* powder was accurately weighed and impregnated with 25 times 70% ethanol for 2 times at room temperature, each time for 2 days. The extraction was filtered, and filtrate was combined and concentrated. The extract was added with 70% ethanol to 1 g/mL of the original materials and then reserved. 200 μL was sent to BGI Co., Ltd., for chemical composition identification.

2.5. Chromatographic Conditions. Hypersil GOLD aQ col-umn (100 mm × 2.1 mm, 1.9 μm) was used to do LC-MS ex-periment. The mobile phase was 0.1% formic acid-water (liquid A) and 0.1% formic acid-acetonitrile (liquid B). The following gradients were used for elution: 0–2 min 5% B; 2–22 min 5%–95% B; 22–27 min 95% B; 27.1–30 min 5% B. The flow rate was 0.3 mL/min, the column temperature was 40°C, and the in-jection volume was 5 μL.

2.6. Mass Spectrometry Conditions. The mass range was 150–1500, the MS resolution was 70000, the AGC was 1e^6, and the maximum injection time was 100 ms. According to the strength of the MS ions, TOP3 was selected for frag-mentation. The MS^2 resolution was 35000, AGC is 2e^5, the maximum injection time was 50 ms, and the fragmentation energy were set as 20, 40, and 60 eV. Ion source (ESI) pa-rameter settings: sheath gas flow rate was 40, aux gas flow rate was 10, spray voltage (|KV|) of positive ion mode was 3.80, spray voltage (|KV|) of negative ion mode was 3.20, ion capillary temp was 320°C, and aux gas heater temp was 350°C.

2.7. Data Analysis. UPLC-MS/MS technology was used to systematically analyze the chemical constituents of *A. argyi*. High-resolution mass spectrometer Q Exactive (Thermo Fisher Scientific, USA) was used to collect data in positive and negative ion modes, respectively, to im-prove the chemical constituent coverage. Raw mass spectrum data collected by UPLC-MS/MS were imported into Com-pound Discoverer 3.1 (Thermo Fisher Scientific, USA) for data processing. It mainly includes peak extraction, retention time correction within and between groups, additive ion merging, missing value filling, background peak labeling, and metabolite identification. Finally, the molecular weight, re-tention time, peak area, and identification results of the compound were derived. The compounds were identified by comparing the retention time, accurate molecular weight, and MS^2 data with standard databases such as MZVault, MZCloud, and BGI Library (self-built standard Library by BGI Co., Ltd).

3. Results

3.1. Total Ion Chromatogram. Total ion chromatogram of *A. argyi* is shown in Figures 1 and 2.

3.2. Identification Results of Chemical Composition. In this study, UPLC-Q-Exactive-MS/MS technology was used to rapidly identify the chemical constituents in *A. argyi*. The identification of compounds was based on the retention time, MS data, and MS2 data compared with the standard database (MZVault, MZCloud and BGI Library (self-built standard Library by BGI Co., Ltd)). Most flavonoids, phe-nylpropanoids, and organic acids were easily deprotonated and responded in negative ion mode. Most steroids and terpenoids were easily protonated and responded in pos-itive ion mode. The identification results are shown in Ta-ble 1. A total of 125 chemical constituents were identified in
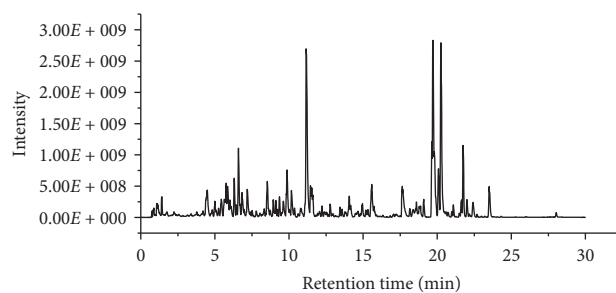
Figure 1: Total ion chromatogram of *A. argyi* in positive ion mode.
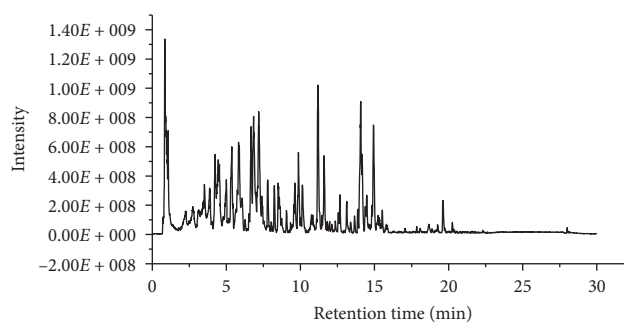
Figure 2: Total ion chromatogram of *A. argyi* in negative ion mode.

A. argyi, including 49 flavonoids, 30 organic acids, 13 phenylpropanoids, 9 terpenoids, 5 amino acids, 2 steroids, 1 phenolic acid, 1 alkaloid, and 15 other compounds.

4. Discussion

Eupatilin and jaceosidin as flavonoids and chlorogenic acid as phenylpropanoids were the main components of *A. argyi*, which were often used as the index components for content determination and quality evaluation [18–22], and the content of total flavonoids in *A. argyi* leaves was as high as 4.48%–11.46% [18]. Flavonoids and phenylpropanoids of *A. argyi* were also the active ingredients. The flavonoids in *A. argyi* leaves had anti-tumor, antioxidation, anti-platelet aggregation, gastrointestinal smooth muscle protection, and other pharmacological effects. And the phenylpropanoids in *A. argyi* leaves had pharmacological effects such as antibacterial, anti-inflammatory, antiviral, free radical scavenging, liver protection and gallbladder protection, and lowering blood pressure and blood lipid [12].

Previous studies showed that the chemical components isolated from the *A. argyi* leaves include flavonoids, terpenoids, phenylpropanoids, organic acids, steroids, etc. [2], and the above chemical components were all contained in *A. argyi* from Zhumadian, indicating that the chemical components in *A. argyi* from Zhumadian were relatively diverse with good quality. In this study, in addition to the reported flavonoids, eupafolin, eupatilin, jaceosidin, apigenin, kaempferol, luteolin, hispidulin, isoschaftoside, eriodictyol, naringenin, acacetin, and artemetin isolated from *A. argyi* leaves, *A. argyi* from Zhumadian contained 37 other flavonoids such as schaftoside, rutin, isovitexin, and

taxifolin. These results revealed that there were abundant flavonoids in *A. argyi* from Zhumadian. *A. argyi* from Zhumadian contained most of the reported phenylpropanoids identified from *A. argyi* [2], such as neochlorogenic acid, cryptochlorogenic acid, chlorogenic acid, isochlorogenic acid B, isochlorogenic acid C, scopoletin, and isofraxidin; besides, *A. argyi* from Zhumadian also contained other phenylpropanoid compounds, such as 2-hydroxycinnamic acid, esculetin, fraxetin, and 3-coumaric acid. In addition, *A. argyi* from Zhumadian was rich in terpenoids and organic acids. There were many kinds of active ingredients in *A. argyi* from Zhumadian, and it was worthy to study systematically to find more natural active ingredients.

Ultra-high performance liquid chromatography (UPLC) has the advantages of high analytical speed, high sensitivity, and solvent saving compared with high-performance liquid chromatography (HPLC) [23]. UPLC is often combined with mass spectrometry for rapid detection of chemical constituents of traditional Chinese medicine. Ultra-high performance liquid chromatography tandem quadruple-time of flight mass spectrometry (UPLC-Q-TOF-MS/MS) and UPLC-Q-Exactive-MS/MS are currently commonly used. Compared to traditional LC-MS/MS, UPLC-Q-Exactive-MS/MS has higher resolution, which can eliminate the interference of sample matrix [17]. Wang et al. [12] investigated the chemical constituents of *A. argyi* produced in Nanyang by UPLC-Q-TOF-MS/MS technology, and 23 chemical constituents were identified, including 12 flavonoids and flavonoid glycosides, 9 phenylpropionic acids, and 1 coumarin. Li et al. [14] used RRLC-TOFMS technology to rapidly identify the chemical components in *A. argyi* leaves and identified 31 chemical components. In this study, 125 chemical

TABLE 1: Identification results of chemical composition in *A. argyi*.

Number	Retention time (min)	Molecular formula	[M−H]− Theoretical value (Da)	The measured values (m/z)	Error (ppm)	[M+H]+/ [M+NH4]+/ [M+H−H2O]+ Theoretical value (Da)	The measured values (m/z)	Error (ppm)	Compound name	Compound type
1	0.798	$C_4H_8N_2O_3$	131.04622	131.04616	−0.44	—	—	—	Asparagine	Amino acids
2	0.905	$C_{16}H_{18}O_9$	353.08778	353.08707	−1.99	—	—	—	Neochlorogenic acid	Phenylpropanoids
3	0.913	$C_7H_{12}O_6$	191.05601	191.05557	−2.30	—	—	—	D-(−)-quinic acid	Organic acids
4	0.966	$C_4H_6O_5$	133.01430	133.01425	−0.34	—	—	—	Dl-malic acid	Organic acids
5	1.072	$C_6H_8O_7$	191.01970	191.01927	−2.22	—	—	—	Citric acid	Organic acids
6	1.092	$C_9H_8O_3$	—	—	—	182.08117	182.08139	1.33	2-Hydroxycinnamic acid	Phenylpropanoids
7	1.12	$C_4H_6O_4$	117.01932	117.01909	−1.99	—	—	—	Succinic acid	Organic acids
8	1.323	$C_6H_{10}O_4$	145.05062	145.05022	−2.74	—	—	—	3-Methylglutaric acid	Organic acids
9	1.332	$C_5H_8O_4$	131.03497	131.03461	−2.73	—	—	—	Glutaric acid	Organic acids
10	1.41	$C_9H_{11}NO_2$	—	—	—	166.08628	166.08643	0.94	L-phenylalanine	Amino acids
11	1.455	$C_9H_{17}NO_5$	218.10339	218.10284	−2.52	—	—	—	Pantothenic acid	Organic acids
12	3.163	$C_{11}H_9NO_2$	—	—	—	188.07052	188.07053	0.07	Indole-3-acrylic acid	Organic acids
13	4.337	$C_7H_{12}O_4$	159.06628	159.06586	−2.63	—	—	—	Pimelic acid	Organic acids
14	4.452	$C_{16}H_{18}O_9$	353.08772	353.08716	−1.59	—	—	—	Cryptochlorogenic acid	Phenylpropanoids
15	4.492	$C_9H_6O_4$	177.01937	177.01929	−0.42	—	—	—	Esculetin	Phenylpropanoids
16	4.591	$C_6H_{12}O_3$	131.07130	131.07104	−1.98	—	—	—	2-Hydroxycaproic acid	Organic acids
17	4.63	$C_9H_8O_4$	179.03491	179.03459	−1.80	—	—	—	Caffeic acid	Phenolic acid
18	4.839	$C_8H_8O_3$	151.04013	151.03972	−2.70	—	—	—	2-Hydroxyphenylacetic acid	Organic acids
19	4.873	$C_8H_{15}NO_3$	172.09792	172.09763	−1.68	—	—	—	N-Acetyl-d-alloisoleucine	Amino acids
20	4.922	$C_{16}H_{18}O_9$	353.08798	353.08734	−1.80	—	—	—	Chlorogenic acid	Phenylpropanoids
21	4.994	$C_{18}H_{28}O_9$	387.16599	387.16553	−1.20	—	—	—	{(1r,2r)-2-[(2z)-5-(Hexopyranosyloxy)-2-penten-1-yl]-3-oxocyclopentyl}acetic acid	Others
22	5.054	$C_{19}H_{30}O_8$	—	—	—	387.20113	387.20114	0.03	3-Hydroxy-3,5,5-trimethyl-4-(3-oxo-1-buten-1-ylidene)cyclohexyl β-d-glucopyranoside	Others
23	5.304	$C_{27}H_{30}O_{15}$	593.15126	593.1507	−0.94	—	—	—	Vicenin II	Flavonoids
24	5.319	$C_{10}H_8O_5$	207.02985	207.02951	−1.64	—	—	—	Fraxetin	Phenylpropanoids
25	5.362	$C_{25}H_{24}O_{12}$	515.11974	515.11871	−2.00	—	—	—	1,3-Dicaffeoylquinic acid	Phenylpropanoids
26	5.46	$C_{11}H_{13}NO_3$	206.08221	206.08176	−2.17	—	—	—	N-Acetyl-L-phenylalanine	Amino acids
27	5.607	$C_{17}H_{20}O_9$	367.10343	367.10269	−2.01	—	—	—	(3r,5r)-1,3,5-Trihydroxy-4-[[(2e)-3-(4-hydroxy-3-methoxyphenyl)-2-propenoyl]oxy]cyclohexanecarboxylic acid	Others
28	5.684	$C_9H_8O_3$	163.04006	163.03973	−2.03	—	—	—	3-Coumaric acid	Phenylpropanoids
29	5.745	$C_{26}H_{28}O_{14}$	563.14063	563.13977	−1.52	—	—	—	Isoschaftoside	Flavonoids
30	5.789	$C_8H_{14}O_4$	173.08194	173.08148	−2.65	—	—	—	Suberic acid	Organic acids
31	5.862	$C_{21}H_{20}O_{11}$	447.09332	447.09247	−1.89	—	—	—	Homoorientin	Flavonoids
32	5.993	$C_{26}H_{28}O_{14}$	563.14072	563.13983	−1.57	—	—	—	Schaftoside	Flavonoids
33	6.012	$C_{27}H_{30}O_{16}$	—	—	—	611.16078	611.16064	−0.23	Orientin-2″-O-β-L-galactoside	Flavonoids
34	6.109	$C_{10}H_8O_4$	—	—	—	193.04977	193.04984	0.37	Scopoletin	Phenylpropanoids
35	6.118	$C_{27}H_{32}O_{15}$	—	—	—	579.17105	579.17102	−0.05	Eriocitrin	Flavonoids
36	6.226	$C_{15}H_{12}O_7$	303.05103	303.05057	−1.51	—	—	—	Taxifolin	Flavonoids
37	6.334	$C_{11}H_{10}O_5$	—	—	—	223.06025	223.06018	−0.32	Isofraxidin	Phenylpropanoids
38	6.346	$C_{26}H_{28}O_{15}$	579.13551	579.13507	−0.76	—	—	—	Leucoside	Flavonoids
39	6.351	$C_{27}H_{30}O_{16}$	609.14620	609.14587	−0.54	—	—	—	Rutin	Flavonoids
40	6.421	$C_{21}H_{20}O_{10}$	431.09831	431.09772	−1.36	—	—	—	Isovitexin	Flavonoids
41	6.438	$C_{27}H_{30}O_{15}$	—	—	—	595.16575	595.16589	0.24	Lonicerin	Flavonoids
42	6.456	$C_9H_7NO_2$	160.04040	160.04007	−2.06	—	—	—	Indole-2-carboxylic acid	Organic acids

TABLE 1: Continued.

Number	Retention time (min)	Molecular formula	[M-H]− Theoretical value (Da)	[M-H]− The measured values (m/z)	[M-H]− Error (ppm)	[M+H]+/[M+NH4]+/[M+H-H2O]+ Theoretical value (Da)	The measured values (m/z)	Error (ppm)	Compound name	Compound type
43	6.474	$C_9H_6O_4$	177.01934	177.01897	-2.05	—	—	—	5,7-Dihydroxychromone	Flavonoids
44	6.511	$C_{21}H_{20}O_{12}$	463.08810	463.08774	-0.78	—	—	—	Isoquercitrin	Flavonoids
45	6.515	$C_{21}H_{20}O_{12}$	—	—	—	465.10303	465.10312	0.20	Hyperoside	Flavonoids
46	6.516	$C_{27}H_{30}O_{14}$	577.15627	577.15533	-1.63	—	—	—	Vitexin rhamnoside	Flavonoids
47	6.546	$C_{21}H_{18}O_{12}$	461.07248	461.07205	-0.93	—	—	—	Luteolin 7-glucuronide	Flavonoids
48	6.568	$C_{21}H_{20}O_{11}$	447.09318	447.09268	-1.11	—	—	—	Cynaroside	Flavonoids
49	6.587	$C_5H_9NO_2$	114.05603	114.05582	-1.85	—	—	—	D-Proline	Amino acids
50	6.682	$C_{10}H_{14}O$	—	—	—	151.11175	151.11176	0.09	Carvone	Others
51	6.685	$C_7H_6O_3$	137.02446	137.02411	-2.55	—	—	—	3-Hydroxybenzoic acid	Organic acids
52	6.72	$C_{27}H_{32}O_{14}$	579.17146	579.17126	-0.34	—	—	—	Naringin	Flavonoids
53	6.724	$C_{27}H_{32}O_{14}$	—	—	—	581.18648	581.1864	-0.14	Narirutin	Flavonoids
54	6.827	$C_{27}H_{30}O_{15}$	—	—	—	595.16605	595.1662	0.25	Kaempferol-3-O-rutinoside	Flavonoids
55	6.841	$C_{25}H_{24}O_{12}$	515.11944	515.11853	-1.76	517.13405	517.13422	0.34	4,5-Dicaffeoylquinic acid	Phenylpropanoids
56	6.958	$C_{27}H_{30}O_{14}$	—	—	—	579.17034	579.17065	0.53	Rhoifolin	Flavonoids
57	7.018	$C_{21}H_{20}O_{11}$	447.09319	447.09268	-1.13	—	—	—	Astragalin	Flavonoids
58	7.076	$C_9H_{16}O_4$	187.09763	187.09727	-1.90	—	—	—	Azelaic acid	Organic acids
59	7.126	$C_{28}H_{32}O_{15}$	—	—	—	609.18158	609.18158	-0.004	Diosmin	Flavonoids
60	7.158	$C_{15}H_{18}O_4$	—	—	—	263.12782	263.12778	-0.15	(3as,10ar,10br)-6,10a-Dimethyl-3-methylene-3,3a,4,5,7,8,10a,10b-octahydrofuro[3',2':6,7] cyclohepta[1,2-b]pyran-2,9-dione	Others
61	7.187	$C_{25}H_{24}O_{12}$	515.11931	515.11853	-1.51	—	—	—	Isochlorogenic acid B	Phenylpropanoids
62	7.19	$C_{21}H_{18}O_{11}$	—	—	—	447.09180	447.09186	0.14	Apigenin 7-O-glucuronide	Flavonoids
63	7.245	$C_{28}H_{32}O_{16}$	623.16176	623.16132	-0.71	—	—	—	Isorhamnetin-3-O-nehesperidine	Flavonoids
64	7.346	$C_{15}H_{23}NO_4$	—	—	—	282.16995	282.16992	-0.11	Actidione	Alkaloids
65	7.362	$C_{22}H_{22}O_{11}$	—	—	—	463.12359	463.12366	0.16	Tectoridin	Flavonoids
66	7.544	$C_{15}H_{20}O_4$	263.12884	263.12845	-1.47	—	—	—	Abscisic acid	Organic acids
67	8.024	$C_{15}H_{12}O_6$	287.05610	287.05576	-1.17	—	—	—	Eriodictyol	Flavonoids
68	8.392	$C_{28}H_{32}O_{14}$	—	—	—	593.18581	593.18622	0.69	Linarin	Flavonoids
69	8.398	$C_{15}H_{10}O_7$	301.03549	301.03497	-1.74	—	—	—	Morin	Flavonoids
70	8.471	$C_{15}H_{10}O_6$	285.04044	285.04001	-1.52	287.05492	287.05484	-0.29	Luteolin	Flavonoids
71	8.522	$C_{11}H_{12}O_4$	207.06631	207.06586	-2.15	—	—	—	Ethyl caffeate	Phenylpropanoids
72	8.618	$C_{16}H_{12}O_7$	315.05096	315.0506	-1.14	317.06558	317.06552	-0.18	Eupafolin	Flavonoids
73	9.028	$C_{15}H_{18}O_3$	—	—	—	229.12240	229.1223	-0.40	Arglabin	Terpenoids
74	9.039	$C_{15}H_{12}O_5$	271.06122	271.06082	-1.45	—	—	—	Naringenin	Flavonoids
75	9.057	$C_{12}H_{18}O_3$	209.11834	209.11795	-1.84	—	—	—	Jasmonic acid	Organic acids
76	9.063	$C_{16}H_{12}O_7$	315.05111	315.05069	-1.31	—	—	—	3-Methoxy-5,7,3',4'-tetrahydroxy-flavone	Flavonoids
77	9.158	$C_{17}H_{14}O_7$	329.06682	329.06631	-1.56	331.08129	331.08112	-0.53	Jaceosidin	Flavonoids
78	9.233	$C_{16}H_{14}O_6$	301.07175	301.07138	-1.23	—	—	—	Hesperetin	Flavonoids
79	9.234	$C_{15}H_{18}O_2$	—	—	—	231.13794	231.13792	-0.07	Atractylenolide I	Terpenoids
80	9.424	$C_{15}H_{10}O_5$	269.04550	269.04517	-1.24	271.06013	271.0600	-0.49	Apigenin	Flavonoids
81	9.431	$C_{15}H_{10}O_6$	285.04055	285.04007	-1.69	—	—	—	Kaempferol	Flavonoids
82	9.556	$C_{18}H_{32}O_5$	327.21768	327.21722	-1.40	—	—	—	Corchorifatty acid f	Organic acids
83	9.623	$C_{16}H_{12}O_6$	299.05608	299.0556	-1.58	301.07058	301.07053	-0.16	Hispidulin	Flavonoids

TABLE 1: Continued.

Number	Retention time (min)	Molecular formula	[M-H]⁻ Theoretical value (Da)	[M-H]⁻ The measured values (m/z)	[M-H]⁻ Error (ppm)	[M+H]⁺/[M+NH4]⁺/[M+H-H₂O]⁺ Theoretical value (Da)	[M+H]⁺/[M+NH4]⁺/[M+H-H₂O]⁺ The measured values (m/z)	[M+H]⁺/[M+NH4]⁺/[M+H-H₂O]⁺ Error (ppm)	Compound name	Compound type
84	9.82	$C_{18}H_{16}O_8$	359.07727	359.0769	−1.03	—	—	—	5,7,3′-Trihydroxy-6,4′,5′-trimethoxyflavone	Flavonoids
85	10.426	$C_{12}H_{22}O_4$	229.14456	229.14415	−1.80	—	—	—	Dodecanedioic acid	Organic acids
86	10.832	$C_{17}H_{14}O_6$	—	—	—	315.08616	315.08582	−1.10	Scrophulein	Flavonoids
87	11.028	$C_{19}H_{18}O_8$	373.09286	373.09241	−1.21	375.10744	375.10736	−0.22	Casticin	Flavonoids
88	11.177	$C_{18}H_{16}O_7$	343.08239	343.08182	−1.67	345.09679	345.09668	−0.31	Eupatilin	Flavonoids
89	11.294	$C_{15}H_{22}O_2$	—	—	—	235.16921	235.16913	−0.35	Artemisinic acid	Terpenoids
90	11.393	$C_{15}H_{12}O_4$	255.06630	255.06595	−1.36	—	—	—	Pinocembrin	Flavonoids
91	11.533	$C_{15}H_{10}O_4$	253.05071	253.05026	−1.76	—	—	—	Chrysin	Flavonoids
92	11.54	$C_{19}H_{18}O_8$	373.09297	373.09238	−1.57	—	—	—	Chrysosplenetin B	Flavonoids
93	11.668	$C_{15}H_{16}O_3$	—	—	—	245.11738	245.11719	−0.76	Linderalactone	Terpenoids
94	11.723	$C_{15}H_{10}O_5$	269.04555	269.04514	−1.52	—	—	—	Galangin	Flavonoids
95	11.754	$C_{16}H_{12}O_5$	283.06138	283.06125	−0.46	—	—	—	Acacetin	Flavonoids
96	12.071	$C_{17}H_{14}O_6$	313.07213	313.07175	−1.21	—	—	—	Pectolinarigenin	Flavonoids
97	12.587	$C_{18}H_{26}O_2$	—	—	—	275.20053	275.2005	−0.09	19-Nortestosterone	Steroids
98	12.774	$C_{20}H_{20}O_8$	—	—	—	389.12315	389.12289	−0.67	Artemetin	Flavonoids
99	12.896	$C_{24}H_{30}O_6$	—	—	—	415.21151	415.2114	−0.26	Bis (4-ethylbenzylidene) sorbitol	Others
100	13.107	$C_{20}H_{32}O_2$	—	—	—	305.24757	305.24741	−0.53	Arachidonic acid	Organic acids
101	13.216	$C_{18}H_{34}O_4$	313.23846	313.23868	0.70	—	—	—	(±)9,10-Dihydroxy-12z-octadecenoic acid	Organic acids
102	13.396	$C_{15}H_{18}O_2$	—	—	—	231.13808	231.13791	−0.74	Dehydrocostus lactone	Terpenoids
103	13.636	$C_{24}H_{36}O_2$	—	—	—	357.27881	357.27863	−0.51	Docosahexaenoic acid ethyl ester	Others
104	13.709	$C_{18}H_{28}O_3$	291.19672	291.1968	0.29	—	—	—	12-Oxo phytodienoic acid	Organic acids
105	14.035	$C_{16}H_{26}O_2$	—	—	—	251.20046	251.20039	−0.30	Clareolide	Terpenoids
106	14.515	$C_{20}H_{32}O_2$	—	—	—	305.24747	305.24731	−0.53	Mesterolone	Steroids
107	14.543	$C_{15}H_{22}O$	—	—	—	219.17439	219.17432	−0.33	Germacrone	Terpenoids
108	14.59	$C_{18}H_{28}O_3$	—	—	—	293.21100	293.21091	−0.32	9s,13r-12-Oxophytodienoic acid	Organic acids
109	14.648	$C_{16}H_{30}O_2$	—	—	—	255.23177	255.23166	−0.43	Palmitoleic acid	Organic acids
110	14.94	$C_{18}H_{30}O_2$	—	—	—	279.232023	279.23166	−1.32	A-eleostearic acid	Organic acids
111	15.294	$C_{14}H_{28}O_3$	243.19660	243.19652	−0.33	—	—	—	(r)-3-Hydroxy myristic acid	Organic acids
112	15.515	$C_{18}H_{30}O_3$	—	—	—	295.22663	295.22675	0.41	9-Oxo-10(e),12(e)-octadecadienoic acid	Organic acids
113	16.018	$C_{14}H_{28}O_3$	243.19657	243.19649	−0.33	—	—	—	2-Hydroxymyristic acid	Organic acids
114	18.083	$C_{16}H_{32}O_3$	271.22796	271.22803	0.25	—	—	—	16-Hydroxyhexadecanoic acid	Organic acids
115	18.536	$C_{30}H_{48}O_3$	—	—	—	439.35730	439.35718	−0.27	Ursolic acid	Terpenoids
116	18.586	$C_{18}H_{37}NO_2$	—	—	—	300.28971	300.28955	−0.52	Palmitoyl ethanolamide	Others
117	18.595	$C_{20}H_{39}NO_2$	—	—	—	326.30542	326.30524	−0.55	Oleoyl ethanolamide	Others
118	18.908	$C_{18}H_{32}O_2$	279.23298	279.233	0.07	—	—	—	Linoleic acid	Organic acids
119	19.712	$C_{18}H_{35}NO$	—	—	—	282.27920	282.27905	−0.55	Oleamide	Others
120	20.083	$C_{16}H_{33}NO$	—	—	—	256.26379	256.26352	−1.06	Hexadecanamide	Others
121	20.759	$C_{20}H_{34}O_2$	—	—	—	307.26319	307.26306	−0.41	Linolenic acid ethyl ester	Others
122	20.841	$C_{20}H_{41}NO_2$	—	—	—	328.32113	328.32086	−0.81	Stearoyl ethanolamide	Others
123	22.408	$C_{18}H_{37}NO$	—	—	—	284.29494	284.29468	−0.92	Stearamide	Others
124	23.526	$C_{22}H_{43}NO$	—	—	—	338.34147	338.34155	0.23	Erucamide	Others
125	23.702	$C_{30}H_{48}O$	—	—	—	425.37782	425.37772	−0.23	Lupenone	Terpenoids

Note: "—" indicates undetected.

constituents of *A. argyi* from Zhumadian were preliminarily identified by UPLC-MS/MS. All of them contain isochlorogenic acid C and eupatilin. The chemical constituents identified in this study were relatively comprehensive, which provides a certain reference for the subsequent studies of *A. argyi*.

5. Conclusion

In this study, a total of 125 chemical constituents of *A. argyi* were identified by UPLC-Q-Exactive-MS/MS technology. The UPLC-Q-Exactive-MS/MS technology could be used to quickly and preliminarily identify the chemical constituents of *A. argyi*, providing a basis for further study on the pharmacological substance basis and resource utilization of *A. argyi*.

Data Availability

The data used to support the findings of this study are included within the article.

Conflicts of Interest

The authors declare that there are no conflicts of interest regarding this study.

Acknowledgments

References

[1] Editorial Committee of flora of China, *Flora of China*, Science press, vol. 76, no. 2, , p. 87, Beijing, China, 1991.

[2] X. Y. Lang, Y. Zhang, L. B. Zhu et al., "Research progress on chemical constituents from Artemisiae Argyi Folium and their pharmacological activities and quality control," *China Journal of Chinese Materia Medica*, vol. 45, no. 17, pp. 4017–4030, 2020.

[3] National Pharmacopoeia Commission, *Pharmacopoeia of the People's Republic of China*, Vol. 91, China Medical Science and Technology Press, Beijing, China, 2020.

[4] X. L. Zhang and X. W. Chen, "Research progress on chemical constituents and pharmacological activities of Artemisia argyi volatile oil," *Chinese Archives of Traditional Chinese Medicine*, pp. 1–19, 2020.

[5] X. L. Zhao and Y. L. Dang, "Advance on chemical constituents and pharmacological effects of *Artemisia argyi* volatile oils," *Natural Product Research and Development*, vol. 31, no. 12, pp. 2182–2188, 2019.

[6] L. Cao, D. Yu, L. Cui et al., "Research progress on chemical composition, pharmacological effects and product development of *Artemisia argyi*," *Drug Evaluation Research*, vol. 41, no. 5, pp. 918–923, 2018.

[7] S. J. Zhang, Y. L. Ma, J. L. Wang et al., "Chemical constituents of *Artemisia argyi*," *Chinese Traditional and Herbal Drugs*, vol. 50, no. 8, pp. 1906–1914, 2019.

[8] J. L. Wang, Y. L. Ma, D. Wang et al., "Chemical constituents of *Artemisia argyi* (II)," *Chinese Traditional and Herbal Drugs*, vol. 51, no. 20, pp. 5114–5122, 2020.

[9] M. Fan, T. Guo, W. Li et al., "Isolation and identification of novel casein-derived bioactive peptides and potential functions in fermented casein with Lactobacillus helveticus," *Food Science and Human Wellness*, vol. 8, no. 2, pp. 156–176, 2019.

[10] J. Ma, S. Fan, L. Sun, L. He, Y. Zhang, and Q. Li, "Rapid analysis of fifteen sulfonamide residues in pork and fish samples by automated on-line solid phase extraction coupled to liquid chromatography-tandem mass spectrometry," *Food Science and Human Wellness*, vol. 9, no. 4, pp. 363–369, 2020.

[11] F. Yang, H. L. Wang, G. Q. Feng et al., "Rapid identification of chemical constituents in *Hericium erinaceus* based on LC-MS/MS metabolomics," *Journal of Food Quality*, vol. 2021, Article ID 5560626, 10 pages, 2021.

[12] Y. Q. Wang, R. H. Geng, and X. X. Zhang, "Analysis of chemical constituents in *Artemisia argyi* (Nanyang) by UPLC-Q-TOF-MS/MS," *Chinese Hospital Pharmacy Journal*, vol. 38, no. 5, pp. 500–505, 2018.

[13] D. D. Luo, H. S. Peng, Y. Zhang et al., "Comparison of chemical components between Artemisia stolonifera and *Artemisia argyi* using UPLC-Q-TOF-MS," *China Journal of Chinese Materia Medica*, vol. 45, no. 17, pp. 4057–4064, 2020.

[14] L. Li, L. Lv, X. Dong et al., "Rapid identification of chemical components in Artemisiae argyi folium by RRLC-TOFMS," *Journal of Pharmaceutical Practice*, vol. 32, no. 6, pp. 448–452, 2014.

[15] J.-X. Xia, B.-B. Zhao, J.-F. Zan, P. Wang, and L.-L. Chen, "Simultaneous determination of phenolic acids and flavonoids in Artemisiae Argyi Folium by HPLC-MS/MS and discovery of antioxidant ingredients based on relevance analysis," *Journal of Pharmaceutical and Biomedical Analysis*, vol. 175, p. 112734, 2019.

[16] B. Zeng, H. M. Liu, X. M. Liu et al., "Application of UPLC-Q-exactive orbitrap MS technology in analysis of traditional Chinese medicine," *Journal of Chinese Medicinal Materials*, vol. 43, no. 9, pp. 2313–2319, 2020.

[17] H. J. Dong, X. H. Chen, and R. Zeng, "Rapid analysis on chemical constituents in roots of Rheum pumilum by UPLC coupled with hybrid quadrupole-orbit trap MS," *Chinese Traditional and Herbal Drugs*, vol. 47, no. 14, pp. 2428–2435, 2016.

[18] M. Gong, J. Q. Lu, and Y. S. Xiao, "Determination of total flavonoids and three main aglycones in folium Artemisiae argyi from different origins," *China Pharmacist*, vol. 22, no. 5, pp. 966–968+975, 2019.

[19] Q. Jiao, *The Study of the Fingerprint and Multicomponent Content of Artemisia Argyi Folium and Artemisiae Lavandulaefoliae Folium*, Hebei Medical University, Shijiazhuang, China, 2018.

[20] Q. Zhou, L. L. Sun, B. Jiang et al., "Simultaneous determination of eupatilin and jaceosidin in *Artemisia argyi* and its processed products by RP-HPLC," *China Pharmacy*, vol. 24, no. 47, pp. 4464–4466, 2013.

[21] L. Long, Y. J. Li, X. H. Cheng et al., "Determination of Eupatilin in Herb Artemisia," *Journal of Hubei University for Nationalities (Natural Science Edition)*, vol. 28, no. 4, pp. 395-396+404, 2010.

[22] J. L. Wu, Y. L. Wang, W. Liu et al., "Simultaneous determination of 7 components in *Artemisia argyi* leaves by HPLC," *Chinese Traditional Patent Medicine*, vol. 39, no. 9, pp. 1876–1879, 2017.

[23] J. Wang, Z. Z. Han, L. W. Yang et al., "Comparison of UPLC and HPLC for the determination of 6,8,3',4'-tetramethoxy flavone in Murraya paniculate (L.) Jack," *Chinese Journal of Pharmaceutical Analysis*, vol. 30, no. 8, pp. 1499–1501, 2010.

WILEY | Hindawi

Research Article

Rapid Identification of Chemical Constituents in *Hericium erinaceus* Based on LC-MS/MS Metabolomics

Fei Yang [iD],[1,2] **Honglin Wang** [iD],[1] **Guoquan Feng** [iD],[3] **Sulan Zhang** [iD],[4] **Jinmei Wang** [iD],[1] **and Lili Cui** [iD][1]

[1]*National R & D Center for Edible Fungus Processing Technology, Henan University, Kaifeng 475004, China*
[2]*Zhengzhou Institute for Food and Drug Control, Zhengzhou 450006, Henan, China*
[3]*International School of Qiushi, Kaifeng 475009, China*
[4]*The First Affiliated Hospital of Zhengzhou University, Zhengzhou 450052, Henan, China*

Correspondence should be addressed to Lili Cui; cuill@vip.henu.edu.cn

Hericium erinaceus is a precious edible and medicinal fungus with high nutritional value. It has many functions, such as enhancing immunity, antitumor antioxidation, antihyperglycemic, antihyperlipidemic, and protecting gastric mucosa. However, there are few researches about the *H. erinaceus* compounds. In this paper, ultraperformance liquid chromatography tandem high-resolution mass spectrometry (UPLC-Q-exactive-MS/MS) was used to isolate and identify the compounds in *H. erinaceus*. 102 compounds were identified in *H. erinaceus* by comparing with standard databases such as MZVault, MZCloud, and BGI Library (self-built standard Library by BGI Co., Ltd), including flavonoids, terpenoids, phenolic acids, phenylpropanoids, steroids, organic acids, and amino acids.

1. Introduction

Hericium erinaceus is a precious edible and medicinal fungus, and it is listed as one of the "Four Famous Cuisines" of China, together with bear's paws, trepang, and shark's fin [1]; it has been used for a long time in traditional Chinese medicine [2]. Researches showed that the chemical constituents of *H. erinaceus* include terpenoids, phenolics, steroids, pyranones, fatty acids, and alkaloids; about 80 small molecular compounds were isolated and identified from *H. erinaceus* [3]. Terpenoids in *H. erinaceus* were mainly diterpenoids with cyathane skeleton. Terpenoids in *H. erinaceus* were first isolated and identified by Kawagishi et al. from mycelia of *H. erinaceus*, named Erinacines A-C [4]. Subsequently, Kawagishi et al. isolated and identified Erinacines D-G, Erinacines J, and Erinacines K from mycelia of *H. erinaceus* [5–7]; Lee et al. isolated and identified Erinacines H and Erinacines I from mycelia of *H. erinaceus* [8]; Kenmoku et al. isolated and identified Erinacine P and Erinacine Q from mycelia of *H. erinaceus*

[9, 10]. Most of these diterpenoids compounds were stimulators of nerve growth factor-synthesis. Phenolics were also main constituents in *H. erinaceus*. 8 phenolics were isolated and identified from fruiting bodies of *H. erinaceus* by the Kawagishi team between 1990 and 1993, named Hericenone A-H [11–13]. After that, three phenolics were isolated and identified by Arnone et al. [14] with 5'- carbonyl group replaced by 5'- methylene, named Hericenes A-C. Subsequently, two new phenolics were isolated from fruiting bodies of *H. erinaceus* by Ma et al. [15], named Hericenone I and Hericenone D; they have the same fatty acid chain. A new skeleton phenolic compound was isolated from fruiting bodies of *H. erinaceus* by Li et al. [16], named Erinacene D. In addition to terpenoids and phenolics compounds, *H. erinaceus* was rich in steroids, six new (erinarols A-F), and five known ergostane-type sterol fatty acid esters were isolated from the fruiting bodies of *H. erinaceus*; erinarols A and B significantly activated the transcriptional activity of PPARs, PPARα, and PPARγ [17]. Previous pharmacological studies showed that *H. erinaceus*

had many pharmacological activities, such as regulating immunity [18, 19], neuroprotection [20, 21], antidepressant [22, 23], antioxidant [24], antitumor [25], antihyperglycemic [26], and antihyperlipidemic properties [27], and protecting gastric mucosa [28, 29].

High-performance liquid chromatography tandem mass spectrometry (LC-MS/MS) technology has the advantage of rapid identification of compounds. With the maturity of LC-MS/MS technology, it is more and more widely used in the field of food and medicine [30–35]. In this study, ultraperformance liquid chromatography tandem high-resolution mass spectrometry (UPLC-Q-Exactive-MS/MS) combined with standard substance database was used to rapidly identify the chemical components of H. erinaceus.

2. Materials and Methods

2.1. Instrument. The LC-MS experiment was carried out by ultraperformance liquid chromatography (Waters 2D UPLC, USA) and high-resolution mass spectrometry (Q Exactive, Thermo, USA). The Hypersil GOLD aQ column (100 mm*2.1 mm, 1.9 μm) was purchased from Thermo Fisher Scientific, USA. Low-temperature high-speed centrifuge (Centrifuge 5430) was purchased from Eppendorf. The vortex finder (QL-901) was purchased from Qilinbeier Instrument Manufacturing Co., Ltd. The pure water meter (Milli-Q) was purchased from Integral Millipore Corporation, USA.

2.2. Reagent. d_3-leucine, $^{13}C_9$-phenylalanine, d_5-tryptophan, and $^{13}C_3$-progesterone were used as internal standards. Methanol (A454-4) and acetonitrile (A996-4) were both in mass spectral grade, which were purchased from Thermo Fisher Scientific, USA. Ammonium formate (17843–250 G) was obtained from Honeywell Fluka, USA. Formic acid (50144–50 mL) was obtained from DIMKA, USA.

2.3. Materials. Fruiting bodies of H. erinaceus were obtained from Henan Longfeng Industrial Co., Ltd. The specimens (No. 2020-09-09) were saved in National Research and Development Center of Edible Fungi Processing Technology, Henan University.

2.4. Preparation of Sample. According to the methods commonly used by our team, dry fruiting bodies of H. erinaceus were crushed by the grinding machine. 100 g of H. erinaceus powder was immersed with 50% ethanol (1000 mL) for 2 times at room temperature, each time for 3 days. The filtrate was concentrated to obtain 48.6 g extract. 50 mg extract of H. erinaceus was weighed, and then 800 μL of solution with 70% methanol: internal standard (V/V = 85 : 1) was added to the sample. Two small steel beads were added to the sample and ground in a tissue grinder (50 Hz, 5 min), ultrasound for 10 min at 4°C water, and the sample was placed for 1 h at −20°C. After that, the sample was centrifuged for 15 min at 4°C, 25000 rpm, 500 μL of supernatant was filtered through 96-well filter plate, and the filtrate was used to detect.

2.5. Chromatographic Conditions. The LC-MS experiment was carried out on Hypersil GOLD a Q column (100 mm*2.1 mm, 1.9 μm). The mobile phase was 0.1% formic acid-water (liquid A) and 0.1% formic acid-acetonitrile (liquid B). The elution gradient was as follows: 0–2 min 5% B; 2–22 min 5%–95% B; 22–27 min 95% B; 27.1–30 min 5% B. The flow rate was 0.3 mL/min, the column temperature was 40°C, and the injection volume was 5 μL.

2.6. Mass Spectrometry Conditions. The MS and MS^2 data were collected by the Q Exactive mass spectrometer. The range of m/z was 150–1500 with the MS resolution 70000, and the AGC was 1 e^6, and the maximum injection time was 100 ms. According to the strength of the MS ions, top3 was selected for determining MS^2 fragmentation. The MS^2 resolution was 35000, AGC was 2 e^5, the maximum injection time was 50 ms, and the fragmentation energy was set as 20, 40, and 60 eV. Ion source (ESI) parameters are as follows: sheath gas flow rate was 40, aux gas flow rate was 10, spray voltage (|KV|) of positive ion mode was 3.80, spray voltage (|KV|) of negative ion mode was 3.20, capillary temp was 320°C, and aux gas heater temp was 350°C.

2.7. Data Analysis. High-resolution mass spectrometer (Q Exactive, Thermo Fisher Scientific, USA) was used to collect data in positive and negative ion modes, respectively, to improve the chemical constituent coverage. Raw mass spectrum data collected by LC-MS/MS were imported into Compound Discoverer 3.1 (Thermo Fisher Scientific, USA) for data processing. It mainly includes peak extraction, retention time correction within and between groups, additive ion merging, missing value filling, background peak labeling, and metabolite identification. Finally, the molecular weight, retention time, peak area, and identification results of the compound were derived.

3. Results

3.1. Total Ion Chromatogram. The total ion chromatogram of H. erinaceus is shown in Figure 1.

3.2. Results of Compound Identification. The compounds of H. erinaceus were analyzed by LC-MS/MS; the identification of structure was based on the retention time, MS data, and MS^2 data compared with the standard database. The identified compounds were classified into three grades (Level 1, Level 2, and Level 3) according to the comparison results, there into, Level 2 was confirmed on the basis of MS data, MS^2 data, and properties of compounds, and Level 3 was identified on the basis of MS data and MS^2 data. The credibility sequence is as follows: Level 1> Level 2> Level 3. Detailed results are shown in Table 1. 102 compounds were preliminarily identified in H. erinaceus with grade of identification as Level 1 and Level 2, including 31 organic acids, 10 nucleotides and analogues, 8 amino acids, 6 carbohydrates and derivatives, 5 flavonoids, 3 unsaturated fatty acids, 3 terpenoids, 3 phenolic acids, 1 phenylpropanoid, 1
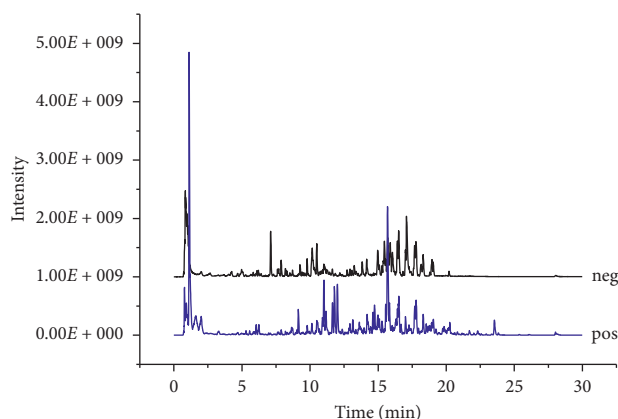
FIGURE 1: Total ion chromatogram of *H. erinaceus* in the positive ion mode (pos) and negative ion mode (neg).

steroid, and 32 other compounds. Most flavonoids and organic acids were easily deprotonated and responded in the negative ion mode. Most nucleoside compounds were easily protonated and responded in the positive ion mode. The identification process of some compounds was as follows.

Compound 49, $C_{15}H_{10}O_6$, was easily deprotonated in the negative ion mode to produce ion m/z 285 $[M − H]^−$ and then RDA cracking to get 2 fragment ions m/z 133 $[C_8H_6O_2 − H]^−$ and m/z 151 $[C_7H_4O_4 − H]^−$. Compound 49 was identified as luteolin compared to the database and references [36]. The MS^2 spectrum is shown in Figure 2.

Compound 60 produced ion m/z 283 $[M − H]^−$, then lost the methyl group, and got ion 268 $[M − H − CH_3]^−$, combined with retention time, MS data, and MS^2 data, compound 60 was identified as acacetin by comparin with the database and references [37]. The MS^2 spectrum is shown in Figure 3.

Compound 62 was easily protonated in the positive ion mode to produce ion m/z 249 $[M + H]^+$, then lost the hydroxyl group, and got ion m/z 231 $[M + H − H_2O]^+$, Compound 62 was identified as atractylenolide III by comparing with the database and references [38]. The MS^2 spectrum is shown in Figure 4.

4. Discussion and Conclusion

In this study, 102 compounds were preliminarily identified in *H. erinaceus*, including organic acids, nucleotides and analogues, amino acids, carbohydrates and derivatives, flavonoids, unsaturated fatty acids, terpenoids, phenolic acids, phenylpropanoid, and steroid. It revealed that the compounds in *H. erinaceus* were diverse. Previous studies showed that the chemical constituents of *H. erinaceus* include terpenoids, phenolics, steroids, pyranones, fatty acids, and alkaloids; thereinto, reports about terpenoids and phenolics in *H. erinaceus* were more [3–16]. Terpenoids and phenolics were less in this study; the reasons may be different material parts, different origins, different varieties, different extraction methods, and so on. In addition, nucleotides were also the main constituents in *H. erinaceus*. Yan et al. [39] studied the content of five nucleosides in *H. erinaceus* from different habitats by high-performance liquid chromatography; the results showed that different origins of *H. erinaceus* had the same nucleoside components, such as cytosine, inosine, and adenosine, and the content of inosine and adenosine in *H. erinaceus* was higher. In this study, 10 nucleotides and analogues were identified, including adenosine, adenine, guanosine, guanine, and uridine.

Most of the compounds in *H. erinaceus* had a good biological activity; researches about polysaccharide were more, which had a wide variety of pharmacological functions such as antimicrobial, antidiabetic, and antihypertension ones [1]. Small molecular compounds isolated from *H. erinaceus* also had many biological activities. Diterpenoids in *H. erinaceus* could promote the synthesis of nerve growth factors, such as Erinacines A, Erinacines B, Erinacines C, Erinacines D, Erinacines E, Erinacines F, Erinacines G, Erinacines H, and Erinacines I [4–6]. Phenolics compounds in *H. erinaceus* could also promote the synthesis of nerve growth factors, such as Hericenone C, Hericenone D, Hericenone E, and Hericenone H [12, 13]. Hericenones A and B showed cytotoxicity against HeLa cells [11]. In addition, Hericenone B was found to be a potential antiplatelet aggregation agent [40]. Steroids in *H. erinaceus* could activate the transcriptional activity of PPARs, PPARα, and PPARγ, such as erinarols A and erinarols B. In addition, nucleosides and flavonoids may be the main active components of *H. erinaceus*. Nucleoside components have many biological activities, such as antitumor, antivirus, and gene therapy. Studies have shown that adenosine, inosine, and guanosine have many pharmacological effects such as regulating immunity, neuroprotection, and treatment of cardiovascular diseases [41]. Flavonoids also have many pharmacological effects, such as neuroprotection, antimyocardial ischemia, hypotension, improved learning and memory, antigastric ulcer, protection of reproductive tissue, anti-inflammatory, and antitumor [42].

In a word, *H. erinaceus* has high nutritional value and medicinal value. At present, it has been developed into a variety of functional foods, including health wine, health drinks, healthy yogurt, tea, cans, and health vinegar [2], which was of great significance to study the chemical composition of *H. erinaceus*. In this study, 102 compounds were preliminarily identified to provide reference for the follow-up study of *H. erinaceus*.

TABLE 1: Identification results of compounds in *H. erinaceus*.

Number	Retention time (min)	Molecular formula	Relative molecular weight (Da)	The measured values (m/z)	Adduct ions	Error (ppm)	Peak	Compound name	Compound type	mzVault best match	mzCloud best match	Level
1	0.743	$C_{17}H_{27}N_3O_{17}P_2$	607.08113	606.07379	$[M-H]^-$	−0.72	143833617.1	Udp-*n*-acetylglucosamine	Nucleotides and analogues	NA	95.8	Level 2
2	0.826	$C_7H_{15}NO_3$	161.10508	162.11214	$[M+H]^+$	−0.70	455483170.3	L(−)-Carnitine	Others	77.9	85.7	Level 2
3	0.869	$C_4H_6O_5$	134.02147	133.01422	$[M-H]^-$	−0.41	23529567982	Dl-Malic acid	Organic acids	NA	98.8	Level 2
4	0.87	$C_4H_4O_4$	116.011	115.00369	$[M-H]^-$	0.33	1996525749	Fumaric acid	Organic acids	90.7	98.1	Level 1
5	0.883	$C_5H_7NO_3$	129.04263	128.03534	$[M-H]^-$	0.31	1198916725	4-Oxoproline	Amino acids	NA	88	Level 2
6	0.928	$C_5H_{12}O_5$	152.06831	151.0611	$[M-H]^-$	−1.07	5339098404	Ribitol	Carbohydrates and derivatives	90.6	98.1	Level 1
7	0.939	$C_6H_{14}O_6$	182.07893	181.07164	$[M-H]^-$	−0.61	3288369180	D-(−)-Mannitol	Carbohydrates and derivatives	93	98.4	Level 2
8	0.94	$C_{12}H_{22}O_{12}$	358.1107	357.10416	$[M-H]^-$	−1.19	58626917.89	Lactobionic acid	Carbohydrates and derivatives	87.8	NA	Level 1
9	1.026	$C_6H_{14}O_6$	182.07914	183.0865	$[M+H]^+$	0.55	272725138.5	Galactitol	Carbohydrates and derivatives	85.6	93.8	Level 1
10	1.061	$C_9H_{13}N_3O_5$	243.08565	487.17841	$[2M+H]^+$	0.55	1565196711	Cytarabine	Nucleotides and analogues	79	85.6	Level 2
11	1.066	$C_9H_{11}NO_3$	181.07393	182.08116	$[M+H]^+$	0.21	226778893.2	L-Tyrosine	Amino acids	86.5	91.3	Level 2
12	1.079	$C_8H_{14}O_7$	222.07377	221.06636	$[M-H]^-$	−0.81	939035522.5	Ethyl-β-d-glucuronide	Others	NA	96.2	Level 2
13	1.08	$C_9H_{12}N_2O_6$	244.0691	243.0618	$[M-H]^-$	−1.77	270847192.6	Uridine	Nucleotides and analogues	87.9	86.2	Level 2
14	1.084	$C_6H_8O_7$	192.02693	191.01961	$[M-H]^-$	−0.38	2611016825	Citric acid	Organic acids	92.1	96.7	Level 1
15	1.088	$C_5H_8O_5$	148.03713	147.02985	$[M-H]^-$	−0.31	355626048.3	D-α-hydroxyglutaric acid	Organic acids	NA	91.2	Level 2
16	1.094	$C_6H_6O_6$	174.0163	173.00929	$[M-H]^-$	−0.82	116011083.2	Trans-aconitic acid	Organic acids	43.7	81.9	Level 2
17	1.095	$C_7H_{11}NO_5$	189.06359	188.05672	$[M-H]^-$	−0.67	91397041.99	N-acetyl-dl-glutamic acid	Amino acids	NA	87.1	Level 2
18	1.099	$C_6H_{10}O_6$	178.04763	177.04068	$[M-H]^-$	−0.59	177666674.9	Δ-Gluconic acid δ-lactone	Carbohydrates and derivatives	NA	90.6	Level 2
19	1.106	$C_9H_8O_3$	164.04747	182.0813	$[M+NH4]^+$	0.74	246283118.7	2-Hydroxycinnamic acid	Phenylpropanoids	77.2	86.1	Level 2
20	1.134	$C_4H_6O_4$	118.02667	117.01939	$[M-H]^-$	0.54	319647862.4	Succinic acid	Organic acids	91.9	91	Level 1
21	1.14	$C_{10}H_{13}N_5O_4$	267.09628	312.09454	$[M+FA-H]^-$	−1.76	302054711.9	Adenosine	Nucleotides and analogues	86.1	85.2	Level 2
22	1.142	$C_7H_{10}O_7$	206.0424	205.03548	$[M-H]^-$	−1.25	118715221	3-Hydroxy-3-(methoxycarbonyl) pentanedioic acid	Others	4.8	87.8	Level 2
23	1.143	$C_5H_5N_5$	135.05446	134.04736	$[M-H]^-$	−0.25	1110258417	Adenine	Nucleotides and analogues	76.2	81.1	Level 1
24	1.15	$C_{10}H_{13}N_5O_5$	283.0917	284.09888	$[M+H]^+$	0.12	843230783.7	Guanosine	Nucleotides and analogues	84.8	NA	Level 2
25	1.153	$C_5H_5N_5O$	151.04949	152.05672	$[M+H]^+$	0.53	291864775.2	Guanine	Nucleotides and analogues	80	91.6	Level 1
26	1.181	$C_{10}H_{13}N_5O_3$	251.10188	252.10921	$[M+H]^+$	0.17	597455561.5	2′-Deoxyadenosine	Nucleotides and analogues	84.5	93.6	Level 2

TABLE 1: Continued.

| Number	Retention time (min)	Molecular formula	Relative molecular weight (Da)	The measured values (m/z)	Adduct ions	Error (ppm)	Peak	Compound name	Compound type	mzVault best match	mzCloud best match	Level
27	1.187	$C_6H_{12}O_6$	180.06332	161.0457	$[M-H-H_2O]^-$	−0.40	136214268.5	L-Sorbose	Carbohydrates and derivatives	66.2	89.4	Level 1
28	1.47	$C_{11}H_{15}N_5O_4$	281.11214	282.11905	$[M+H]^+$	−0.94	592442404.4	2′-o-Methyladenosine	Nucleotides and analogues	NA	85.2	Level 2
29	3.116	$C_{11}H_9NO_2$	187.06332	188.07059	$[M+H]^+$	−0.03	184845897.5	Indole-3-acrylic acid	Others	83.9	90.6	Level 2
30	3.123	$C_{11}H_{12}N_2O_2$	204.08972	203.08231	$[M-H]^-$	−0.75	46680672.16	L-Tryptophan	Amino acids	92	92.9	Level 1
31	3.29	$C_{11}H_{15}N_5O_3S$	297.08932	298.09692	$[M+H]^+$	−0.82	822526337.5	5′-s-Methyl-5′-thioadenosine	Nucleotides and analogues	NA	93	Level 2
32	4.218	$C_6H_6O_3$	126.03166	125.02444	$[M-H]^-$	−0.27	23877907.51	Pyrogallol	Phenolic acids	85.7	69.8	Level 2
33	4.221	$C_7H_6O_5$	170.02147	169.01414	$[M-H]^-$	−0.33	71859123.52	Gallic acid	Phenolic acids	85.5	84.6	Level 2
34	4.236	$C_7H_{12}O_4$	160.07347	159.06624	$[M-H]^-$	−0.56	770557559.2	3-Methyladipic acid	Organic acids	87.1	96.9	Level 2
35	4.352	$C_{12}H_{12}N_2O_2$	216.08996	217.09717	$[M+H]^+$	0.37	179365585.2	2,3,4,9-Tetrahydro-1h-β-carboline-3-carboxylic acid	Organic acids	NA	92.9	Level 2
36	4.734	$C_6H_{12}O_3$	132.07867	131.07133	$[M-H]^-$	0.21	111408164.4	2-Hydroxycaproic acid	Organic acids	NA	89.2	Level 2
37	5.007	$C_8H_{15}NO_3$	173.10533	174.11256	$[M+H]^+$	0.77	49085835.4	N-Acetyl-l-leucine	Amino acids	84.2	88.9	Level 2
38	5.273	$C_8H_{15}NO_3$	173.10522	172.09795	$[M-H]^-$	0.17	228758811.1	2-(Acetylamino)hexanoic acid	Organic acids	NA	94.9	Level 2
39	5.495	$C_9H_{10}O_3$	166.06292	165.05562	$[M-H]^-$	−0.47	7120276779	L-(-)-3-Phenyllactic acid	Others	79.8	92.4	Level 2
40	5.783	$C_{11}H_{18}N_2O_2$	210.13664	211.14392	$[M+H]^+$	−0.87	148811351.4	Cyclo(leucylprolyl)	Amino acids	NA	86.6	Level 2
41	5.832	$C_8H_{14}O_4$	174.08912	173.08185	$[M-H]^-$	−0.50	361132054.6	Suberic acid	Organic acids	89.2	92.8	Level 2
42	5.85	$C_{11}H_{13}NO_3$	207.08931	206.08209	$[M-H]^-$	−1.14	135547722	N-Acetyl-L-phenylalanine	Amino acids	89.4	88.5	Level 2
43	6.629	$C_9H_{14}O_4$	186.08906	185.0818	$[M-H]^-$	−0.78	68946334.82	1-(Carboxymethyl)cyclohexanecarboxylic acid	Organic acids	NA	89.1	Level 2
44	7.097	$C_{12}H_{10}N_4O_2$	242.08046	243.08763	$[M+H]^+$	0.35	161472292.4	Lumichrome	Others	89.6	39.1	Level 2
45	7.105	$C_9H_{16}O_4$	188.10468	187.09747	$[M-H]^-$	−0.97	3465873760	Azelaic acid	Organic acids	93.2	96.7	Level 1
46	7.755	$C_{12}H_{14}O_2$	190.09933	191.1066	$[M+H]^+$	−0.27	20998200.24	Ligustilide	Others	87.5	NA	Level 1
47	7.998	$C_{12}H_{16}O_3$	208.10987	209.11719	$[M+H]^+$	−0.38	8947399.972	B-Asarone	Others	82	85.7	Level 2
48	8.296	$C_{10}H_{18}O_4$	202.12036	201.1131	$[M-H]^-$	−0.74	435644695.3	3-Tert-butyladipic acid	Organic acids	NA	86.6	Level 2
49	8.504	$C_{15}H_{10}O_6$	286.04722	285.04053	$[M-H]^-$	−1.80	17137849.28	Luteolin	Flavonoids	94.3	86.7	Level 1
50	9.458	$C_{15}H_{10}O_5$	270.05241	269.04538	$[M-H]^-$	−1.52	9772253.507	Apigenin	Flavonoids	96.2	86.7	Level 1
51	9.756	$C_{16}H_{12}O_6$	300.06343	301.07077	$[M+H]^+$	0.15	17886631.77	Diosmetin	Flavonoids	78	88.5	Level 2
52	9.757	$C_{16}H_{12}O_6$	300.06297	299.05612	$[M-H]^-$	−1.39	1002007346	Hispidulin	Flavonoids	93	79.8	Level 1
53	9.785	$C_{15}H_{20}O_3$	248.14096	249.14859	$[M+H]^+$	−1.14	765330608.2	(3ar,8r,8ar,9ar)-8-Hydroxy-8a-methyl-3,5-bis(methylene)decahydronaphtho[2,3-b]furan-2(3 h)-one (	Others	81.7	89.9	Level 2
54	10.161	$C_{12}H_{18}O_2$	194.13062	195.13806	$[M+H]^+$	−0.32	139186228.7	Sedanolide	Others	NA	88.1	Level 2

Table 1: Continued.

Number	Retention time (min)	Molecular formula	Relative molecular weight (Da)	The measured values (m/z)	Adduct ions	Error (ppm)	Peak	Compound name	Compound type	mzVault best match	mzCloud best match	Level
55	10.163	$C_{18}H_{34}O_5$	330.24027	329.23309	$[M-H]^-$	−1.08	4975697767	(15z)-9,12,13-Trihydroxy-15-octadecenoic acid	Organic acids	NA	90.2	Level 2
56	10.459	$C_{12}H_{22}O_4$	230.15155	229.1442	$[M-H]^-$	−1.13	18453143.37	Dodecanedioic acid	Organic acids	NA	90.1	Level 2
57	11.508	$C_{20}H_{30}O_4$	334.21425	335.22144	$[M+H]^+$	−0.48	288459427.2	2-Hydroxy-4,5′,8a′-trimethyl-1′-oxo-4-vinyloctahydro-1′h-spiro[cyclopentane-1,2′-naphthalene]-5′-carboxylic acid	Organic acids	68.1	85.2	Level 2
58	11.573	$C_{10}H_{20}O_3$	188.14116	187.13385	$[M-H]^-$	−0.46	6112620.09	10-Hydroxydecanoic acid	Organic acids	NA	85.5	Level 2
59	11.73	$C_{22}H_{26}O_6$	386.17282	387.17999	$[M+H]^+$	−0.30	162320645.1	Bis(methylbenzylidene) sorbitol	Others	15.4	91.5	Level 2
60	11.791	$C_{16}H_{12}O_5$	284.06798	283.06070	$[M-H]^-$	−1.75	1982601.94	Acacetin	Flavonoids	94.6	83.2	Level 1
61	11.863	$C_{15}H_{18}O_3$	246.12566	247.13295	$[M+H]^+$	0.27	4367290.94	Arglabin	Terpenoids	65	86.7	Level 2
62	12.006	$C_{15}H_{20}O_3$	248.14096	249.14842	$[M+H]^+$	−1.14	16706391.7	Atractylenolide III	Terpenoids	92.9	92.4	Level 1
63	12.437	$C_{14}H_{26}O_4$	258.18284	257.17584	$[M-H]^-$	−1.03	3550240.872	Tetradecanedioic acid	Organic acids	NA	88.7	Level 2
64	12.818	$C_{20}H_{32}O_3$	320.23487	321.24219	$[M+H]^+$	−0.87	240249419.6	3-Methyl-5-[(1s,2r,4ar)-1,2,4a,5-tetramethyl-7-oxo-1,2,3,4,4a,7,8,8a-octahydro-1-naphthalenyl] pentanoic acid	Organic acids	78.1	90.5	Level 2
65	12.858	$C_{20}H_{32}O_2$	304.23998	305.24768	$[M+H]^+$	−0.83	6899745.63	Arachidonic acid	Organic acids	61.9	89.3	Level 2
66	12.934	$C_{24}H_{30}O_6$	414.20434	415.21118	$[M+H]^+$	0.24	1507553854	Bis(4-ethylbenzylidene) sorbitol	Others	NA	94.9	Level 2
67	12.976	$C_9H_{10}O_3$	166.06299	167.07022	$[M+H]^+$	−0.02	92932147.44	Ethyl paraben	Others	84	87.1	Level 2
68	12.977	$C_{11}H_{14}O_3$	194.09427	195.1017	$[M+H]^+$	−0.12	215420117.3	4-Ethoxy ethylbenzoate	Others	69	90.6	Level 2
69	13.247	$C_{18}H_{34}O_4$	314.24521	313.23795	$[M-H]^-$	−1.60	1064033527	(±)9,10-Dihydroxy-12z-octadecenoic acid	Organic acids	NA	94.9	Level 2
70	13.379	$C_{12}H_{26}O_4S$	266.15457	265.14728	$[M-H]^-$	−2.31	919909720.2	Dodecyl sulfate	Others	NA	94.3	Level 2
71	13.427	$C_{20}H_{28}O_2$	300.20881	301.21606	$[M+H]^+$	−0.39	260138250.1	Isotretinoin	Organic acids	NA	85.1	Level 2
72	13.908	$C_{18}H_{35}NO_2$	297.26671	298.27426	$[M+H]^+$	−0.22	57608549.56	2-Aminooctadec-4-yne-1,3-diol	Others	NA	92.4	Level 2
73	14.152	$C_{18}H_{28}O_3$	292.20372	293.21088	$[M+H]^+$	−0.42	477279239	9s,13r-12-Oxophytodienoic acid	Organic acids	NA	92.4	Level 2
74	14.574	$C_{12}H_{16}O_2$	192.11508	193.12238	$[M+H]^+$	0.28	134018825.8	Senkyunolide A	Others	85.9	NA	Level 2
75	14.763	$C_{21}H_{44}NO_7P$	453.28511	452.27756	$[M-H]^-$	−0.95	115696629.3	Glycerophospho-n-palmitoyl ethanolamine	Others	NA	93.5	Level 2
76	14.975	$C_{18}H_{30}O_2$	278.22423	279.23184	$[M+H]^+$	−1.24	3057598727	A-Eleostearic acid	Unsaturated fatty acids	91	96.7	Level 2

TABLE 1: Continued.

Number	Retention time (min)	Molecular formula	Relative molecular weight (Da)	The measured values (m/z)	Adduct ions	Error (ppm)	Peak	Compound name	Compound type	mzVault best match	mzCloud best match	Level
77	15.058	$C_{18}H_{30}O_3S$	326.19129	325.18396	$[M-H]^-$	−0.84	934129316.5	4-Dodecylbenzenesulfonic acid	Others	NA	92.4	Level 2
78	15.149	$C_{20}H_{32}O_3$	320.23482	321.24207	$[M+H]^+$	−1.02	654199927.6	(3 s)-3-Methyl-5-[(1 s,8ar)-2,5,5,8a-tetramethyl-4-oxo-1,4,4a,5,6,7,8,8a-octahydro-1-naphthalenyl] pentanoic acid	Organic acids	64.3	89.1	Level 2
79	15.292	$C_{18}H_{30}O_2$	278.22423	279.23172	$[M+H]^+$	−1.26	1402325459	Pinolenic acid	Organic acids	90.2	95.8	Level 2
80	15.332	$C_{14}H_{28}O_3$	244.20347	243.19621	$[M-H]^-$	−1.52	22659032.03	(r)-3-Hydroxy myristic acid	Organic acids	NA	88.9	Level 2
81	15.832	$C_{18}H_{30}O_3$	294.2195	295.22685	$[M+H]^+$	0.003	5846063601	9-Oxo-10(e),12(e)-octadecadienoic acid	Organic acids	NA	97.6	Level 2
82	16.357	$C_{30}H_{46}O_4$	470.33934	471.34756	$[M+H]^+$	−0.57	3098680480.74	18-β-glycyrrhetinic acid	Terpenoids	87.3	90.6	Level 2
83	17.175	$C_{20}H_{32}O_3$	320.23482	321.24222	$[M+H]^+$	−1.02	129134534.2	Ginkgolic acid 9(z),11(e),13(e)-	Phenolic acids	66	86.1	Level 2
84	17.422	$C_{19}H_{32}O_2$	292.23998	293.24725	$[M+H]^+$	−0.87	84449956.04	Octadecatrienoic acid methyl ester	Others	NA	94	Level 2
85	17.727	$C_{20}H_{34}O_2$	306.25582	307.26297	$[M+H]^+$	−0.21	59379266.82	Linolenic acid ethyl ester	Others	91.1	96.2	Level 2
86	17.935	$C_{21}H_{38}O_4$	354.27685	355.28397	$[M+H]^+$	−0.44	469393052.8	1-Linoleoyl glycerol	Others	NA	94.4	Level 2
87	18.154	$C_{16}H_{32}O_3$	272.23457	271.22726	$[M-H]$-	−2.12	2322316874	16-Hydroxyhexadecanoic acid	Organic acids	NA	93.3	Level 2
88	18.184	$C_{22}H_{36}O_3$	348.26628	349.2735	$[M+H]^+$	−0.47	79521502.69	3-Methyl-5-(5,5,8a-trimethyl-2-methylene-7-oxodecahydro-1-naphthalenyl) pentyl acetate	Others	NA	85	Level 2
89	18.301	$C_{20}H_{30}O_3$	318.21935	319.22678	$[M+H]^+$	−0.46	87070678.64	11-α-hydroxy-17-methyltestosterone	Steroids	74.9	85.5	Level 2
90	18.528	$C_{16}H_{30}O_2$	254.22444	255.23161	$[M+H]^+$	−0.54	93625271.65	Palmitoleic acid	Organic acids	79.8	97.2	Level 2
91	18.532	$C_{16}H_{30}O_2$	254.22421	253.21733	$[M-H]^-$	−1.45	75050753.73	Δ2-Trans-hexadecenoic acid	Unsaturated fatty acids	NA	86.4	Level 2

TABLE 1: Continued.

Number	Retention time (min)	Molecular formula	Relative molecular weight (Da)	The measured values (m/z)	Adduct ions	Error (ppm)	Peak	Compound name	Compound type	mzVault best match	mzCloud best match	Level
92	18.608	$C_{18}H_{37}NO_2$	299.28227	300.28955	$[M+H]^+$	−0.52	60691604.46	Palmitoyl ethanolamide	Others	NA	95.2	Level 2
93	18.618	$C_{20}H_{39}NO_2$	325.29787	326.30499	$[M+H]^+$	−0.64	205900632.2	Oleoyl ethanolamide	Others	NA	94.2	Level 2
94	18.94	$C_{20}H_{32}O_3$	320.23475	319.228	$[M-H]^-$	−1.22	11930213.5	5-[(3z)-5-Hydroxy-3-methyl-3-penten-1-yl]-1,4a-dimethyl-6-methylenedecahydro-1-naphthalenecarboxylic acid	Organic acids	80.5	86.2	Level 2
95	18.948	$C_{18}H_{32}O_2$	280.23944	279.23248	$[M-H]^-$	−2.81	1954067053	9(z),11(e)-Conjugated linoleic acid	Unsaturated fatty acids	85.8	87.3	Level 2
96	19.741	$C_{18}H_{35}NO$	281.27169	282.27902	$[M+H]^+$	−0.61	800775254.3	Oleamide	Others	NA	97.3	Level 2
97	20.138	$C_{16}H_{33}NO$	255.25604	256.26334	$[M+H]^+$	−0.68	144475650.8	Hexadecanamide	Others	NA	90.2	Level 2
98	20.821	$C_{20}H_{34}O_2$	306.25582	307.26343	$[M+H]^+$	−0.21	6347388.901	Linolenic acid ethyl ester	Others	90.2	96.2	Level 1
99	20.977	$C_{21}H_{42}O_4$	358.30821	359.31543	$[M+H]^+$	−0.27	268288479.9	1-Stearoylglycerol	Others	NA	89.1	Level 2
100	21.524	$C_{18}H_{34}O_2$	282.25578	283.26306	$[M+H]^+$	−0.34	21237622.49	Ethyl palmitoleate	Others	64.8	93.9	Level 2
101	22.225	$C_{18}H_{37}NO$	283.28734	284.29741	$[M+H]^+$	−0.61	133000171.1	Stearamide	Others	NA	90.6	Level 2
102	22.746	$C_{20}H_{38}O_2$	310.28707	311.29428	$[M+H]^+$	−0.37	22068099.07	Ethyl oleate	Others	57.8	96.3	Level 2
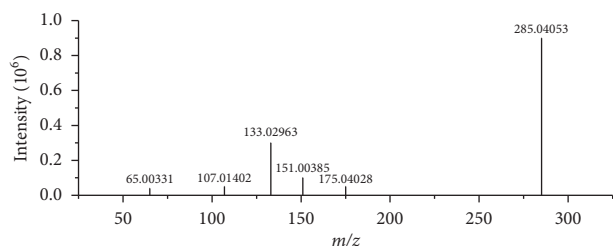
Figure 2: The MS² spectrum of luteolin.
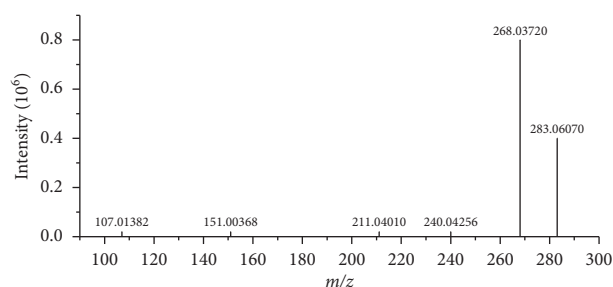
Figure 3: The MS² spectrum of acacetin.
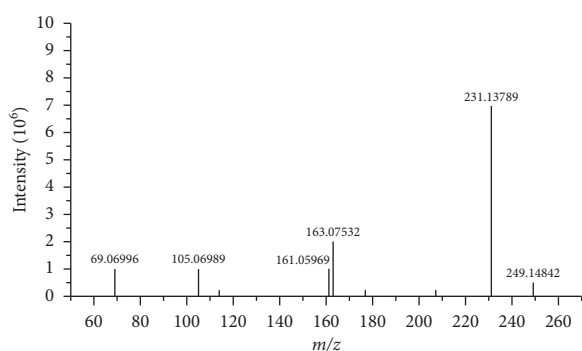
Figure 4: The MS² spectrum of acacetin atractylenolide III.

Data Availability

The data used to support this study are available within the article.

Conflicts of Interest

The authors declare that there are no conflicts of interest regarding this study.

Acknowledgments

References

[1] M. Wang, Y. Gao, D. Xu, T. Konishi, and Q. Gao, "*Hericium erinaceus* (Yamabushitake): a unique resource for developing functional foods and medicines," *Food & Function*, vol. 5, no. 12, pp. 3055–3064, 2014.

[2] J. Y. Tan, J. J. Wang, X. L. Wang et al., "The health value of *Hericium erinaceus* (Review)," *Edible and Medicinal Mushroom*, vol. 23, no. 3, pp. 188–193, 2015.

[3] Y. Zhang, *Chemical Constituents of Hericium erinaceus*, Northwest A & F University, Xianyang, China, 2016.

[4] H. Kawagishi, A. Shimada, R. Shirai et al., "Erinacines A, B and C, strong stimulators of nerve growth factor (NGF)-synthesis, from the mycelia of Hericium erinaceum," *Tetrahedron Letters*, vol. 35, no. 10, pp. 1569–1572, 1994.

[5] H. Kawagishi, A. Simada, K. Shizuki et al., "Erinacine D, a stimulator of NGF-synthesis, from the mycelia of Hericium erinaceum," *Heterocyclic Communications*, vol. 2, no. 1, pp. 51–54, 1996.

[6] H. Kawagishi, A. Shimada, S. Hosokawa et al., "Erinacines E, F, and G, stimulators of nerve growth factor (NGF)-synthesis, from the mycelia of Hericium erinaceum," *Tetrahedron Letters*, vol. 37, no. 41, pp. 7399–7402, 1996.

[7] H. Kawagishi, A. Masui, S. Tokuyama, and T. Nakamura, "Erinacines J and K from the mycelia of Hericium erinaceum," *Tetrahedron*, vol. 62, no. 36, pp. 8463–8466, 2006.

[8] E. W. Lee, K. Shizuki, S. Hosokawa et al., "Two novel diterpenoids, erinacines H and I from the mycelia of Hericium erinaceum," *Bioscience, Biotechnology, and Biochemistry*, vol. 64, no. 11, pp. 2402–2405, 2000.

[9] H. Kenmoku, T. Sassa, and N. Kato, "Isolation of erinacine P, a new parental metabolite of cyathane-xylosides, from Hericium erinaceum and its biomimetic conversion into erinacines A and B," *Tetrahedron Letters*, vol. 41, no. 22, pp. 4389–4393, 2000.

[10] H. Kenmoku, T. Shimai, T. Toyomasu, N. Kato, and T. Sassa, "Erinacine Q, a new erinacine from Hericium erinaceum, and its biosynthetic route to erinacine C in the basidiomycete," *Bioscience, Biotechnology, and Biochemistry*, vol. 66, no. 3, pp. 571–575, 2002.

[11] H. Kawagishi, M. Ando, and T. Mizuno, "Hericenone A and B as cytotoxic principles from the mushroom," *Tetrahedron Letters*, vol. 31, no. 3, pp. 373–376, 1990.

[12] H. Kawagishi, M. Ando, H. Sakamoto et al., "Hericenones C, D and E, stimulators of nerve growth factor (NGF)-synthesis, from the mushroom Hericium erinaceum," *Tetrahedron Letters*, vol. 32, no. 35, pp. 4561–4564, 1991.

[13] H. Kawagishi, M. Ando, and K. Shinba, "Chromans, hericenones F, G and H from the mushroom of Hericium erinaceum," *Phytochemistry*, vol. 32, no. 1, pp. 175–178, 1993.

[14] A. Arnone, R. Cardillo, G. Nasini, and O. V. de Pava, "Secondary mold metabolites: part 46. hericenes A-C and erinapyrone C, new metabolites produced by the fungus Hericium erinaceus," *Journal of Natural Products*, vol. 57, no. 5, pp. 602–606, 1994.

[15] B.-J. Ma, H.-Y. Yu, J.-W. Shen et al., "Cytotoxic aromatic compounds from Hericium erinaceum," *The Journal of Antibiotics*, vol. 63, no. 12, pp. 713–715, 2010.

[16] W. Li, Y. N. Sun, W. Zhou, S. H. Shim, and Y. H. Kim, "Erinacene D, a new aromatic compound from Hericium erinaceum," *The Journal of Antibiotics*, vol. 67, no. 10, pp. 727–729, 2014.

[17] W. Li, W. Zhou, S. B. Song, S. H. Shim, and Y. H. Kim, "Sterol fatty acid esters from the mushroom Hericium erinaceum and their PPAR transactivational effects," *Journal of Natural Products*, vol. 77, no. 12, pp. 2611–2618, 2014.

[18] Z. Liu, L. Liao, Q. Chen et al., "Effects of *Hericium erinaceus* polysaccharide on immunity and apoptosis of the main immune organs in muscovy duck reovirus-infected ducklings,"

International Journal of Biological Macromolecules, vol. 171, pp. 448–456, 2021.

[19] F. Wu and H. Huang, "Surface morphology and protective effect of *Hericium erinaceus* polysaccharide on cyclophosphamide-induced immunosuppression in mice," *Carbohydrate Polymers*, vol. 251, p. 116930, 2021.

[20] S. Y. Lew, S. H. Lim, L. W. Lim et al., "Neuroprotective effects of *Hericium erinaceus* (Bull.: Fr.) Pers. against high-dose corticosterone-induced oxidative stress in PC-12 cells," *BMC Complementary Medicine and Therapies*, vol. 20, no. 1, p. 340, 2020.

[21] P. S. Chong, S. Khairuddin, A. C. K. Tse et al., "*Hericium erinaceus* potentially rescues behavioural motor deficits through ERK-CREB-PSD95 neuroprotective mechanisms in rat model of 3-acetylpyridine-induced cerebellar ataxia," *Scientific Reports*, vol. 10, no. 1, p. 14945, 2020.

[22] F. Limanaqi, F. Biagioni, C. L. Busceti, M. Polzella, C. Fabrizi, and F. Fornai, "Potential antidepressant effects of scutellaria baicalensis, Hericium erinaceus and Rhodiola Rosea," *Antioxidants (Basel, Switzerland)*, vol. 9, no. 3, p. 234, 2020.

[23] P. S. Chong, M.-L. Fung, K. H. Wong, and L. W. Lim, "Therapeutic potential of *Hericium erinaceus* for depressive disorder," *International Journal of Molecular Sciences*, vol. 21, no. 1, p. 163, 2019.

[24] T. Qin, X. Liu, Y. Luo et al., "Characterization of polysaccharides isolated from *Hericium erinaceus* and their protective effects on the DON-induced oxidative stress," *International Journal of Biological Macromolecules*, vol. 152, pp. 1265–1273, 2020.

[25] W. Li, W. Zhou, E.-J. Kim, S. H. Shim, H. K. Kang, and Y. H. Kim, "Isolation and identification of aromatic compounds in lion's mane mushroom and their anticancer activities," *Food Chemistry*, vol. 170, pp. 336–342, 2015.

[26] B. Liang, Z. D. Guo, F. Xie, and F. Zhao, "Antihyperglycemic and antihyperlipidemic activities of aqueous extract of *Hericium erinaceus* in experimental diabetic rats," *BioMed Central*, vol. 13, no. 1, p. 253, 2013.

[27] K. Hiwatashi, Y. Kosaka, N. Suzuki et al., "Yamabushitake mushroom (Hericium erinaceus) improved lipid metabolism in mice fed a high-fat diet," *Bioscience, Biotechnology, and Biochemistry*, vol. 74, no. 7, pp. 1447–1451, 2014.

[28] E. D. Yuan, M. Huang, L. Li et al., "Protective effect of Hericium erinaceus mycelium/fruit body polysaccharide on gastric mucosa," *Journal of Chinese Institute of Food Science and Technology*, vol. 20, no. 11, pp. 71–78, 2020.

[29] W. Chen, D. Wu, Y. Jin et al., "Pre-protective effect of polysaccharides purified from Hericium erinaceus against ethanol-induced gastric mucosal injury in rats," *International Journal of Biological Macromolecules*, vol. 159, pp. 948–956, 2020.

[30] M. Hamza, E. Imane, A. Amal et al., "Antioxidant, anti-inflammatory and antidiabetic proprieties of LC-MS/MS identified polyphenols from coriander seeds," *Molecules*, vol. 26, no. 2, p. 487, 2021.

[31] Q. Y. Zhang, X. J. Wang, X. M. Wang et al., "Development of a pass-through SPE cartridge for the rapid determination of fipronil and its metabolites in chicken eggs by LC-MS/MS," *Food Analytical Methods*, 2021.

[32] W. Li, Y. Zhang, S. Shi et al., "Spectrum-effect relationship of antioxidant and tyrosinase activity with malus pumila flowers by UPLC-MS/MS and component knock-out method," *Food and Chemical Toxicology*, vol. 133, p. 110754, 2019.

[33] J. Ma, S. Fan, L. Sun, L. He, Y. Zhang, and Q. Li, "Rapid analysis of fifteen sulfonamide residues in pork and fish samples by automated on-line solid phase extraction coupled to liquid chromatography-tandem mass spectrometry," *Food Science and Human Wellness*, vol. 9, no. 4, pp. 363–369, 2020.

[34] S. Fan, J. Ma, M. Cao et al., "Simultaneous determination of 15 pesticide residues in Chinese cabbage and cucumber by liquid chromatography-tandem mass spectrometry utilizing online turbulent flow chromatography," *Food Science and Human Wellness*, vol. 10, no. 1, pp. 78–86, 2021.

[35] J. M. Ma, Q. Li, S. F. Fan et al., "Determination of 8 endogenous alkaloid components in boletus using ultrahigh-performance liquid chromatography combined with quadrupole-time of flight mass spectrometry," *Journal of Food Quality*, vol. 2020, Article ID 8865725, 10 pages, 2020.

[36] Q. Q. Xu, B. H. Bao, L. Zhang et al., "UPLC-QTOF-MS analysis and multicomponent quantitative analysis of cayratia japonica," *Journal of Nanjing University Traditional Chinese Medicine*, vol. 36, no. 4, pp. 517–524, 2020.

[37] X. N. Lu, Y. W. Zheng, F. Wen et al., "Study of the active ingredients and mechanism of Sparganii rhizoma in gastric cancer based on HPLC-Q-TOF–MS/MS and network pharmacology," *Scientific Reports*, vol. 11, no. 1, p. 1905, 2021.

[38] Y.-Y. Shi, S.-H. Guan, R.-N. Tang, S.-J. Tao, and D.-A. Guo, "Simultaneous determination of atractylenolide II and atractylenolide III by liquid chromatography-tandem mass spectrometry in rat plasma and its application in a pharmacokinetic study after oral administration of atractylodes macrocephala rhizoma extract," *Biomedical Chromatography*, vol. 26, no. 11, pp. 1386–1392, 2012.

[39] X. X. Yan, H. Zhang, F. K. Zhang et al., "Determination of five nucleosides in *Hericium erinaceus* from different habitats by high performance liquid chromatography," *Chinese Journal of Traditional Medical Science and Technology*, vol. 25, no. 4, pp. 520–522, 2018.

[40] K. Mori, H. Kikuchi, Y. Obara et al., "Inhibitory effect of hericenone B from *Hericium erinaceus* on collagen-induced platelet aggregation," *Phytomedicine*, vol. 17, no. 14, pp. 1082–1085, 2010.

[41] X. J. Ding, L. Xiong, Q. M. Zhou et al., "Advances in studies on chemical structure and pharmacological activities of natural nucleosides," *Journal of Chengdu University of TCM*, vol. 41, no. 2, pp. 102–108, 2018.

[42] J. H. Qi and F. X. Dong, "Research progress of the pharmacological action of flavonoids," *Journal of Beijing Union University*, vol. 34, no. 3, pp. 89–92, 2020.